

UC Merced

UC Merced Electronic Theses and Dissertations

Title

Microalgae Cultivation using Offshore Membrane Enclosures for Growing Algae (OMEGA)

Permalink

<https://escholarship.org/uc/item/0586c8p5>

Author

Wiley, Patrick Edward

Publication Date

2013

Peer reviewed|Thesis/dissertation

UNIVERSITY OF CALIFORNIA, MERCED

Microalgae Cultivation using Offshore Membrane Enclosures for Growing Algae
(OMEGA)

A dissertation submitted in partial satisfaction of the requirements
for the degree Doctor of Philosophy

in

Environmental Systems

by

Patrick Edward Wiley

Committee in charge:

Professor Thomas Harmon, Chair
Professor J. Michael Beman
Professor J. Elliott Campbell
Professor Jonathan D. Trent

2013

Copyright

Patrick Edward Wiley, 2013

All rights reserved

The Dissertation of Patrick Edward Wiley is approved, and it is acceptable
in quality and form for publication on microfilm and electronically:

Professor J. Michael Beman

Professor J. Elliott Campbell

Professor Jonathan D. Trent

Professor Thomas Harmon, Chair

University of California, Merced

2013

TABLE OF CONTENTS

LIST OF FIGURES	vi
LIST OF TABLES	xii
ACKNOWLEDGEMENTS	xiii
CURRICULUM VITAE.....	xiv
ABSTRACT OF THE DISSERTATION	xvi
Chapter 1: Introduction	1
1.1 Microalgae as a Biofuel Feedstock	1
1.2 Combining Microalgae Cultivation with Wastewater Treatment	1
1.3 The OMEGA Concept.....	2
1.4 Dissertation Outline.....	5
1.5 Acknowledgements	6
1.6 References.....	6
Chapter 2: Development of an OMEGA Prototype System	10
2.1 Introduction.....	10
2.2 Prototype Development	10
2.3 Photobioreactor (PBR) System	12
2.4 Gas Exchange and Harvesting Column (GEHC).....	13
2.4.1 Predicting GEHC Gas Injection Rate and CO ₂ Mass Transfer Efficiency	16
2.4.2 Balancing Carbon Consumption in the PBR with Carbon Injection in the GEHC.....	18
2.5 Process Automation and Data Collection	20
2.5.1 Monitoring and Controlling the GEHC with the HMI	27
2.5.2 PBR Monitoring with the HMI.....	28
2.6 Chapter Summary	28
2.7 Acknowledgements.....	29
2.8 References.....	29
Chapter 3: Deployment and Performance Evaluation of the OMEGA Prototype System	31
3.1 Introduction.....	31

3.2 Prototype Configuration and Experimental Details	31
3.3 Module Deployment and System Inoculation.....	32
3.4 Harvesting Procedures, Microalgal Yields and CO ₂ Utilization Efficiency.....	34
3.5 Nutrient Recovery from FPE Wastewater	35
3.6 OMEGA Prototype Performance	36
3.6.1 GEHC Performance	38
3.6.2 CO ₂ Utilization and Biomass Production	40
3.6.3 OMEGA and Wastewater Treatment.....	43
3.7 Conclusion	49
3.8 Acknowledgements.....	50
3.9 References.....	50
Chapter 4: The Future of the OMEGA Concept.....	53
4.1 Introduction.....	53
4.2 Impact of Biofouling on Microalgal Photosynthesis within OMEGA PBRs	53
4.2.1 Quantifying the Impacts of Biofouling on Microalgal Photosynthesis	55
4.3 Improving Microalgal Harvesting Procedures for the OMEGA System.....	57
4.3.1 Harvesting Through the GEHC	59
4.3.2 Construction and Operation of an EC Unit for the GEHC	61
4.3.3 Preliminary Performance Results of the EC System	69
4.4 Concluding Thoughts.....	74
4.5 Acknowledgements.....	74
4.6 References.....	75

LIST OF FIGURES

Figure 1.1.	The OMEGA system cultivates microalgae using wastewater contained in PBR modules deployed offshore. This approach eliminates competition with agriculture for land and nutrients, while enabling co-location with large wastewater treatment facilities constructed in coastal urban areas. The surrounding ocean water provides structural support, temperature regulation and could produce a “simulated reef” that enriches local species diversity. The osmotic gradient between the PBR contents and the surrounding seawater can be used to drive forward osmosis, which is effective at concentrating nutrients, dewatering microalgae and producing clean water	3
Figure 1.2.	A hypothetical OMEGA deployment in the San Francisco Bay. This deployment, co-located with the San Francisco Southeast Wastewater Treatment Plant, has the capacity to accept five days of wastewater discharged from the facility ($1.23 \times 10^6 \text{ m}^3$) as a source of water and nutrients for microalgae cultivation and occupies approximately 11 km^2 . The inset in the blue box shows the floating infrastructure needed to support the OMEGA deployment.	4
Figure 2.1.	Microalgae grown in FPE wastewater following nutrient concentration using an FO membrane. The 1X flask contains FPE that was not concentrated, while 2X and 3X have nutrient concentrations that were doubled and tripled, respectively. The increasing cell density due to higher nutrient availability is evidenced by the darker color of the flasks.	11
Figure 2.2.	Early OMEGA prototype deployment with internal sparging network during leak testing with tap water (Bottom) and after inoculation with microalgae (Top). The sparging network was used to inject CO_2 and provide aeration intended to keep the microalgae suspended. This design was abandoned due to engineering challenges and difficulty in sustaining microalgal biology.	12
Figure 2.3.	Illustration of OMEGA PBR tubes with swirl vanes. PBRs were made of flexible, clear LLDPE connected with cam-lock fittings to a U-shaped PVC manifold. The six swirl vanes (see insert enlargement) directed the flow into a helical path to improve mixing and light exposure of the microalgae.....	13
Figure 2.4.	VFDs used to control the pumping rate of the culture through the PBR tubes. Two independent prototype systems, each requiring a VFD, were constructed during the OMEGA project.	14

Figure 2.5.	Sensor manifold for measuring pH, temperature, DO, and flow rate. The culture was pumped from the PBR past the sensors. Part of the circulating flow was diverted to the GEHC (see Figure 2.6) at the GEHC suction fitting by a positive displacement pump (not shown) and returned to the PBR flow at the GEHC return. The valved bypass was used to isolate the sensors for cleaning and maintenance without disrupting the overall circulation.	14
Figure 2.6.	Gas exchange and harvesting column (GEHC) controls pH, removes settled microalgae and provides a location for wastewater addition into the PBR system. An oxygen stripping device (OSD, top) designed to remove excessive concentrations of photosynthetically generated dissolved oxygen was built into the GEHC. CO ₂ is added by gas bubbles injected with the diffuser at a rate controlled by pH. Biomass collected in the settling chamber is removed, whereas suspended microalgae are returned to the PBR (return flow pipe, left). The pressure transducer controls a pinch valve position to maintain a consistent liquid level in the GEHC. The volume of the GEHC was periodically harvested from the drain valve at the bottom and replaced with wastewater to replenish nutrients in the PBRs.	15
Figure 2.7.	Efficiency of CO ₂ mass transfer in the GEHC relative to the height of the column and the pH of the solution. Data were obtained (n = 76) experimentally using tap water, pH adjusted (>11.00) with NaOH. For practical reasons a maximum column height of 1.8 meters was used for the functional OMEGA prototype system.	19
Figure 2.8.	The natural log of total carbon absorbed by the NaOH solution between pH 7.5 and 9.0 as a function of time. The three experimental trials were conducted using a column height of 1.8 meters and a gas flow rate of 0.5 lpm of 8.5% CO ₂ . These parameters were selected because they were expected to closely mimic operating conditions of the OMEGA prototype. These data enabled determination of the CO ₂ mass transfer rate, which is required to estimate the GEHC recycle rate.	21
Figure 2.9.	Components of the SCADA system. Inputs from the sensors were routed through a multi-parameter transmitter (A) or directly into a PLC (B) were transferred to a computer database. Setpoint values established using an HMI modulated PLC outputs that controlled a mass flow controller for CO ₂ injection (C) and an I/P transducer (D) to regulate pinch valve positioning.....	24
Figure 2.10.	Control Cabinet A (Left) and Control Cabinet B (Right) containing PLCs that receive input signals from field sensors and generate output signals connected to mass flow controllers for CO ₂ injection and I/P transducers for GEHC level control. The cabinets were designed to accommodate two independent prototype systems.	25

Figure 2.11.	The HMI screen of the OMEGA SCADA system. The HMI displayed data from field sensors and provided operators with the ability to specify the desired pH and liquid level in the GEHC. Clicking on the “View Data” buttons displayed trending data for the specified parameter. All data displayed by the HMI was logged to a database every three minutes.	26
Figure 3.1.	Component and flow diagram of the OMEGA system showing the circulation through the PBRs, sensor manifold, and side loop for the GEHC.....	31
Figure 3.2.	(A) Tubular OMEGA PBR modules with internal swirl vanes deployed in a seawater tank located at the California Department of Fish and Game, Marine Wildlife Veterinary Care and Research Center in Santa Cruz, CA. (B) The operational GEHC mounted on the exterior of the salt water tank. Flow from the PBR enters the top of the GEHC and cascades through the OSD (clear pipe on top), before entering the CO ₂ gas injection section (small diameter pipe with red hash marks). The large diameter section of pipe at the bottom of the GEHC is the settling chamber. The SCADA system modulates a pneumatic pinch valve to maintain the desired liquid level in the GEHC.....	32
Figure 3.3.	DO concentration, PAR and F _v /F _M values for experiment 1 (Left) and experiment 2 (Right). (Top) Mean hourly (± SE) concentration photosynthetically generated DO (solid line) increases and decreases as a function of PAR (dotted line). (Bottom) The mean hourly F _v /F _m ratio (dotted line) overlaying the range of data points (shaded area) measured by FRRF indicates that the culture has maintained high photoconversion efficiency. The slight suppression of the F _v /F _m ratio during mid-day is a result of photoinhibition caused by PAR intensity and elevated concentrations of DO (solid line).....	36
Figure 3.4.	The mean hourly (± SE) pH, gas flow, and PAR recorded during experiment 1 (Left) and experiment 2 (Right). (Top) pH values measured inside the GEHC (solid line) compared to pH in the PBR (dotted line). The differential between the GEHC and PBRs increases during the day due to carbon assimilation for photosynthesis. The rate of CO ₂ injection was controlled to maintain the GEHC pH setpoint during the day. The slow decrease in pH at night is attributed to respiration. (Bottom) Gas flow rates (solid lines) indicating CO ₂ demand correlated with PAR (dotted lines), and inferred rates of photosynthesis. The pH of the GEHC and PBRs equalize at night due to respiration.	38

Figure 3.5.	Totalized gas flow (8.5% CO ₂ V/V) (bold black line) and biomass production (histogram) plotted for experiment 1 (Bottom) and experiment 2 (Top) with the day/night cycle indicated by vertical stripes. The totalized gas flow has a “staircase” shape because CO ₂ was injected on demand; photosynthesis caused injection during the day (slope up), but not at night (plateaus). The histogram shows biomass production in the height of bars (right axis, g) and the time between harvesting in the width of the bars (bottom axis, days).	41
Figure 3.6.	The mean hourly temperatures (± SE) inside the GEHC (solid lines) and PBR (dotted lines) for experiment 1 and experiment 2. The slightly warmer temperature in the PBR is likely due to the heat capacity of the surrounding seawater and the use of a thermal pool cover during the evening to prevent heat loss.	43
Figure 3.7.	Time course for the addition and utilization of ammonia (Bottom) and nitrate (Top) during experiment 1 and experiment 2. Solid lines represent changes in nutrient concentration between harvest periods, while dotted lines indicate the addition of fresh FPE to replenished nutrients consumed by the microalgae. The day/night cycle is represented by white/gray shading on the vertical bars.	44
Figure 3.8.	Removal rates are shown as positive when nutrients were depleted or negative when nutrient concentrations increased. The ammonia removal rates (black bars) were always positive, but nitrate removal rates (grey bar) were occasionally negative due to nitrification. The microalgae preferred ammonia as their nitrogen source and consume nitrate once the supply of ammonia was exhausted.	45
Figure 3.9.	Time course for the addition and utilization of phosphate for experiment 1 (Bottom) and experiment 2 (Top). Solid lines represent changes in nutrient concentration between harvest periods, while dotted lines indicate the addition of fresh FPE to the system. The day/night cycle is represented by white/gray shading on the vertical bars.	46
Figure 3.10.	Phosphate removal rates for experiment 1 (Bottom) and experiment 2 (Top). X’s signify missing data points between harvest intervals during experiment 1, which prevented calculation of removal rates. In both experiments, the rate of phosphate recovery increased with increasing concentration.	47
Figure 4.1.	The 1500-liter OMEGA system deployed at the SF SEP. (Top) The system consisted of four PBR tubes 10 m in length connected to a centrifugal circulation pump. (Bottom) A scaled version of the GEHC was constructed for supplemental CO ₂ injection and as a harvesting location.	53

Figure 4.2.	<p>(Top Left) The biofouled LLDPE PBR tubes deployed at Moss Landing Harbor at Time 0 and 12 weeks later. (Top Right) The PBR tubes were removed from the harbor and transported to the OMEGA test facility in Santa Cruz, where one of the modules was cleaned while biofouling on the other was left intact. (Above) The biofouled (treatment) and clean (control) LLDPE tubes were cut into sleeves and wrapped around PBR modules deployed in a seawater tanks. The CO₂ consumption, used as a proxy for photosynthetic activity, was used to quantify the light attenuating effects of biofouling. The sleeves were swapped after three days to ensure that biofouling was the driving force inhibiting photosynthesis.....</p>	55
Figure 4.3.	<p>The totalized gas flow rate used to express rates of photosynthesis for biofouled and clean OMEGA PBRs. The dotted line during the first three days of the experiment represents CO₂ consumed by the microalgal culture in the biofouled PBR, while the solid line designates the clean PBR. The sleeves were switched at day three (dashed vertical line) and produced a similar trend, indicating that biofouling is the dominant factor suppressing photosynthesis. The grey and white vertical stripes signify the day night cycle, during which time photosynthesis ceases and no CO₂ was demanded by the microalgae.</p>	56
Figure 4.4.	<p>Illustration of microalgal cells as they approach each other in the bulk solution. Overlapping EDLs produce an electrostatic force that prevents aggregation and keeps cells suspended in the culture broth.</p>	57
Figure 4.5.	<p>Zeta potential of microalgae cultivated using the OMEGA prototype with changing pH. The zeta potential remains strongly negative regardless of pH, indicating that coagulating agents are needed to improve the sedimentation efficiency in the GEHC.</p>	58
Figure 4.6.	<p>Conceptual illustration of a full-scale OMEGA deployment. The red circle identifies one of many GEHCs distributed throughout the system. The GEHC serves as both a harvesting point and an effluent discharge point.</p>	59
Figure 4.7.	<p>(Left) Microalgae removed from the surface of a harvesting barrel using a pool skimmer after being thickened with Suspended Air Floatation. (Right) The biomass was then squeezed by hand to produce a more concentrated microalgal paste.....</p>	59
Figure 4.8.	<p>Installation of the EC system into the GEHC. Valves in the plumbing isolated the GEHC from the PBR enabling the GEHC pump to recycle flow between the EC electrode plates. Once the desired coagulant dose was delivered, the GEHC was designed to act as a sedimentation pit to collect flocculated microalgal biomass.....</p>	61

Figure 4.9.	(Left) Freshly fabricated aluminum electrodes with wires for the anode and cathode. The electrodes were held together using non-conductive plastic screws and spacers to prevent shorting. (Right) The electrode assembly was inserted inside transparent PVC tubes with union-style end caps to make installation and removal from the GEHC plumbing fast and easy.	62
Figure 4.10.	Control Cabinet B containing electronics for operating the EC harvest system. The EC process is a low-maintenance, energy efficient process that can be controlled precisely with automation tools.	65
Figure 4.11.	The HMI for operating the EC harvesting system. Boxes with the double border accept operator inputs that control coagulant dosing, polarity cycling and calculate power usage. Operators begin the harvest cycle by clicking the green “Start” button, which automatically initiates data logging. The system stops automatically once the desired coagulant dose has been delivered. Molar mass fractions and total soluble aluminum are calculated using ionization constants, pH and temperature.	66
Figure 4.12.	Solubility of aluminum as influenced by pH. The gray-shaded region designates the zone of precipitation, while vertical red bar represents the pH range observed in the GEHC during prototype operation. This suggests that a “sweep-coagulation” mechanism will likely dominate this application.	69
Figure 4.13.	Total aluminum concentration predicted by Faraday’s Law (dashed line) compared to the actual amount delivered by the EC unit in a sodium chloride solution (green dots). The SCADA system adjusts the voltage of a DC power supply to ensure that the current applied to the electrodes remains constant (gray dots).	70
Figure 4.14.	Theoretical aluminum concentration predicted with Faraday’s Law (dashed line) compared to the actual amount (green dots) measured after an EC cycle was conducted on a microalgal culture. The discrepancy between theoretical and observed dosing is likely due to coagulants binding to the microalgal cells, as current (gray dots), and thus dosing, remained constant throughout the cycle.	71
Figure 4.15.	Sedimentation of microalgal biomass after being subjected to an EC harvest cycle. When used with a GEHC, the dense microalgal mat will be removed, while the clear supernatant is discharged as final effluent.	72

LIST OF TABLES

Table 2.1.	Description and location of field sensors connected to the SCADA system for data logging and process control.	22
Table 3.1.	Harvesting frequency, biomass yields and mass of carbon injected into the GEHC used to calculate carbon conversion efficiency and areal biomass productivity during experiments 1 and 2.	40
Table 4.1.	Description and location of the sensors and equipment used by the EC harvesting system.	63

ACKNOWLEDGEMENTS

I am deeply indebted to Elliott Campbell for the exceptional guidance and unwavering support that he has provided over the past four years. I also want to recognize Jonathan Trent, the original OMEGA man, for allowing me to become part of such an amazing and exciting project. I also extend appreciation to Professors Tom Harmon and Mike Beman for their counsel during my graduate experience.

Additionally, I want to thank members of my OMEGA family, in particular, Steve Ord, Alan Wong, Tsege Embaye, Zbigniew Kolber, Justine Richardson, Brandi McQuin, Hiromi Kagawa, Jon Rask, John Malinoski, Emil Geiger and Matt Claxton for being incredibly helpful and supportive throughout the course of the project. I already miss the liquid debriefings with my colleagues and dear friends Sasha Tozzi, Sigrid Reinsch, Kit Clark, Colin Beal and Linden Harris that often followed long days at the lab. Special thanks to “don’t call me Shirley” Fauth, for her assistance with manuscript preparation and for tolerating my sense of humor.

And of course, I must express appreciation to my beautiful wife-to-be, Caroline, for her encouragement, patience and solace.

Financial support provided by the California Water Environment Association, University of California Merced Energy Research Institute, NASA Graduate Student Researcher Program, California Energy Commission, and the NASA Educational Associated Program are acknowledged and greatly appreciated.

CURRICULUM VITAE

Patrick Wiley

patrickewiley@gmail.com

PROFESSIONAL QUALIFICATIONS

Grade V Wastewater Operator (V-28096) issued by the California State Water Resources Control Board.

Grade 5 Wastewater Operator (#309) issued by the Maine Department of Environmental Protection.

Grade IV Wastewater Operator (#11063) issued by the Oregon Department of Environmental Quality.

Grade I Wastewater Laboratory Analyst (C-0511) issued by the New England Water Environment Association.

Grade I Wastewater Collection System Operator (C-2614) issued by the New England Water Environment Association.

EDUCATION

Ph.D. in Environmental Systems, School of Engineering, University of California, Merced (2013).

M.S. in Natural Resources, Concentration in Wastewater Utilization, Humboldt State University (2007).

B.S. in Natural Resources, Concentration in Soil and Water Conservation, Biology minor, University of Maine (2002).

Certificate in Pollution Abatement Technology, Concentration in Wastewater Treatment, Southern Maine Technical College (1998).

PUBLICATIONS

Wiley, P., L. Harris, S. Reinsch, S. Tozzi, T. Embaye, K. Clark, B. McQuin, Z. Kolber, R. Adams, H. Kagawa, T.M.J. Richardson, J. Malinowski, C. Beal, M. Claxton, E. Geiger, J. Rask, J.E. Campbell and J. Trent (2013). Microalgae cultivation using offshore membrane enclosures for growing algae (OMEGA). *J. Sustainable Bioener. Sys.* 3 (1), 18-32.

Harris, L., S. Tozzi, **P. Wiley**, C. Young, J. Richardson, K. Clark, J. Trent (2013). Potential impact of biofouling on the proposed offshore membrane enclosures for growing algae (OMEGA). *Bioresour. Technol.* Under review.

Trent, J., **P. Wiley**, S. Tozzi, B. McQuin, S. Reinsch (2012). The future of biofuels: is it in the bag? *Biofuels.* 3 (5), 511-513.

Malinowski, J., E.J. Geiger, **P. Wiley**, J. Trent (2012). Wireless ISFET pH sensor network for offshore microalgae cultivation. *Proceedings of the ASME 2012 International Mechanical Engineering Congress & Exposition.*

- Wiley, P.E.**, J.E. Campbell, B. McQuin (2011). Production of biodiesel and biogas from algae: A review of process train options. *Water Environ. Res.* 83 (4), 326-338.
- Wiley, P.E.**, K.J. Breneman, A.E. Jacobson (2009). Improved algal harvesting using suspended air flotation. *Water Environ. Res.* 81 (7), 702-708.
- Wiley, P.E.** (2007). Incorporation of wastewater harvested algae into three-phase compression ignition emulsion fuels. Master's thesis, Humboldt State University Library.
-

PRESENTATIONS

- Wiley, P.E.** (2012). Microalgae cultivation and wastewater treatment using offshore membrane enclosures for growing algae (OMEGA). University of California, Merced Environmental Systems Seminar Series, Merced, CA.
- Strazisar, T., S. Ord, J. Trent, S. Reinsch, **P. Wiley**, S. Tozzi, E. Kolodziej, C. Beal (2012). Offshore membrane enclosures for growing algae (OMEGA) government day briefing. NASA Headquarters, Washington, DC.
- Wiley, P.E.** (2011). Cultivating energy using offshore membrane enclosures for growing algae (OMEGA). Distinguished Keynote Speaker, Rocky Mountain Association of Environmental Professionals Envirofest, Denver, CO.
- Wiley, P.E.**, R.M. Adams (2007). Incorporation of wastewater harvested algae into three-phase compression ignition emulsion fuels. California Water Environment Association Fall Conference, Redding, CA.
- Wiley, P.E.** (2007). Wastewater algae as a source of renewable energy. Humboldt State University, Department of Environmental Resources Engineering, International Development Technology graduate student presentation series, Arcata, CA.
- Wiley, P.E.** (2006). Green building and LEED certification. Organic Planet Festival, Eureka, CA.
-

ACADEMIC AWARDS

- 2012 NASA Education Associates Program (\$48,000)
2012 UC Merced Graduate Student General Fellowship (\$3,885)
2011 UC Merced Energy Research Institute Fellowship (\$9,000)
2011 California Water Environment Association Kirt Brooks Memorial Scholarship (\$1,000)
2010-2011 NASA Graduate Student Researcher Program Fellowship (\$28,000)
-

PROFESSIONAL MEMBERSHIPS

- Water Environment Federation
California Water Environment Association
Maine Wastewater Control Association
New England Water Environment Association

ABSTRACT OF THE DISSERTATION

Microalgae Cultivation using Offshore Membrane Enclosures for Growing Algae (OMEGA)

by

Patrick Edward Wiley

Doctor of Philosophy in Environmental Systems

University of California, Merced, 2013

Professor Thomas Harmon

Offshore Membrane Enclosures for Growing Algae (OMEGA) cultivate microalgae using wastewater contained in floating photobioreactors (PBRs) deployed in marine environments; thereby eliminating competition with agriculture for water, fertilizer, and land. The offshore placement in protected bays near coastal cities co-locates OMEGA with wastewater outfalls and sources of CO₂-rich flue gas on shore, while the seawater supports the PBRs, regulates temperature and can drive forward osmosis to concentrate nutrients and facilitate microalgal dewatering. To evaluate the feasibility of OMEGA, microalgae were grown on secondary-treated wastewater and simulated flue gas (8.5% CO₂ V/V) in a 110-liter prototype system tested in a seawater tank. The flow-through system consisted of tubular PBRs made of transparent linear low-density polyethylene, a gas exchange-harvesting column (GEHC), two pumps, and a custom supervisory control and data acquisition (SCADA) system. The PBRs contained

regularly spaced swirl vanes to impart a helical flow and improve mixing of the circulating culture. About 5% of the culture volume was diverted through the GEHC to remove dissolved oxygen (DO), provide supplemental CO₂, and harvest microalgae in a settling chamber. The SCADA system controlled CO₂ injection and recorded DO levels, totalized CO₂ flow, temperature, circulation rates, photosynthetic active radiation (PAR), and the photosynthetic efficiency as determined by fast repetition rate fluorometry. In two experimental trials, totaling 23 days in April and May 2012, microalgal productivity averaged $14.1 \pm 1.3 \text{ g m}^{-2} \text{ day}^{-1}$ (n = 16), supplemental CO₂ was converted to biomass with >50% efficiency, and >90% of the ammonia-nitrogen was recovered from secondary effluent.

Experimental data collected during prototype evaluation clearly demonstrated that the accumulation of marine biofouling on the PBR tubes strongly suppressed rates of microalgal photosynthesis, as biofouled PBRs consumed less CO₂ than clean PBRs. These results suggest that any OMEGA deployment must have means to remove or prevent biofouling from accumulating on the surface of PBRs. This work also presents preliminary data regarding the use of energy-efficient electrochemical harvesting processes appropriate for the OMEGA configuration presented here. If OMEGA can be optimized for energy efficiency and scaled-up economically, it has the potential to contribute significantly to biofuels production and wastewater treatment.

Chapter 1: Introduction

1.1 Microalgae as a Biofuel Feedstock

The production of renewable fuels is becoming increasingly important as the supply of petroleum reserves diminish and environmental consequences resulting from fossil fuel combustion become more severe. Fuels produced from biomass have the potential to reduce reliance on petroleum resources and reduce greenhouse gas (GHG) emissions. However, Fargione et al. (1) and Searchinger et al. (2) reported that land use practices, such as clearing carbon-rich forests for biofuel production, might actually increase GHG emissions when compared with emissions released from fossil fuel combustion. Additionally, the use of arable land for biofuel production could negatively affect the global food supply (3).

Microalgae are currently under consideration as a significant source of sustainable biofuels because of their high photosynthetic efficiency, fast growth rates and seemingly large capacity to produce oil that can be readily transformed into fuel (4-9). Mata et al. (7) identified over 40 strains of microalgae capable of accumulating lipid content ranging from 2 to 75% by mass that can be extracted and transformed into liquid transportation fuels. These microscopic, single-celled organisms can be cultivated on non-arable land, using saline, brackish, or wastewaters that have few competing uses (7, 8, 10-13), lessening competition with agriculture and thus giving them an advantage over other biofuel crops (4, 13, 14). On the other hand, microalgae require fertilizer and supplemental carbon dioxide (CO₂) for optimal growth, which can generate more environmental pollution and GHG emissions than cultivation of more traditional biofuel feedstocks, such as switchgrass, canola and corn (15-17). Several authors have noted that these environmental drawbacks can be ameliorated by linking microalgae cultivation to wastewater treatment plants (to provide water and nutrients) and flue gas sources (to provide CO₂) (16, 18-20). It has also been shown that an overall net positive energy return on investment (EROI) can be realized when microalgal cultivation systems are combined with wastewater treatment processes for the purpose of nutrient recovery (15, 21). Accordingly, there is growing consensus that any large-scale microalgal cultivation system must be linked to wastewater treatment to establish economic feasibility and reduce the GHG emissions (16, 18, 22).

1.2 Combining Microalgae Cultivation with Wastewater Treatment

The two techniques for microalgal cultivation are raceway pond systems and photobioreactors (PBRs). A raceway pond is a continuously operated, closed-loop recirculation channel typically constructed of concrete or compacted earth (4). A paddlewheel is used to drive water around the circuit and keep the microalgae in a well-mixed suspension. (13, 23, 24). Raceway systems are inexpensive to construct and easy to operate, but must be situated on flat land and have large surface area requirements due to shallow culture depths (15-30 cm) necessary to ensure adequate solar exposure (9, 13, 24). As raceway ponds have a large surface area openly exposed to the surrounding

environment, they experience large evaporative losses and are easily contaminated with organisms capable of reducing culture viability and suppressing microalgal yields (7, 25, 26).

In contrast, PBR systems cultivate microalgae in bags, tubing, or other transparent materials that are not exposed directly to the atmosphere (13, 27). As the microalgae are grown in a closed system, there are fewer concerns regarding species contamination and evaporative losses when compared with open raceway pond systems (28, 29). Several PBR configurations, including tubular (13, 30, 31), flat plate (13, 32, 33) and fence-like (4) have been proposed to maximize surface to volume ratios and provide greater solar exposure than cultures grown in raceway systems. As a result, the concentration of microalgal biomass grown in PBR systems is expected to be greater than that realized using raceway ponds. However, Lee et al. (34) cited numerous publications reporting PBR productivities within the range achievable in open ponds. This inhibition of microalgal growth is likely caused by the photo-oxidative destruction of microalgal cells due to the accumulation of photosynthetically generated oxygen well beyond saturation levels within the PBR system (4, 35). Because the dissolved oxygen cannot be removed inside the tubes, this situation must be remediated by pumping the culture through degassing vessels (4, 35, 36). Furthermore, external cooling or heat exchangers are needed to prevent excessive temperatures within the PBR system (4). The high operating and construction cost of PBR systems may limit their application for large-scale production of low value products, such as biofuel feedstocks (13, 24).

To obtain the maximum EROI, any microalgae cultivation operation must be in close proximity to the wastewater treatment plant to minimize expenses associated with transporting wastewater long distances to the microalgal production facility (21, 37). However, the practical feasibility of co-locating traditional microalgal cultivation systems with wastewater treatment is questionable, as many existing wastewater facilities capable of supporting large-scale microalgal production are deeply embedded within the urban infrastructure and do not have the land resources needed to support such a facility (21). It is also not practical to relocate existing wastewater treatment plants to accommodate microalgal cultivation facilities. Thus, it is not possible to co-locate large-scale microalgae cultivation systems with established urban wastewater treatment facilities using conventional approaches. For coastal cities, however, which use offshore wastewater outfalls, a system of floating PBRs called Offshore Membrane Enclosures for Growing Algae (OMEGA) may resolve these difficulties.

1.3 The OMEGA Concept

The OMEGA system is designed to grow freshwater microalgae in flexible, clear, plastic PBRs attached to a floating infrastructure anchored offshore in protected bays (21, 37-39) (**Figure 1.1**). During operation, treated final plant effluent (FPE) discharged from existing wastewater outfall pipes would be diverted into the PBRs, providing water and nutrients needed to sustain microalgal growth. This approach is advantageous because the offshore placement eliminates the need for terrestrial resources and allows

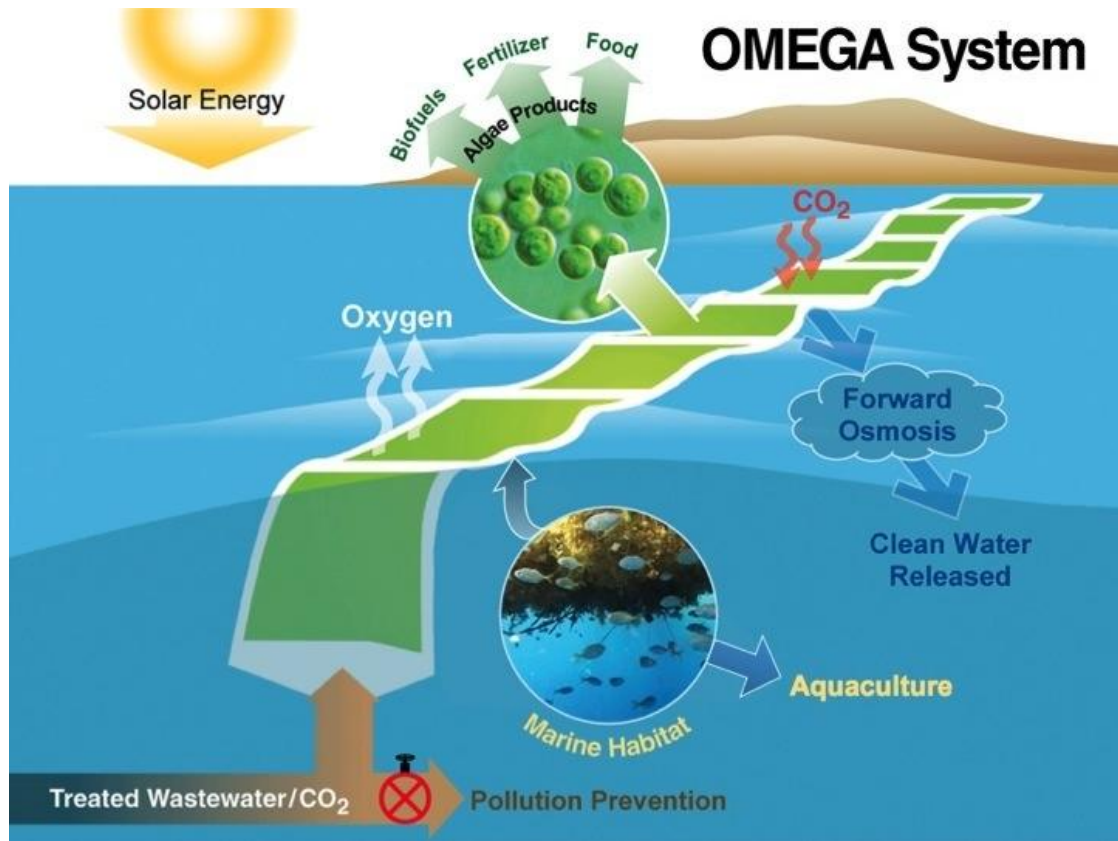


Figure 1.1. The OMEGA system cultivates microalgae using wastewater contained in PBR modules deployed offshore. This approach eliminates competition with agriculture for land and nutrients, while enabling co-location with large wastewater treatment facilities constructed in coastal urban areas. The surrounding ocean water provides structural support, temperature regulation and could produce a “simulated reef” that enriches local species diversity. The osmotic gradient between the PBR contents and the surrounding seawater can be used to drive forward osmosis, which is effective at concentrating nutrients, dewatering microalgae and producing clean water.

the system to be in close proximity to wastewater treatment plants and sources of flue gas, removing the need to pump these wastes long distances to remote locations where land resources for microalgae cultivation may be available. By using wastewater for water and nutrients and by not using arable land the OMEGA system avoids competing with agriculture or disrupting urban infrastructure in the vicinity of wastewater treatment plants.

Another advantage of the OMEGA system is that cooling and structural support are provided by the ocean, rather than with expensive mechanical components that are typical of conventional PBRs (37). Additionally, the osmotic gradient between the freshwater inside the PBRs and the surrounding seawater can be used to drive forward osmosis (FO). An FO system consists of a salt rejecting and water permeable membrane that is placed between two solutions of different osmotic pressures (40). In the case of

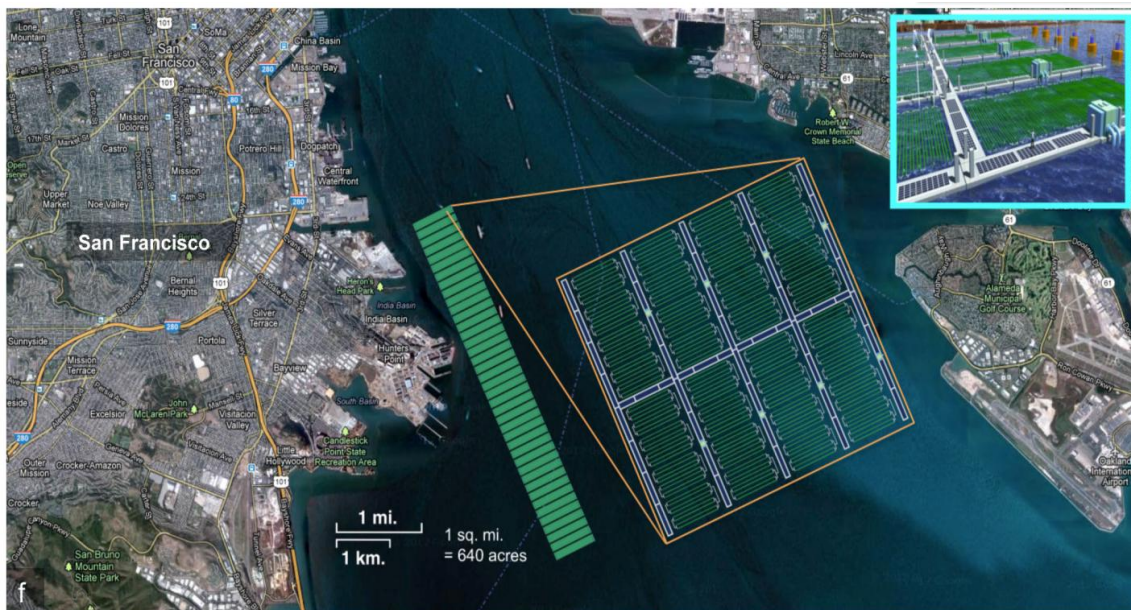


Figure 1.2. A hypothetical OMEGA deployment in the San Francisco Bay. This deployment, co-located with the San Francisco Southeast Wastewater Treatment Plant, has the capacity to accept five days of wastewater discharged from the facility ($1.23 \times 10^6 \text{ m}^3$) as a source of water and nutrients for microalgae cultivation and occupies approximately 11 km^2 . The inset in the blue box shows the floating infrastructure needed to support the OMEGA deployment.

OMEGA, the FO membranes would be built into the surface of the PBR. The freshwater FPE “feed solution” inside the PBR would permeate through the membrane to the more concentrated seawater “draw solution”, thereby dewatering the microalgae, concentrating nutrients while discharging clean water from the OMEGA modules (21, 37, 40-43).

On a scale relevant to biofuels, OMEGA will be intrusive in the marine environment, although the footprint of a full-scale OMEGA deployment will depend on the volume of wastewater utilized. When using the Southeast Wastewater Treatment Plant located in San Francisco (SF SEP) as a hypothetical example, the estimated footprint of an OMEGA system capable of utilizing the daily FPE discharge $246,000 \text{ m}^3$ would be approximately 11 km^2 , assuming a five-day detention time (**Figure 1.2**). It is obvious that to build a microalgae production facility of this size on land adjacent to the SF SEP would impact roads, freeways, bridges, buildings, and many homes. However, offshore, it occupies $<1\%$ of the surface area of San Francisco Bay, it would be in close proximity to the wastewater treatment plant and could use the existing outfall infrastructure.

An OMEGA deployment of this scale may also have beneficial effects for coastal communities. The OMEGA system would remove nutrients from the wastewater that is currently discharged into coastal waters and may thereby mitigate “dead-zone” formation. The infrastructure would provide substrate, refugia, and habitat for an extensive community of sessile and associated organisms (44). It is known that

introduced surfaces in the marine environment become colonized and can form “artificial reefs” or act as “fish aggregating devices,” which increase local species diversity and expand the food web (45, 46). A large-scale deployment of OMEGA systems may also act as floating “turf scrubbers” and function to absorb anthropogenic pollutants, improving coastal water quality (47).

Despite the apparent advantages of the OMEGA concept, the technical feasibility and performance metrics of the OMEGA concept have yet to be evaluated at any scale. This research addresses these knowledge gaps and advances the OMEGA concept through the development, construction and evaluation of a prototype 110-liter OMEGA system deployed in a simulated marine environment. The prototype system was inoculated using freshwater microalgae and secondary-treated wastewater as growth media and monitored to assess the potential of the OMEGA concept as a microalgal cultivation system and wastewater treatment process.

1.4 Dissertation Outline

This chapter highlights the advantages of microalgal biofuels and describes how cultivation must be linked to wastewater treatment processes to provide a positive EROI and reduce GHG emissions. This chapter also describes the traditional approaches to microalgal cultivation and how these techniques cannot be co-located with large existing wastewater treatment facilities due to the limited available space in urban areas. The OMEGA concept is introduced as a solution to these obstacles due to the offshore location and other advantages associated with deployment in marine environments are described.

Chapter 2 focuses on the engineering of a 110-liter prototype system with emphasis on the construction and components of the PBR system and the gas exchange and harvesting column used harvest from the system and inject supplementary CO₂. This chapter also describes the sensors used to drive the process control logic for the OMEGA deployment and details the supervisory control and data acquisition system designed to provide a high degree of operator control, enable autonomous operation and log process data.

Chapter 3 presents the performance data collected during continuous operation of the OMEGA prototype for 23 days during April and May 2012. Nutrient recovery from FPE, microalgal areal productivity, CO₂ utilization efficiency and photoconversion efficiency were metrics used to assess the viability of the OMEGA concept as microalgal cultivation system and as a nutrient recovery process for wastewater treatment.

Chapter 4 discusses the future of the OMEGA concept and identifies areas needing more research to advance the technology. This includes an assessment of marine biofouling on the microalgal photosynthesis within the PBR modules and suggests improvements that can be made to the existing harvesting approach using a low-energy, automated electrochemical harvesting system. The chapter concludes with a general discussion of broader research needs including structural engineering and PBR manufacturing challenges.

1.5 Acknowledgements

Material in this chapter has appeared in the following publications:

- P. Wiley *et al.*, Microalgae cultivation using offshore membrane enclosures for growing algae (OMEGA). *Journal of Sustainable Bioenergy Systems* 3, 18 (2013).
- P. E. Wiley, J. E. Campbell, B. McKuin, Production of Biodiesel and Biogas from Algae: A Review of Process Train Options. *Water Environment Research* 83, 326 (2011).
- J. Trent, P. Wiley, S. Tozzi, B. McKuin, S. Reinsch, Research Spotlight: The future of biofuels: is it in the bag? *Biofuels* 3, 521 (2012).

The author thanks the NASA Ames Research Center and Jonathan Trent for granting permission to use images used in **Figures 1.1** and **1.2**.

1.6 References

1. J. Fargione, J. Hill, D. Tilman, S. Polasky, P. Hawthorne, Land clearing and the biofuel carbon debt. *Science* 319, 1235 (2008).
2. T. Searchinger *et al.*, Use of US croplands for biofuels increases greenhouse gases through emissions from land-use change. *Science* 319, 1238 (2008).
3. D. Johansson, C. Azar, A scenario based analysis of land competition between food and bioenergy production in the US. *Climatic Change* 82, 267 (2007).
4. Y. Chisti, Biodiesel from microalgae. *Biotechnology Advances* 25, 294 (2007).
5. G. C. Dismukes, D. Carrieri, N. Bennette, G. M. Ananyev, M. C. Posewitz, Aquatic phototrophs: efficient alternatives to land-based crops for biofuels. *Current Opinion in Biotechnology* 19, 235 (2008).
6. S. Mandal, N. Mallick, Microalga *Scenedesmus obliquus* as a potential source for biodiesel production. *Applied Microbiology and Biotechnology* 84, 281 (2009).
7. T. Mata, A. Martins, N. Caetano, Microalgae for biodiesel production and other applications: A review. *Renewable and Sustainable Energy Reviews* 14, 217 (2010).
8. V. H. Smith, B. S. M. Sturm, F. J. Denoyelles, S. A. Billings, The ecology of algal biodiesel production. *Trends in Ecology & Evolution* 25, 301 (2010).
9. L. Lardon, A. Hélias, B. Sialve, J. Steyer, O. Bernard, Life-Cycle Assessment of Biodiesel Production from Microalgae. *Environmental Science & Technology* 43, 6475 (2009).
10. S. Aaronson, Z. Dubinsky, Mass production of microalgae. *Cellular and Molecular Life Sciences* 38, 36 (1982).
11. W. Oswald, Ponds in the twenty-first century. *Water Science & Technology* 31, 1 (1995).

12. P. Pienkos, A. Darzins, The promise and challenges of microalgal-derived biofuels. *Biofuels, Bioproducts and Biorefining* 3, 431 (2009).
13. Y. Shen, W. Yuan, Z. Pei, Q. Wu, E. Mao, Microalgae Mass Production Methods. *Transactions of the ASABE* 52, 1275 (2009).
14. M. Johnson, Z. Wen, Production of Biodiesel Fuel from the Microalga *Schizochytrium limacinum* by Direct Transesterification of Algal Biomass. *Energy & Fuels* 23, 294 (2009).
15. C. M. Beal *et al.*, Energy return on investment for algal biofuel production coupled with wastewater treatment. *Water Environment Research* 89, 692 (2012).
16. A. Clarens, E. Resurreccion, M. White, L. Colosi, Environmental Life Cycle Comparison of Algae to Other Bioenergy Feedstocks. *Environmental Science & Technology* 44, 1813 (2010).
17. A. F. Clarens, H. Nassau, E. P. Resurreccion, M. A. White, L. M. Colosi, Environmental impacts of algae-derived biodiesel and bioelectricity for transportation. *Environmental Science & Technology* 45, 7554 (2011).
18. T. Lundquist, I. Woertz, N. Quinn, J. Benemann, "A Realistic Technology and Engineering Assessment of Algae Biofuel Production" Energy Biosciences Institute, University of California, Berkeley, 2010.
19. J. Park, R. Craggs, A. Shilton, Wastewater Treatment High Rate Algal Ponds for Biofuel Production. *Bioresource Technology* 102, 35 (2011).
20. R. Levine, A. Oberlin, P. Adriaens, A Value Chain and Life Cycle Assessment Approach to Identify Technological Innovation Opportunities in Algae Biodiesel. *Nanotech* 3, 1 (2009).
21. J. Trent, P. Wiley, S. Tozzi, B. McQuin, S. Reinsch, Research Spotlight: The future of biofuels: is it in the bag? *Biofuels* 3, 521 (2012).
22. J. Park, R. Craggs, A. Shilton, Wastewater treatment high rate algal ponds for biofuel production. *Bioresource Technology* 102, 35 (2011).
23. D. Chaumont, Biotechnology of algal biomass production: a review of systems for outdoor mass culture. *Journal of Applied Phycology* 5, 593 (1993).
24. J. Sheehan, T. Dunahay, J. Benemann, P. Roessler, A look back at the US Department of Energy's Aquatic Species Program-Biodiesel from Algae. *Prepared for the US Department of Energy, Prepared by The National Renewable Energy Laboratory (NREL)*, (1998).
25. S. Chinnasamy, B. Ramakrishnan, A. Bhatnagar, K. Das, Biomass Production Potential of a Wastewater Alga *Chlorella vulgaris* ARC 1 Under Elevated Levels of CO₂ and Temperature. *International Journal of Molecular Sciences* 10, 518 (2009).

26. M. Packer, Algal capture of carbon dioxide; biomass generation as a tool for greenhouse gas mitigation with reference to New Zealand energy strategy and policy. *Energy Policy* 37, 3428 (2009).
27. F. Lehr, C. Posten, Closed photo-bioreactors as tools for biofuel production. *Current Opinion in Biotechnology* 20, 280 (2009).
28. C. Posten, G. Schaub, Microalgae and terrestrial biomass as source for fuels-A process view. *Journal of Biotechnology* 142, 64 (2009).
29. K. Yeang, Biofuel from Algae. *Architectural Design* 78, 118 (2008).
30. O. Pulz, Photobioreactors: production systems for phototrophic microorganisms. *Applied Microbiology and Biotechnology* 57, 287 (2001).
31. C. Ugwu, H. Aoyagi, H. Uchiyama, Photobioreactors for mass cultivation of algae. *Bioresource Technology* 99, 4021 (2008).
32. Q. Hu, H. Guterman, A. Richmond, A flat inclined modular photobioreactor for outdoor mass cultivation of photoautotrophs. *Biotechnology and Bioengineering* 51, 51 (1996).
33. K. Zhang, S. Miyachi, N. Kurano, Evaluation of a vertical flat-plate photobioreactor for outdoor biomass production and carbon dioxide bio-fixation: effects of reactor dimensions, irradiation and cell concentration on the biomass productivity and irradiation utilization efficiency. *Applied Microbiology and Biotechnology* 55, 428 (2001).
34. D. Lee, C. Jeon, J. Park, Biological nitrogen removal with enhanced phosphate uptake in a sequencing batch reactor using single sludge system. *Water Research* 35, 3968 (2001).
35. Y. Chisti, Biodiesel from microalgae beats bioethanol. *Trends in Biotechnology* 26, 126 (2008).
36. M. Tredici, P. Carlozzi, G. Chini Zittelli, R. Materassi, A vertical alveolar panel(VAP) for outdoor mass cultivation of microalgae and cyanobacteria. *Bioresource Technology* 38, 153 (1991).
37. M.O. P. Fortier, B. S. M. Sturm, A Geographic Analysis of the Feasibility of Collocating Algal Biomass Production with Wastewater Treatment Plants. *Environmental Science & Technology*, (2012).
38. J. Trent, in *International Workshop on Offshore Algae Cultivation*. Lolland, Denmark, 2009, pp. 274.
39. P. E. Wiley, J. E. Campbell, B. McKuin, Production of Biodiesel and Biogas from Algae: A Review of Process Train Options. *Water Environment Research* 83, 326 (2011).
40. P. Wiley *et al.*, Microalgae cultivation using offshore membrane enclosures for growing algae (OMEGA). *Journal of Sustainable Bioenergy Systems* 3, 18 (2013).

41. L. A. Hoover, W. A. Phillip, A. Tiraferri, N. Y. Yip, M. Elimelech, Forward with Osmosis: Emerging Applications for Greater Sustainability. *Environmental Science & Technology*, 9824 (2011).
42. P. Buckwalter, S. Gormly, T. Embaye, J. Trent, Harvesting Microalgae by Forward Osmosis. *The Open Energy and Fuels Journal*, (2010).
43. R. W. Holloway, A. E. Childress, K. E. Dennett, T. Y. Cath, Forward osmosis for concentration of anaerobic digester centrate. *Water Research* 41, 4005 (2007).
44. S. Zou, Y. Gu, D. Xiao, C. Y. Tang, The role of physical and chemical parameters on forward osmosis membrane fouling during algae separation. *Journal of Membrane Science* 366, 356 (2011).
45. L. Harris *et al.*, Potential impact of biofouling on the proposed offshore membrane enclosures for growing algae (OMEGA). *Bioresource Technology* Under review, (2012).
46. J. H. Bailey-Brock, Fouling community development on an artificial reef in Hawaiian waters. *Bulletin of Marine Science* 44, 580 (1989).
47. K. A. Dafforn, T. M. Glasby, E. L. Johnston, Comparing the Invasibility of Experimental “Reefs” with Field Observations of Natural Reefs and Artificial Structures. *PloS one* 7, e38124 (2012).
48. W. Mulbry, P. Kangas, S. Kondrad, Toward scrubbing the bay: Nutrient removal using small algal turf scrubbers on Chesapeake Bay tributaries. *Ecological Engineering* 36, 536 (2010).

Chapter 2: Development of an OMEGA Prototype System

2.1 Introduction

Maintaining stable and productive microalgal cultures outdoors beyond laboratory scale is challenging due to changing environmental conditions, growth of pathogens and microalgal predators that disrupt culture stability, and the lack of robust, rapid and automated monitoring and control systems capable of sustaining a healthy culture (1). To better understand the technical feasibility of the OMEGA concept a functional prototype system was developed and deployed in an outdoor seawater tank. The design criteria and target performance goals of the prototype system were to:

- 1) Sustain productive, viable microalgal cultures;
- 2) Maintain well-mixed cultures throughout the photobioreactor (PBR) system to maximize nutrient exchange rates and prevent development of anaerobic conditions;
- 3) Generate biomass yields comparable to other cultivation systems;
- 4) Effectively recover nutrients from secondary-treated wastewater final plant effluent (FPE);
- 5) Include efficient means of delivering supplemental CO₂; and
- 6) Have a monitoring and control system capable of providing autonomous operation and maintaining environmental conditions that favor microalgal growth.

The goal of this chapter is to describe the details and engineering aspects of the major components that comprise the OMEGA prototype system. This includes a description of the PBR tubes and the pumping system used to circulate the flow through the system. The experimental determination of the expected CO₂ mass transfer efficiency during prototype operation is also described. And finally, the placement of field sensors, their function and process control logic used by the supervisory control and data acquisition (SCADA) system for autonomous operation are discussed.

2.2 Prototype Development

An objective of the OMEGA project was to dewater microalgae, concentrate nutrients within the PBR and discharge clean water using forward osmosis (FO) membranes built into the PBR modules. FO is well suited for this application because the osmotic gradient between the freshwater in the PBR and the surrounding seawater drives the process (2). Early experimentation by OMEGA scientists confirmed the validity of this approach by quantifying microalgal dewatering rates (3) and demonstrating that nutrient concentration using FO can stimulate microalgal growth (**Figure 2.1**). However, issues related to membrane fouling and durability prevented this technology from being



Figure 2.1. Microalgae grown in FPE wastewater following nutrient concentration using an FO membrane. The 1X flask contains FPE that was not concentrated, while 2X and 3X have nutrient concentrations that were doubled and tripled, respectively. The increasing cell density due to higher nutrient availability is evidenced by the darker color of the flasks.

integrated larger prototype deployments. Instead, PBR tubes were constructed using either polyurethane or linear low-density polyethylene (LLDPE).

Early OMEGA prototypes consisted of PBR tubes with an internal “sparging” network to inject CO₂, strip excessive concentrations of photosynthetically generated dissolved oxygen (DO), and mix the culture (**Figure 2.2**). The approach was ultimately abandoned due to complicated construction and problems associated with venting and over-pressurization of the PBR. In addition to these engineering challenges, this type of PBR failed to sustain viable, well mixed microalgal cultures for more than a few days.

The final configuration selected to satisfy the design criteria and performance targets consisted of two closed (unvented) PBR tubes through which the microalgal culture was circulated. A portion of the culture was diverted from the PBR system to an external gas exchange and harvesting column (GEHC), where it received a supplemental CO₂ injection. Excess DO was removed and accumulated microalgal biomass was harvested from the system. This configuration was selected because the GEHC enhanced CO₂ mass transfer efficiency when compared the convention practice of sparging CO₂ into shallow cultures. The GEHC also greatly simplified PBR construction, by eliminating the need to incorporate gas distribution network *inside* the PBR modules. Furthermore, the GEHC could be completely isolated from the PBR, drained and refilled without disturbing the flow circulating through the PBR tubes, which made harvesting and refilling the system easy and uncomplicated. The prototype also featured a custom SCADA system capable of monitoring and controlling key process control parameters, logging data and providing autonomous system operation.

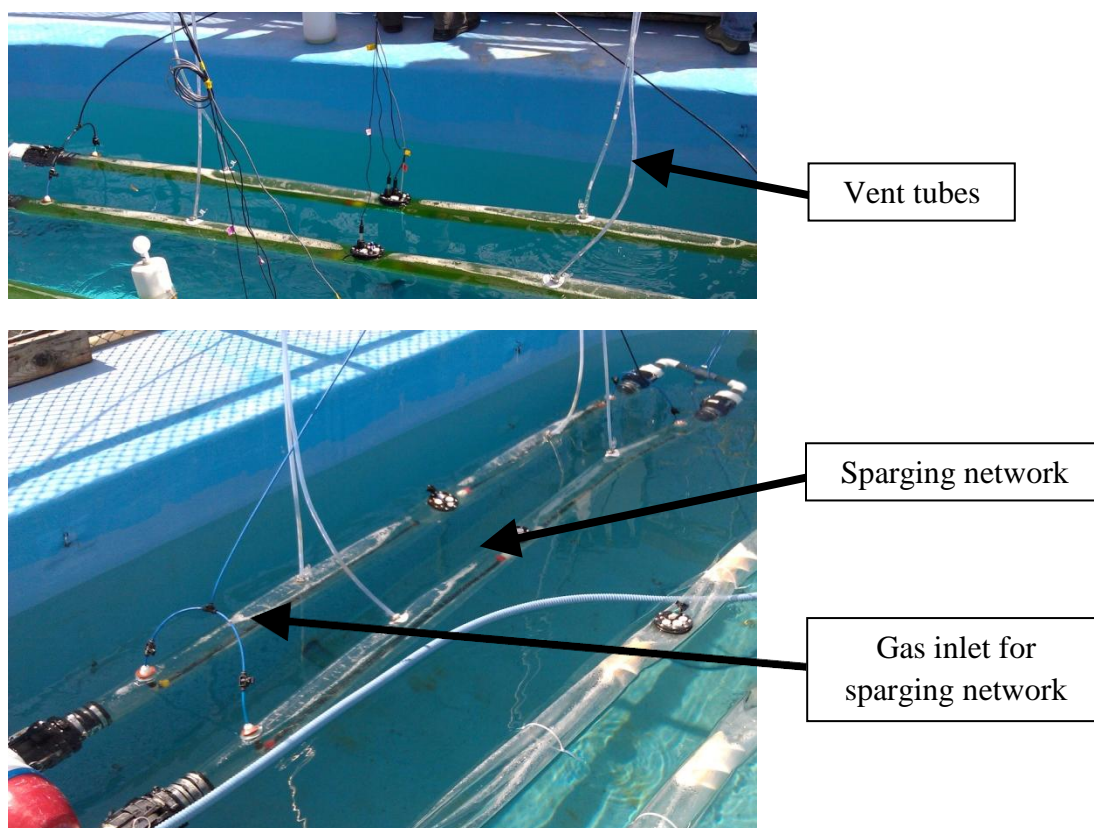


Figure 2.2. Early OMEGA prototype deployment with internal sparging network during leak testing with tap water (**Bottom**) and after inoculation with microalgae (**Top**). The sparging network was used to inject CO₂ and provide aeration intended to keep the microalgae suspended. This design was abandoned due to engineering challenges and difficulty in sustaining microalgal biology.

2.3 Photobioreactor (PBR) System

The OMEGA PBRs were constructed by welding sheets of 15-mil clear LLDPE into tubes (I.D. 11.4 cm × 3 m long) using an AIE double impulse foot heat sealer (Industry, CA). Each PBR tube contained swirl vanes that enhanced mixing by imparting a spiral flow pattern. The swirl vanes, improvised from polyethylene grain augers (Lundell Plastics Corporation, Odebolt, IA), were fixed inside a transparent schedule 40 polyvinyl chloride (PVC) collar (O.D. 11.4 cm × 5.1 cm long) with a steel pin. The sharp edges of the PVC collar were removed with a bench grinder to prevent damaging the LLDPE. The swirl vanes were spaced 0.9 m apart and held in place using cable ties wrapped around the collar on the outside of the PBRs (**Figure 2.3**).

The ends of the PBR tubes were attached to cam-lock fittings (Model 400D, Banjo Corporation, Crawfordsville, IN) and connected in series by a U-shaped manifold constructed of two schedule 40 PVC 90° elbows (10.2 cm). The 10.2-cm cam-lock

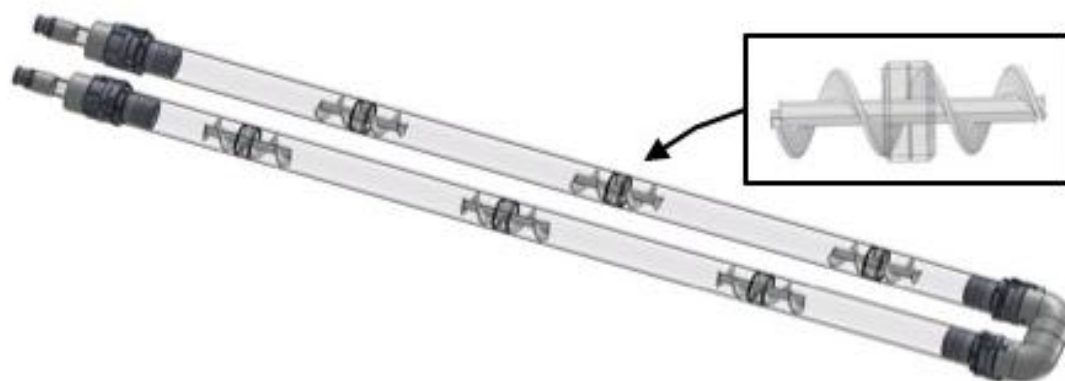


Figure 2.3. Illustration of OMEGA PBR tubes with swirl vanes. PBRs were made of flexible, clear LLDPE connected with cam-lock fittings to a U-shaped PVC manifold. The six swirl vanes (see insert enlargement) directed the flow into a helical path to improve mixing and light exposure of the microalgae.

fittings on the PBR inlet and outlet were reduced to 5.1 cm to accommodate the transparent flexible PVC tubing that was connected to the suction and discharge side of a centrifugal pump (Model 1MC1D5D0, ITT-Goulds, Seneca Falls, NY) (**Figure 2.3**). The speed of the centrifugal pump was adjusted using a 0.746 kW GS-2 variable frequency drive (Automation Direct, Cumming, GA) (**Figure 2.4**). A sensor manifold located before the pump inlet housed a paddlewheel flow meter (Model 2537, Georg Fischer LLC, Tustin, CA), pH probe (Model 2750, Georg Fischer LLC, Tustin, CA), and DO sensor (Sensorex, Garden Grove, CA) and provided connection to the GEHC (**Figure 2.5**).

2.4 Gas Exchange and Harvesting Column (GEHC)

Both carbon availability and pH control are dependent on efficient CO₂ delivery, and both are critical to the productivity and economics of large-scale microalgae cultivation (4-8). Beal *et al.* (9, 10) have shown that commercial CO₂ supply is one of the biggest contributors to overall energy use and cost of microalgal biofuel production. However, use of conventional sparging systems for gas injection typically results in 80-90% of the CO₂ being lost to the atmosphere due to limited gas-liquid contact time caused by shallow culture depths required to minimize light attenuation (11-13). Diffusion methods, using silicon membranes or hollow fibers reduce CO₂ loss to the atmosphere but are cost prohibitive and prone to biofouling (6, 12, 14, 15). In contrast, bubble columns, like the GEHC, are simple, low cost and capable of reducing CO₂ losses to less than 20% (11, 12).

The GEHC (**Figure 2.6**) used with the OMEGA prototype was designed to: (1) remove excess concentrations of photosynthetically-generated DO using an oxygen stripping device (OSD) based on a design by Barnhart (16), (2) supply CO₂ to the



Figure 2.4. VFDs used to control the pumping rate of the culture through the PBR tubes. Two independent prototype systems, each requiring a VFD, were constructed during the OMEGA project.

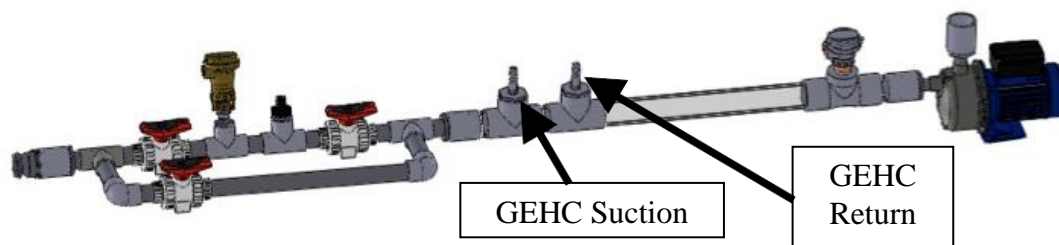


Figure 2.5. Sensor manifold for measuring pH, temperature, DO, and flow rate. The culture was pumped from the PBR past the sensors. Part of the circulating flow was diverted to the GEHC (see **Figure 2.6**) at the GEHC suction fitting by a positive displacement pump (not shown) and returned to the PBR flow at the GEHC return. The valved bypass was used to isolate the sensors for cleaning and maintenance without disrupting the overall circulation.

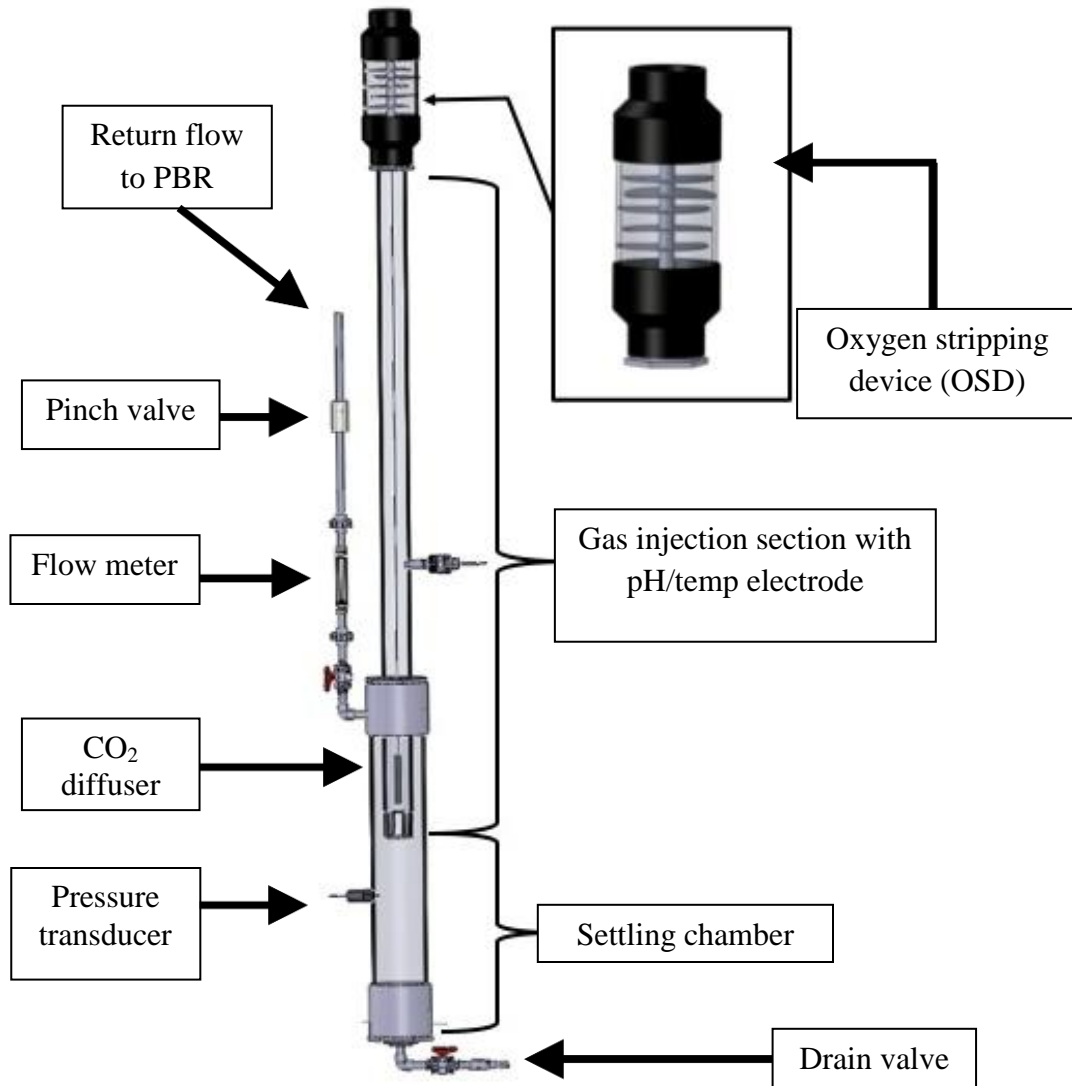


Figure 2.6. Gas exchange and harvesting column (GEHC) controls pH, removes settled microalgae and provides a location for wastewater addition into the PBR system. An oxygen stripping device (OSD, top) designed to remove excessive concentrations of photosynthetically generated dissolved oxygen was built into the GEHC. CO₂ is added by gas bubbles injected with the diffuser at a rate controlled by pH. Biomass collected in the settling chamber is removed, whereas suspended microalgae are returned to the PBR (return flow pipe, left). The pressure transducer controls a pinch valve position to maintain a consistent liquid level in the GEHC. The volume of the GEHC was periodically harvested from the drain valve at the bottom and replaced with wastewater to replenish nutrients in the PBRs.

microalgal culture and control pH, and (3) provide a settling chamber to collect aggregating microalgae for harvesting. A portion of the total system volume was diverted from the PBR to the GEHC using a 12 VDC SHUR-FLO diaphragm pump (Model 2088-343-135, SHUR-FLO, Costa Mesa, CA). The pumping rate into the GEHC was adjusted by changing the voltage setting on the variable DC power supply (Model HY3005D, Mastec Power Supply, San Jose, CA).

The culture from the PBR entered the GEHC through the OSD section and cascaded over five stacked PVC plates (20 cm² each) housed in a pipe (schedule 40 PVC: 15.2 cm diameter x 0.3 m) attached to the top of the GEHC with a rubber coupling (model 1056-63, Fernco Inc., Davidson, MI). After the OSD, the culture entered the gas injection section (schedule 40 clear PVC 7.6 cm diameter x 2.13 m), containing a CO₂ diffuser made from soaker hose (22 cm²) submerged 1.8 m in the culture medium. The compressed CO₂ source injected through the diffuser was a mixture of 8.5% CO₂ in air (V/V) to simulate the concentration of CO₂ in typical flue gas (17). A custom SCADA system (see section **2.5: Process Automation and Data Collection**) modulated the CO₂ injection rate based in the pH in the GEHC, which was measured using GF Signet model 2750 pH sensor electronics (Georg Fischer LLC, Tustin, CA).

After the gas injection section, the culture entered the settling chamber, which consisted of a section of clear pipe (schedule 40 PVC 15.2 cm diameter x 0.91 m) with a ball valve (1.3 cm) drain at the bottom. The cultured entered from the gas injection pipe, which protruded 0.3 m into the settling chamber, and was capped to direct the outflow to the sides and prevent resuspending biomass collected at the bottom of the chamber. The culture returned to the PBRs from the settling chamber through a pipe (schedule 80 PVC 1.3 cm diameter) with a flow meter (model F-40377LN-8, Blue-White Industries LTD, Huntington Beach, CA) and a pneumatic pinch valve (1.3 cm VMP Series, AKO Armaturen & Separations GmbH, Germany). The pinch valve maintained a constant liquid height in the GEHC using a feedback signal generated by a pressure transducer (model PTD25-10-0015H, Automation Direct, Cumming, GA) in the settling chamber (see section **2.5: Process Automation and Data Collection**).

2.4.1 Predicting GEHC Gas Injection Rate and CO₂ Mass Transfer Efficiency

The CO₂ mass transfer efficiency of the GEHC refers to the amount of CO₂ dissolved into solution versus the quantity injected. Maximizing the CO₂ mass transfer efficiency is advantageous because it limits losses of CO₂ to the atmosphere and reduces operating costs. A factor influencing the GEHC mass transfer efficiency is the gas injection rate capable of delivering enough inorganic carbon to sustain the desired level of microalgal productivity. For the OMEGA prototype, a target productivity of 20 g m⁻² day⁻¹ was selected based on average performance numbers cited by Putt *et al.* (12). Within this yield, several authors have noted that carbon content of microalgal biomass is approximately 50% carbon (5, 18, 19), a value corroborated by elemental analysis of the microalgae grown in the OMEGA system (data not shown). These values, together with a 2× overdesign factor, were used in **Equation 2.1** to estimate a peak gas injection rate of 0.5 lpm into the GEHC.

$$Q_{\text{Gas}} = \frac{P_{\text{Algae}} \cdot f_{\text{Carbon}} \cdot A_{\text{PBR}} \cdot RT}{D_{\text{Solar}} \cdot \frac{60 \text{ min}}{\text{hr}} \cdot M_{\text{Car}} \cdot p_{\text{CO}_2}} \quad (2.1)$$

Where,

Q_{Gas}	= Peak gas flow rate, lpm
P_{Algae}	= Microalgal productivity, $\text{g m}^{-2} \text{ day}^{-1}$
f_{Carbon}	= Fraction carbon of microalgal biomass, 0.5
A_{PBR}	= PRB area, m^2
R	= Ideal gas constant, $0.008206 \text{ mol l}^{-1} \text{ atm}^{-1}$
T	= Temperature, K
D_{Solar}	= Length of solar day, hours
M_{Car}	= Carbon molar mass, g mol^{-1}
p_{CO_2}	= CO_2 partial pressure, atm

In addition to gas injection rates, the mass transfer efficiency of the GEHC is highly dependent upon the column height and pH of the solution. The impact of these variables on mass transfer efficiency were determined experimentally for six different GEHC water column levels (0.3 m, 0.6 m, 0.9 m, 1.8 m, 2.1 m or 2.7 m) using a transparent PVC test column (3 m \times 7.6 cm) and tap water, pH adjusted to >11.00 with NaOH. The tap water solution was prepared in a plastic barrel and weighed using an Ohaus Defender scale (Ohaus Corporation, Pine Brook, NJ). The mass of water corresponding to the desired liquid height was transferred from the barrel and added to the test column.

A precision rotometer (Model WU-03218-52, Cole Palmer, Vernon Hills, IL) calibrated with an Agilent ADM1000 Flowmeter (Agilent Technologies Inc., Wilmington, DE) was used to inject the simulated flue gas at 0.5 lpm (from **Equation 2.1**) through a diffuser (previously described) lowered to the bottom of the test column. The mass of CO_2 dissolved into the NaOH solution was based on the stoichiometry of the acid-base reaction relationship between the NaOH and H_2CO_3^* described in **Equations 2.2** and **2.3**.



The total moles of CO_2 injected into the test column were determined using **Equation 2.4**, which enabled calculation of the mass transfer efficiency with **Equation 2.5**. For this experiment, the mass transfer efficiency was calculated based on the amount of CO_2 required to change the pH of the solution from 10 to 9, 9 to 8, 8 to 7 and below 7.

$$M_{\text{CO}_2} = \frac{Q \cdot t \cdot p_{\text{CO}_2}}{RT} \quad (2.4)$$

Where,

M_{CO_2}	= Moles CO ₂ injected into solution
Q	= Gas flow rate, lpm
t	= Time, minutes
p_{CO_2}	= CO ₂ partial pressure, atm
R	= Ideal gas constant, 0.008206 mol l ⁻¹ atm ⁻¹
T	= Temperature, K

$$\text{CO}_{2\text{Eff}} = \frac{M_{\text{NaOH}}}{2M_{\text{CO}_2}} (100) \quad (2.5)$$

Where,

$\text{CO}_{2\text{Eff}}$	= Mass transfer efficiency, %
M_{NaOH}	= Moles of NaOH
M_{CO_2}	= Moles CO ₂ injected into solution

Results obtained from the test column indicated that higher pH and a taller column height increased CO₂ mass transfer efficiency (**Figure 2.7**). In the OMEGA system tested here, however, site restrictions limited the gassing portion of the GEHC to 1.8 meters, which gave a mass transfer efficiency of approximately 50% for the operating pH range in the GEHC, which was expected to range between 7.60 and 7.80. Larger scale OMEGA deployments can utilize a taller column, which improves mass transfer efficiency due to the increased to gas-liquid contact time. Additionally, selection of a diffuser capable of generating smaller bubbles will also facilitate improved mass transfer efficiency by providing a greater bubble surface-to-volume ratio.

2.4.2 Balancing Carbon Consumption in the PBR with Carbon Injection in the GEHC

Balancing the CO₂ mass transfer rate in the GEHC with the carbon consumption rate of microalgae in the PBR is necessary to prevent conditions of carbon limitation in the system. A comparison of the CO₂ mass transfer rate in the GEHC and carbon consumption rate of microalgae in the PBR gives a “detention time ratio” that estimates the amount of time the culture can remain in the PBR before carbon replenishment is needed. The overall mass transfer coefficient ($K_L a$) and subsequent CO₂ mass transfer rate in the GEHC were calculated from the GEHC test column titration data using **Equations 2.6** and **2.7**, whereas the carbon uptake rate in the PBR was approximated with **Equation 2.8**.

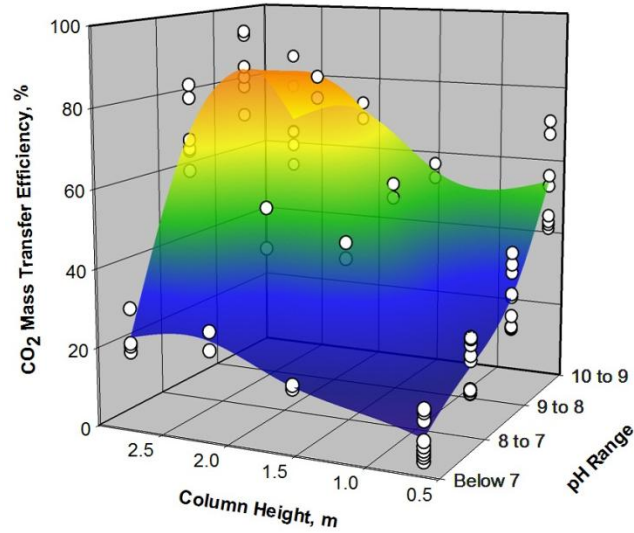


Figure 2.7. Efficiency of CO₂ mass transfer in the GEHC relative to the height of the column and the pH of the solution. Data were obtained (n = 76) experimentally using tap water, pH adjusted (>11.00) with NaOH. For practical reasons a maximum column height of 1.8 meters was used for the functional OMEGA prototype system.

$$K_L a = \ln \frac{C^* - C_2}{C^* - C_1} \quad t_2 - t_1 \quad (2.6)$$

Where,

$K_L a$	= Overall mass transfer coefficient, minutes
C^*	= Equilibrium total carbon concentration, mol l ⁻¹
C	= Total carbon concentration, mol l ⁻¹
t	= Time, minutes

$$\frac{dc}{dt} = K_L a (C^* - C) \quad (2.7)$$

Where,

$\frac{dc}{dt}$	= Carbon injection rate, mol l ⁻¹ min ⁻¹
$K_L a$	= Overall mass transfer coefficient, minutes
C^*	= Equilibrium total carbon concentration, mol l ⁻¹
C	= Total carbon concentration, mol l ⁻¹

$$C_{\text{Uptake}} = \frac{P_{\text{Algae}} \cdot f_{\text{Carbon}} \cdot A_{\text{PBR}}}{D_{\text{Solar}} \cdot \frac{60 \text{ min}}{\text{hr}} \cdot M_{\text{Car}} \cdot \text{PBR}_{\text{Vol}}} \quad (2.8)$$

Where,

C_{Uptake}	= Microalgal carbon uptake, $\text{mol l}^{-1} \text{min}^{-1}$
P_{Algae}	= Microalgal productivity, $\text{g m}^{-2} \text{day}^{-1}$
f_{Carbon}	= Fraction carbon of microalgal biomass, 0.5
A_{PBR}	= PRB area, m^2
D_{Solar}	= Length of solar day, hours
M_{Car}	= Carbon molar mass, g mol^{-1}
PBR_{Vol}	= PBR volume, l

Plotting the natural log of the change in total carbon absorbed between pH 7.5 and 9.0 in a 1.8 meter column using a gas injection rate of 0.5 lpm over time from **Equation 2.6** produced a strong correlation coefficient ($r^2 > 0.99$, $n = 3$) (**Figure 2.8**) and resulted in an estimated K_{La} of 0.21 min^{-1} (SE 0.01, $n = 3$). The corresponding CO_2 mass transfer rate of $1.69 \times 10^{-4} \text{ mol l}^{-1} \text{min}^{-1}$ (SE 1.03×10^{-5} , $n = 3$) was determined with **Equation 2.7**, while the carbon consumption rate in the PBR calculated from **Equation 2.8** was estimated to be $8.72 \times 10^{-6} \text{ mol l}^{-1} \text{min}^{-1}$, which is very close to values obtain by Putt et al.(12) using a similar approach. Dividing the mass transfer rate in the GEHC by the carbon consumed by microalgae indicates that the culture would require one minute in the GEHC for every 20 minutes in the PBR. Therefore, 5 lpm (4.5% total system volume per minute) were diverted from the PBR to the GEHC for gas exchange. This pumping rate provided the GEHC with an overdesign factor of 1.5 to ensure that carbon consumption in the PBR did not exceed the injection capacity in the GEHC and limit microalgal growth.

2.5 Process Automation and Data Collection

A custom SCADA system was constructed for process automation and data logging. The SCADA system consisted of numerous field sensors and instruments that measured pH, temperature, pressure, DO, PBR culture circulation rate, photosynthetically active radiation (PAR) and GEHC gas injection rate of the prototype deployment (**Table 2.1**). Temperature and pH sensors installed in the PBR and GEHC were connected to a GF Signet model 8900 multi-parameter transmitter (Georg Fischer LLC, Tustin, CA) that generated a 0-10 VDC output signal for each measurement. The output signals from the transmitter and other field sensors were connected to the inputs of DL06 programmable logic controllers (PLCs) (Automation Direct, Cumming, GA) (**Figure 2.9**) contained in weather-proof electrical enclosures (**Figure 2.10**). A process control algorithm, written with DirectSoft 5 software (Automation Direct, Cumming, GA), uploaded to the PLCs transferred data to a human-machine interface (HMI) created using LookoutDirect software (Automation Direct, Cumming, GA) that was accessed using a laptop computer. The HMI was central to the operation of the OMEGA prototype system because it displayed real-time data, historical data trending, and enabled operators to specify setpoints that controlled the liquid level and pH in the GEHC (**Figure 2.11**).

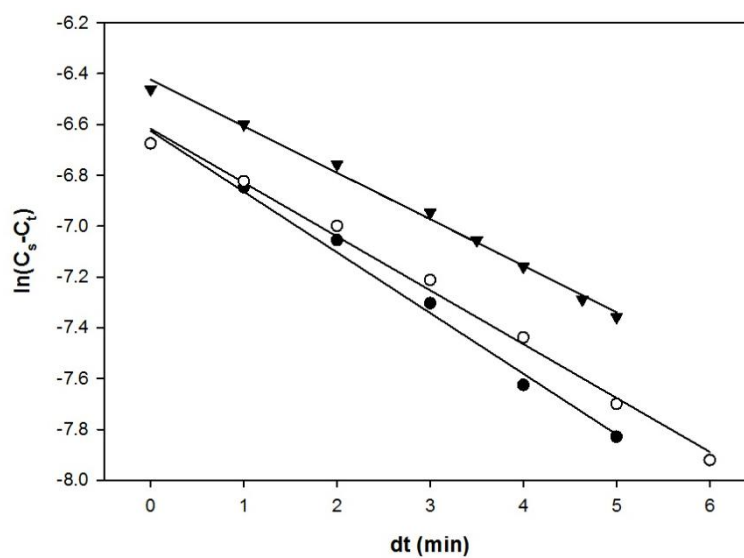


Figure 2.8. The natural log of total carbon absorbed by the NaOH solution between pH 7.5 and 9.0 as a function of time. The three experimental trials were conducted using a column height of 1.8 meters and a gas flow rate of 0.5 lpm of 8.5% CO₂. These parameters were selected because they were expected to closely mimic operating conditions of the OMEGA prototype. These data enabled determination of the CO₂ mass transfer rate, which is required to estimate the GEHC recycle rate.

Table 2.1. Description and location of field sensors connected to the SCADA system for data logging and process control.

Sensor	Manufacturer and Model Number	Input Signal	Output Signal	Scale	Location	Function
Pressure Transducer	Automation Direct, Model PTD25-10-0015H	none	0-10 VDC	0-15 psi	PBR Manifold	Measured pressure within the PBR modules.
Pressure Transducer	Automation Direct, Model PTD25-10-0015H	none	0-10 VDC	0-15 psi	GEHC	Measured head pressure in the GEHC to determine liquid level. PID loop used to modulate I/P transducer, which operated pneumatic pinch valve to maintain desired liquid level in the GEHC.
Mass Flow Controller	Aalborg Model GFC17S-VADL2-COA	0-5 VDC	0-5 VDC	0-5 lpm	Control Cabinet A	Provided "on-demand" CO ₂ injection in the GEHC. Injection rate controlled by PID loop using pH in the GEHC. Output signal used to totalize CO ₂ flow.
PAR	LI-COR LI-190 Quantum Sensor	none	4-20 mA	0-3,000 $\mu\text{E m}^{-2} \text{sec}^{-1}$	Seawater Tank	Measured surface PAR next to PBR modules
Flow Meter	GF Signet Model 2537	none	4-20 mA	0-50 gpm	Sensor Manifold	Measured circulation rate in the PBR.
pH Sensor	GF Signet Model 2750 (combined with temperature sensor)	none	0-10 VDC	0-14	Sensor Manifold and GEHC	Measured pH in the GEHC and in the circulating PBR flow. GEHC measurement used by PID loop to control CO ₂ injection rate.
Temperature Sensor	GF Signet Model 2750 (combined with pH sensor)	none	0-10 VDC	0-50 C	Sensor Manifold and GEHC	Measured temperature in the GEHC and in the circulating PBR flow.

Current Pressure (I/P) Transducer	OMEGA Engineering, Model IP610-060-D	4-20 mA	none	0-450 kPa	Control Cabinet B	Modulated air pressure output to the pneumatic pinch valve used to maintain GEHC liquid level.
DO Sensor	Sensorex, Craig Ocean System	none	0-5 VDC	0-212%	Sensor Manifold	Measured DO concentration of the culture exiting the PBR modules. Data logged by Craig Ocean systems database.

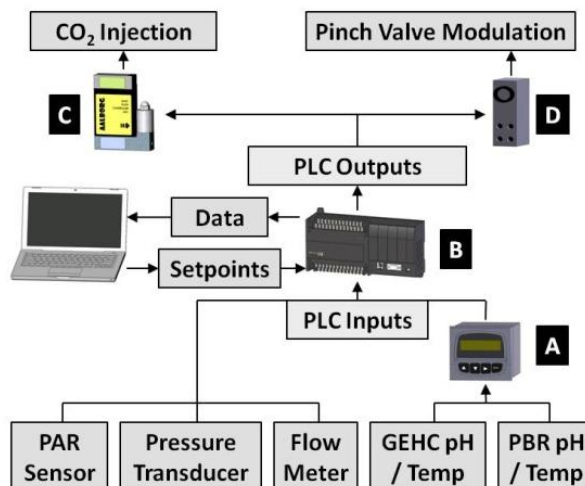


Figure 2.9. Components of the SCADA system. Inputs from the sensors were routed through a multi-parameter transmitter (A) or directly into a PLC (B) were transferred to a computer database. Setpoint values established using an HMI modulated PLC outputs that controlled a mass flow controller for CO₂ injection (C) and an I/P transducer (D) to regulate pinch valve positioning.

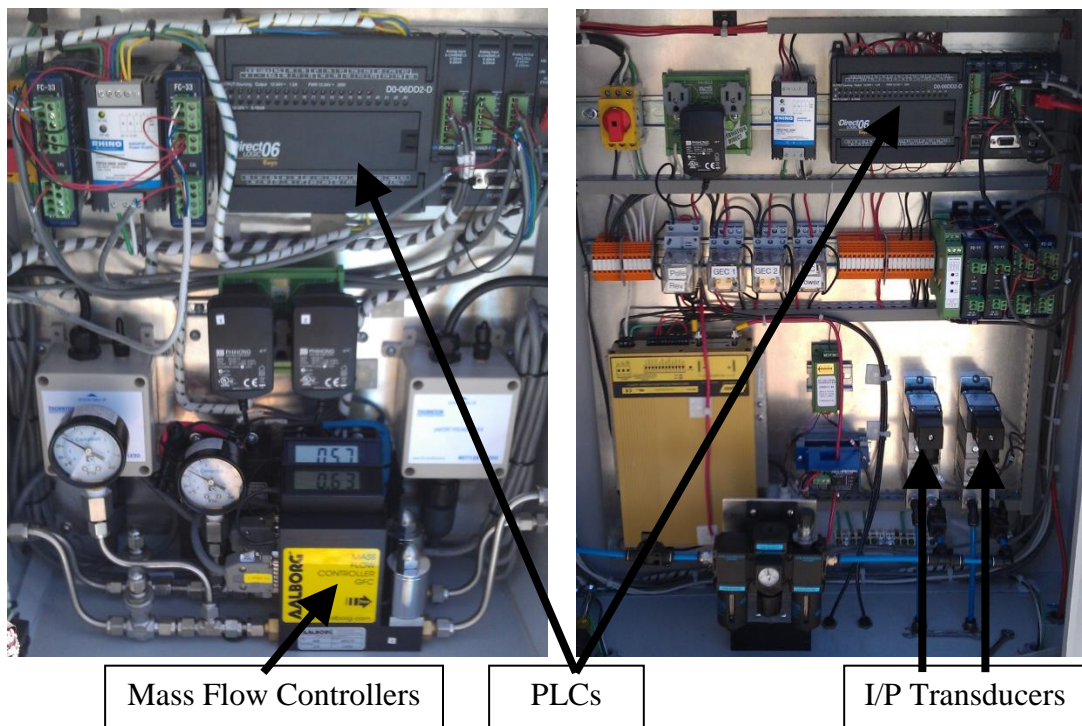


Figure 2.10. Control Cabinet A (Left) and Control Cabinet B (Right) containing PLCs that receive input signals from field sensors and generate output signals connected to mass flow controllers for CO₂ injection and I/P transducers for GEHC level control. The cabinets were designed to accommodate two independent prototype systems.

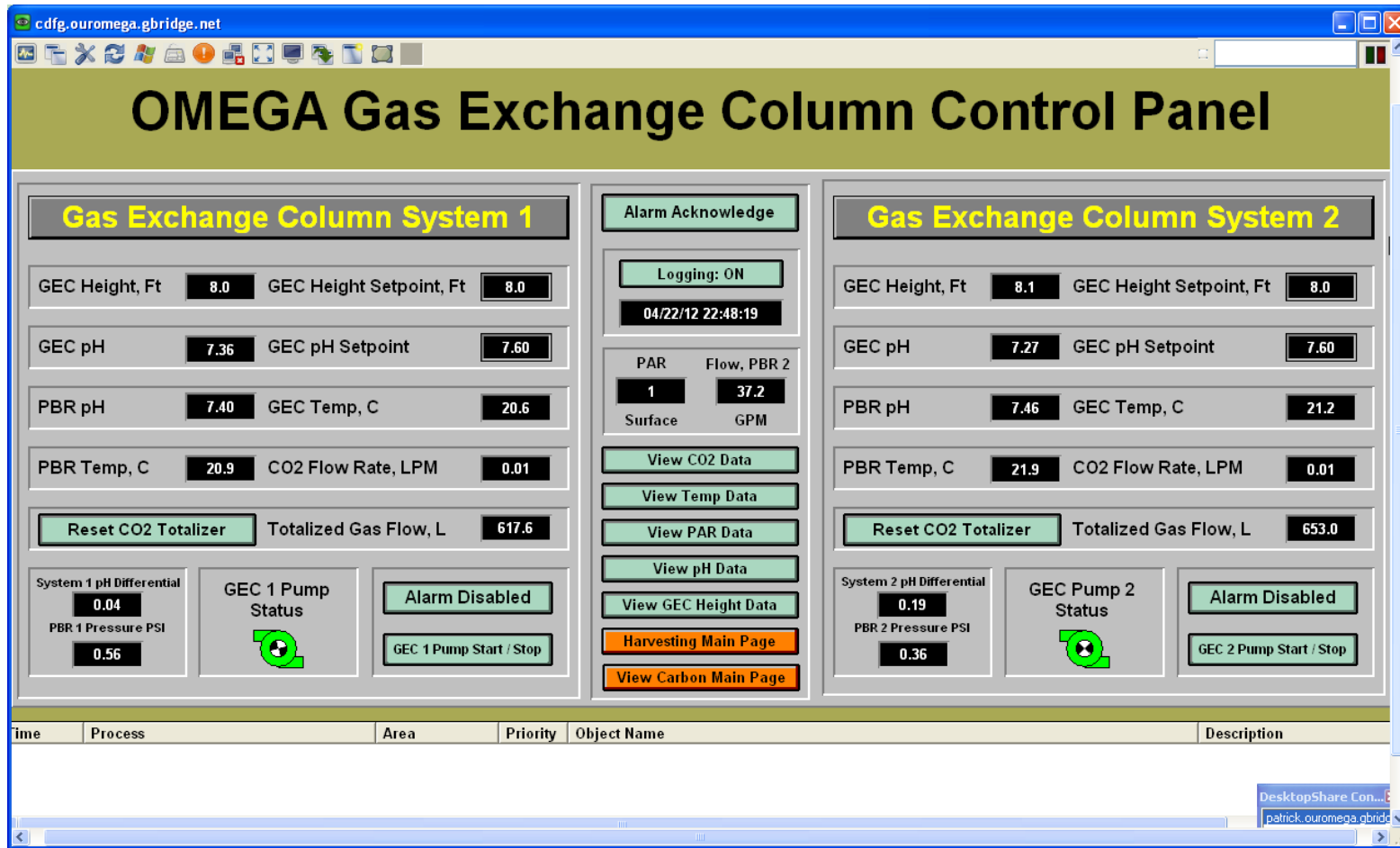


Figure 2.11. The HMI screen of the OMEGA SCADA system. The HMI displayed data from field sensors and provided operators with the ability to specify the desired pH and liquid level in the GEHC. Clicking on the “View Data” buttons displayed trending data for the specified parameter. All data displayed by the HMI was logged to a database every three minutes.

2.5.1 Monitoring and Controlling the GEHC with the HMI

A major objective of the GEHC is to improve CO₂ utilization efficiency by minimizing losses to the atmosphere. As discussed previous sections, this efficiency is influenced by the height of the column and the pH of the solution. However, it is also essential that carbon injection be closely matched with the carbon demand exerted by the microalgae to minimize waste. This presents some difficulty, as microalgal carbon demand varies greatly with solar exposure, nutrient availability and health of the culture. To provide such “on-demand” carbon supply, the SCADA system utilized a control strategy which modulated CO₂ injection rates using pH in the GEHC as a proxy for carbon demand. Using this approach, operators would enter a desired pH value, or *setpoint* (SP), for the GEHC using the HMI. As the microalgae removed carbon from the water during photosynthesis, the pH of the culture would increase. To compensate for this carbon loss, the simulated flue gas would be bubbled into the culture, thereby lowering the pH as CO₂ is dissolved into solution.

The rate of gas injection was proportional to the difference between the SP and the actual value, referred to as the *process variable* (PV), as measured by the pH electrode in the GEHC. The strength of the output signal was calculated by the PLC by multiplying the *error term* (ET), which is the difference between the SP and PV, and the *proportional gain* (PG), which dictates the magnitude of the output signal as the PV deviates from the SP. The objective of this control strategy is to create a situation where the PV = SP by modulating the output signal. In this application, setting the pH in the GEHC (PV) equal to the SP was achieved by varying the rate of CO₂ injection to culture. This approach automatically controlled pH while providing a source of inorganic carbon.

The HMI also displayed the gas injection rate (**Figure 2.11**), which was modulated based on the pH in the GEHC using a mass flow controller. The programming code for the HMI integrated this value and displayed the totalized gas flow during system operation (**Figure 2.11**). This was an essential component of the OMEGA prototype, as tracking carbon usage is necessary to calculate the carbon to microalgal biomass conversion efficiency, which is discussed in depth in Chapter 3.

The same proportional control strategy was used to maintain the liquid level in the GEHC. However, in this case, the input signal originated from a pressure transducer that was converted to display the GEHC level as feet of head on the HMI. The resulting liquid level was the PV, whereas the SP was established using the HMI (**Figure 2.11**). The output signal from the PLC controlled a current / pressure (I/P) transducer that modulated the air pressure to a pneumatically operated pinch valve to maintain the desired liquid level. This approach was advantageous because it enabled constant GEHC liquid level with variable flow rates into the GEHC. It also greatly simplified harvesting from the GEHC because when it was drained, the pinch valve would sense the liquid level being lower than the SP, and would close the pinch valve completely. This isolated the GEHC from the PBR system such that the PBR would circulate uninterrupted during harvesting. This also simplified refilling the system, as when fresh FPE was added to the system and the GEHC level increased, the pinch valve would open and divert liquid to the PBR.

2.5.2 PBR Monitoring with the HMI

In addition to GEHC monitoring, the field instruments also assessed the conditions within the PBRs. This included the temperature and pH of the culture exiting the PBR and the recirculation flow rate as measured with a paddlewheel flow meter. The HMI also displayed the pH differential between the PBR and the GEHC, and the internal PBR pressure quantified using a pressure transducer. Tracking the internal pressure enabled operators to observe changes due to gas build up resulting from photosynthesis (PBR pressure increases), as well as early detection of leaks (PBR pressure decreases). The PAR measured at the surface of the PBRs was also displayed on the HMI and logged to the database by the SCADA system. The DO concentration in the microalgal culture was measured and recorded as the culture exited the PBR tubes using a Craig Ocean Systems (Craig Ocean Systems, Ben Lomond, CA) data logger.

A major challenge of PBR operation is preventing buildup of photosynthetically generated DO, that in combination with high light intensity, decreases microalgal productivity through photoinhibition (20, 21). During photoinhibition, damage occurs to photosystem II (PSII) that depresses the maximum quantum yield of photosynthesis (20). The OMEGA prototype utilized a fast repetition rate fluorometer (FRRF), a rapid non-destructive technique that measures variable chlorophyll fluorescence (F_v) in real time as a tool to monitor culture viability and to detect circumstances of photoinhibition (22). By comparing the ratio of variable chlorophyll fluorescence to maximum fluorescence (F_v/F_M), the FRRF can detect decreases in quantum yield resulting from damage to PSII and is commonly used as an index for photoinhibition. Although FRRF was used strictly as a monitoring tool in this deployment, future OMEGA systems would likely have a control function associated with evidence of photoinhibition. For example, the FRRF could increase pumping rates into the GEHC to facilitate DO removal when signs of photoinhibition are detected.

2.6 Chapter Summary

A pilot-scale prototype system was designed and constructed to evaluate the viability of the OMEGA concept as a microalgal cultivation system capable of recovering nutrients from secondary-treated wastewater FPE. The prototype consisted of two PBR tubes containing swirl vanes designed to enhance mixing by imparting a spiral flow pattern. A portion of the flow from the PBR was diverted to an external GEHC to strip excess DO and provide supplemental CO₂ addition. The GEHC approach was selected to minimize the waste of supplemental CO₂, a major operational expense, by providing improved mass transfer efficiency compared to conventional sparging techniques. The GEHC also featured a sedimentation pit that collected microalgal biomass, greatly simplifying harvesting procedures. All aspects of prototype operation were monitored and controlled using a custom SCADA system that measured numerous process control parameters that were logged to a database. While this chapter focused solely on the design and configuration of the prototype, Chapter 3 discusses the performance of the system deployed in a simulated marine environment evaluated over two experimental trials lasting a total of 23 days.

2.7 Acknowledgements

Parts of this work are published in the following paper:

P. Wiley *et al.*, Microalgae cultivation using offshore membrane enclosures for growing algae (OMEGA). *Journal of Sustainable Bioenergy Systems* 3, 18 (2013).

2.8 References

1. U. S. DOE, “National Algal Biofuels Technology Roadmap” U.S. Department of Energy, Office of Energy Efficiency and Renewable Energy, Biomass Program, 2010.
2. L. A. Hoover, W. A. Phillip, A. Tiraferri, N. Y. Yip, M. Elimelech, Forward with Osmosis: Emerging Applications for Greater Sustainability. *Environmental Science & Technology*, 9824 (2011).
3. P. Buckwalter, S. Gormly, T. Embaye, J. Trent, Harvesting Microalgae by Forward Osmosis. *The Open Energy and Fuels Journal*, (2010).
4. M. Berenguel, F. Rodríguez, F. Acién, J. García, Model predictive control of pH in tubular photobioreactors. *Journal of Process Control* 14, 377 (2004).
5. J. Doucha, F. Straka, K. Lívanský, Utilization of flue gas for cultivation of microalgae *Chlorella* sp. in an outdoor open thin-layer photobioreactor. *Journal of Applied Phycology* 17, 403 (2005).
6. B. S. Ferreira, H. L. Fernandes, A. Reis, M. Mateus, Microporous hollow fibres for carbon dioxide absorption: Mass transfer model fitting and the supplying of carbon dioxide to microalgal cultures. *Journal of Chemical Technology & Biotechnology* 71, 61 (1998).
7. E. Grima, J. Pérez, F. Camacho, R. Medina, Gas-liquid transfer of atmospheric CO₂ in microalgal cultures. *Journal of Chemical Technology and Biotechnology* 56, 329 (1993).
8. P. Talbot, M. Gortares, R. Lencki, J. de la Noüe, Absorption of CO₂ in algal mass culture systems: A different characterization approach. *Biotechnology and Bioengineering* 37, 834 (1991).
9. C. M. Beal, R. E. Hebner, M. E. Webber, R. S. Ruoff, A. F. Seibert, The energy return on investment for algal biocrude: results for a research production facility. *BioEnergy Research* 5, 341 (2012).
10. C. M. Beal *et al.*, Comprehensive Evaluation of Algal Biofuel Production: Experimental and Target Results. *Energies* 5, 1943 (2012).
11. E. W. Becker, *Microalgae: Biotechnology and Microbiology*. Cambridge University Press, 1994, vol. 10.

12. R. Putt, M. Singh, S. Chinnasamy, K. Das, An efficient system for carbonation of high-rate algae pond water to enhance CO₂ mass transfer. *Bioresource Technology* 102, 3240 (2011).
13. J. Doucha, K. Livansky, Productivity, CO₂/O₂ exchange and hydraulics in outdoor open high density microalgal (*Chlorella* sp.) photobioreactors operated in a Middle and Southern European climate. *Journal of Applied Phycology* 18, 811 (2006).
14. A. Carvalho, F. Malcata, Transfer of carbon dioxide within cultures of microalgae: plain bubbling versus hollow-fiber modules. *Biotechnology Progress* 17, 265 (2001).
15. A. Kumar *et al.*, A hollow fiber membrane photo-bioreactor for CO₂ sequestration from combustion gas coupled with wastewater treatment: a process engineering approach. *Journal of Chemical Technology & Biotechnology* 85, 387 (2010).
16. M. C. Barnhart, An improved gas-stripping column for deoxygenating water. *Journal of the North American Benthological Society* 14, 347 (1995).
17. F. Kaštánek *et al.*, In-field experimental verification of cultivation of microalgae *Chlorella* sp. using the flue gas from a cogeneration unit as a source of carbon dioxide. *Waste Management & Research* 28, 961 (2010).
18. A. Carvalho, L. Meireles, F. Malcata, Microalgal reactors: a review of enclosed system designs and performances. *Biotechnology Progress* 22, 1490 (2006).
19. T. Sobczuk, F. Camacho, F. Rubio, F. Fernández, E. Grima, Carbon dioxide uptake efficiency by outdoor microalgal cultures in tubular airlift photobioreactors. *Biotechnology and Bioengineering* 67, 465 (2000).
20. A. Richmond, *Handbook of Microalgal Culture: Biotechnology and Applied Phycology*. Wiley-Blackwell, 2004.
21. F. Rubio, F. Fernández, J. Pérez, F. Camacho, E. Grima, Prediction of dissolved oxygen and carbon dioxide concentration profiles in tubular photobioreactors for microalgal culture. *Biotechnology and Bioengineering* 62, 71 (1999).
22. Z. S. Kolber, O. Prášil, P. G. Falkowski, Measurements of variable chlorophyll fluorescence using fast repetition rate techniques: defining methodology and experimental protocols. *Biochimica et Biophysica Acta (BBA)-Bioenergetics* 1367, 88 (1998).

Chapter 3: Deployment and Performance Evaluation of the OMEGA A Prototype System

3.1 Introduction

The OMEGA system is designed to grow freshwater microalgae in wastewater contained in flexible, clear, plastic photobioreactors (PBRs) attached to a floating infrastructure anchored offshore in protected bays (1-3). The offshore placement allows the system to be in close proximity to wastewater treatment plants and sources of flue gas, eliminating the need to transport these wastes long distances to remote locations where land for microalgal cultivation may be available. By using wastewater for water and nutrients and by not using arable land, the OMEGA system avoids competing with agriculture or disrupting urban infrastructure in the vicinity of wastewater treatment plants. Despite the apparent advantages of the OMEGA approach, microalgal biomass productivity rates and related performance metrics for such systems have not been established. This chapter addresses these knowledge gaps by presenting data collected during two experimental trials aimed at quantifying the performance of an OMEGA prototype deployed in a simulated marine environment. Over the course of these experimental trials, the OMEGA prototype maintained viable microalgae cultures, recovered nutrients from wastewater, sustained areal productivities at levels similar to those reported for other cultivation systems, and utilized supplemental CO₂ with greater efficiency than traditional cultivation systems. These results support the proposal that offshore microalgae cultivation, co-located with waste resources, can contribute to the production of biofuels without competing with agriculture while simultaneously providing valuable wastewater treatment services.

3.2 Prototype Configuration and Experimental Details

A 110-liter prototype OMEGA system was constructed with two tubular PBRs floating in a seawater tank, connected to an external gas exchange and harvesting column (GEHC) and a supervisory control and data acquisition (SCADA) system for process control, autonomous operation and data logging (**Figure 3.1**). To assess the performance of the prototype OMEGA system, two consecutive experiments were conducted in April and May 2012. Experiment 1 lasted 13.5 days and experiment 2 lasted 8.6 days. During both experimental trails, the performance of the OMEGA prototype as a microalgae cultivation system was investigated using areal productivity, CO₂ utilization efficiency and culture viability, as indicated by fast repetition rate fluorometry (FRRF), as performance metrics. Additionally, the ability of OMEGA to provide wastewater treatment services by recovering nitrogen and phosphorus from secondary-treated wastewater final plant effluent (FPE) was evaluated.

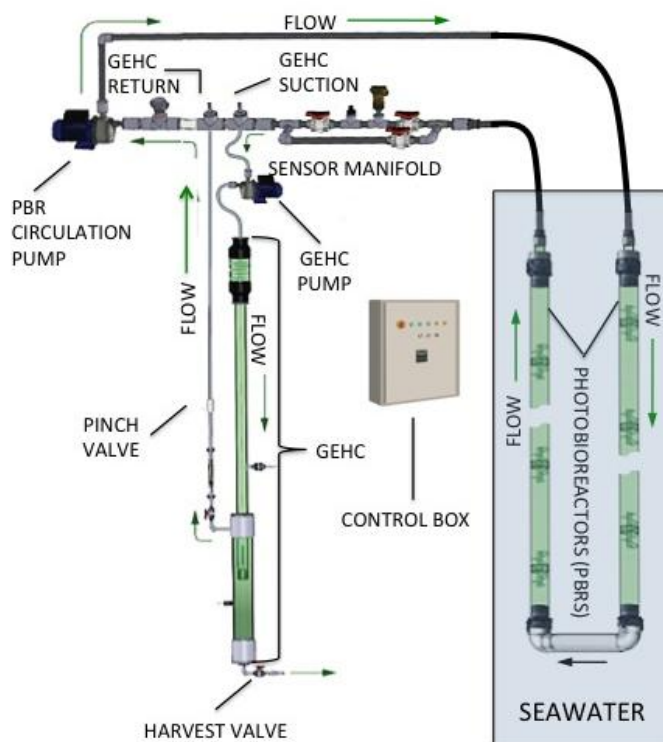


Figure 3.1. Component and flow diagram of the OMEGA system showing the circulation through the PBRs, sensor manifold, and side loop for the GEHC.

3.3 Module Deployment and System Inoculation

Both experiments were conducted at the California Department of Fish and Game, Marine Wildlife Veterinary Care and Research Center in Santa Cruz, CA (Lat: 36° 57' 13", Long: -122° 3' 56") because it provided access to an 8,880-liter salt water tank used to simulate an ocean deployment (**Figure 3.2A**). Due to the cooler temperatures, the tank was covered each night with a thermal pool blanket to minimize heat loss. Bird netting installed around the seawater tank restricted the amount of vertical space available for components of the prototype system, which necessitated that the GEHC be mounted on the exterior of the seawater tank to accommodate its height (**Figure 3.2B**).

A mixed culture of green microalgae used as the system inoculum was dominated by *Desmodesmus* sp. and grown in 19-liter glass carboys containing either BG11 medium (ATCC) or secondary FPE. The carboys were aerated continuously with a regenerative blower (Model VFC084P-5T, Fuji Blowers, Saddle Brook, NJ) and periodically injected with pure CO₂ to lower the culture pH and provide a source of carbon. FPE was collected from the Santa Cruz Wastewater Treatment Facility, mixed with inoculum in a plastic barrel, and weighed with an Ohaus Defender scale (Ohaus Corporation, Parsippany, NJ). The contents of the barrel were transferred into the GEHC using a

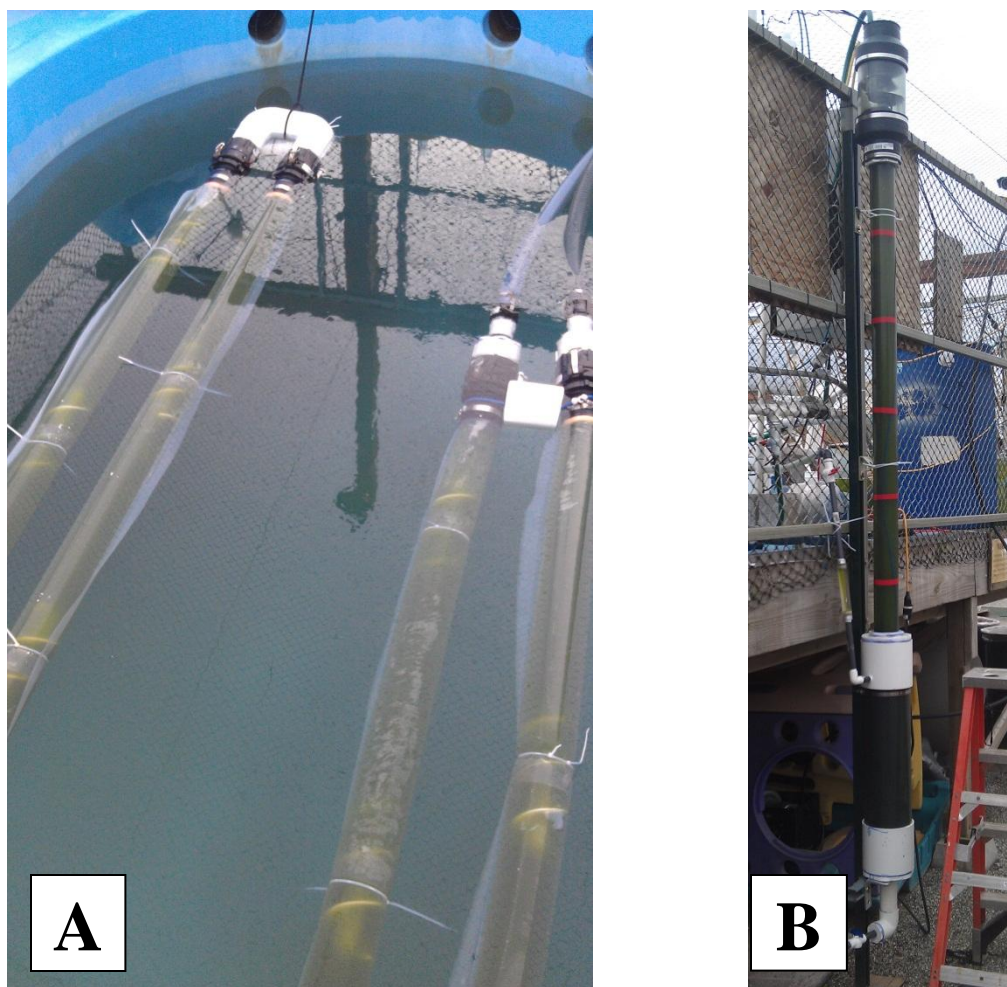


Figure 3.2. (A) Tubular OMEGA PBR modules with internal swirl vanes deployed in a seawater tank located at the California Department of Fish and Game, Marine Wildlife Veterinary Care and Research Center in Santa Cruz, CA. (B) The operational GEHC mounted on the exterior of the salt water tank. Flow from the PBR enters the top of the GEHC and cascades through the OSD (clear pipe on top), before entering the CO₂ gas injection section (small diameter pipe with red hash marks). The large diameter section of pipe at the bottom of the GEHC is the settling chamber. The SCADA system modulates a pneumatic pinch valve to maintain the desired liquid level in the GEHC.

submersible pump. As the liquid level in the GEHC approached the operator-specified level setpoint, the SCADA system opened the pneumatic pinch valve and diverted liquid into the PBR, thereby filling the system. The volume required to fill the entire system was determined by weight. Samples were collected from the barrel and analyzed using method 2540D of Standard Methods (4) to determine total suspended solids (TSS) concentration of the culture. Thus, the initial biomass (B_{Initial}) within the entire prototype system could then be calculated with **Equation 3.1**.

$$B_{\text{Initial}} = \text{SysVol} \cdot \text{TSS}_{\text{Sys}} \quad (3.1)$$

Where,

B_{Initial}	= Initial biomass in the system, g
SysVol	= Total system volume, l
TSS_{Sys}	= Culture TSS concentration, g l ⁻¹

3.4 Harvesting Procedures, Microalgal Yields and CO₂ Utilization Efficiency

Harvesting from the system occurred when the NH₃-N (hereafter “ammonia”) concentration in the system approached zero. This harvest point was selected to prevent conditions of nutrient limitation and to satisfy the wastewater treatment objective of nutrient removal. To harvest from the prototype system, the contents of the GEHC were drained into a barrel and weighed to determine harvest volume (assuming a density of 1 kg l⁻¹). The volume of water remaining in the PBR was determined by subtracting the harvest volume from the total system volume. TSS analyses were then conducted samples collected from the PBR and from the harvest barrel. The harvesting concentration factor (HCF) of the GEHC and total biomass (B_{Total}) in the system could then be calculated with **Equations 3.2** and **3.3** once the TSS concentration and culture volume of PBR and GEHC are known.

$$\text{HCF} = \frac{\text{TSS}_{\text{GEHC}}}{\text{TSS}_{\text{PBR}}} \quad (3.2)$$

Where,

HCF	= Harvesting concentration factor, unitless
TSS_{GEHC}	= Total suspended solids concentration in the GEHC, g l ⁻¹
TSS_{PBR}	= Total suspended solids concentration in the PBRs, g l ⁻¹

$$B_{\text{Total}} = \text{TSS}_{\text{GEHC}} \cdot H_{\text{Vol}} + \text{TSS}_{\text{PBR}} \cdot \text{PBR}_{\text{Vol}} \quad (3.3)$$

Where,

B_{Total}	= Total biomass in the prototype system, g
TSS_{GEHC}	= Total suspended solids concentration in the GEHC, g l ⁻¹
H_{Vol}	= Volume of culture harvested from the GEHC, l
TSS_{PBR}	= Total suspended solids concentration in the PBRs, g l ⁻¹
PBR_{Vol}	= Volume of culture within the PBRs, l

Knowing the B_{Total} from **Equation 3.3** and B_{Initial} value from **Equation 3.1** enabled calculation of the biomass yield (B_{Yield}) using **Equation 3.4**. Then, the areal productivity can be calculated with **Equation 3.5** once the biomass yield (B_{Yield}), elapsed time between harvest cycles (D_{Harvest}), and surface area of the PBR tubes are known.

$$B_{\text{Yield}} = B_{\text{Total}} - B_{\text{Initial}} \quad (3.4)$$

Where,

B_{Yield} = Biomass yield between harvest cycles, g
 B_{Total} = Total biomass in the prototype system, g
 B_{Initial} = Initial biomass in the system, g

$$P_{\text{Algae}} = \frac{A_{\text{Growth}}}{A_{\text{PBR}} \cdot D_{\text{Harvest}}} \quad (3.5)$$

Where,

P_{Algae} = Microalgal areal productivity, $\text{g m}^{-2} \text{ day}^{-1}$
 A_{Growth} = Total biomass produced, g
 A_{PBR} = Surface area of PBR tubes, m^2
 D_{Harvest} = Elapsed time between harvest cycles, days

The biomass yield (B_{Yield}) from **Equation 3.4** and the totalized volume of gas injected into the GEHC recorded by the SCADA system were then used to calculate the CO_2 -to-biomass conversion efficiency ($\text{CO}_{2\text{Conv}}$) between harvest cycles using **Equation 3.6**.

$$\text{CO}_{2\text{Conv}} = \frac{B_{\text{Yield}} \cdot f_{\text{Car}}}{\frac{V_{\text{Gas}} \cdot p_{\text{CO}_2}}{RT} \cdot \frac{12 \text{ g C}}{\text{mol CO}_2}} \cdot 100 \quad (3.6)$$

Where,

$\text{CO}_{2\text{Conv}}$ = CO_2 to biomass conversion efficiency, %
 B_{Yield} = Biomass yield between harvest cycles, g
 f_{Car} = Fraction carbon of microalgal biomass, 0.5
 V_{Gas} = Total volume of gas injected between harvest periods, l
 p_{CO_2} = CO_2 partial pressure, atm
 R = Ideal gas constant, $0.008206 \text{ mol l}^{-1} \text{ atm}^{-1}$
 T = Temperature, K

Once the harvest volume was removed from the GEHC, it was refilled with an equal volume of FPE, which diluted the culture, and the system was put back into operation. The TSS concentration of the entire, well mixed system was again determined and used with **Equation 3.1** to give a new B_{Initial} value with each FPE addition. The ammonia, $\text{NO}_3\text{-N}$ (hereafter “nitrate”) and PO_4^{3-} (hereafter “phosphate”) concentrations we also measured to establish the initial nutrient load. The cycle of harvesting and refilling was repeated throughout the duration of both experiments.

3.5 Nutrient Recovery from FPE Wastewater

A major objective of the OMEGA system is to provide wastewater treatment services in addition to generating microalgal biomass. To assess the potential of OMEGA as a nutrient recovery process, ammonia (Hach method 10031), nitrate (Hach method 8039) and phosphate (Hach method 8048) were measured daily, pre-harvest and post-harvest on samples collected from a port located on the discharge side of the PBR

circulation pump using a Hach DR2800 spectrophotometer (Hach Corporation, Loveland, CO). These data points enabled calculation of nutrient removal rates using **Equation 3.7**.

$$\text{Rate} = \frac{N_{\text{Int}} - N_{\text{Final}}}{D_{\text{Harvest}}} \quad (3.7)$$

Where,

Rate	= Nutrient removal rate, mg l ⁻¹ day ⁻¹ , or mg l ⁻¹ hour ⁻¹
[N] _{Int}	= Initial nutrient concentration, mg l ⁻¹
[N] _{Final}	= Final nutrient concentration, mg l ⁻¹
D _{Harvest}	= Elapsed time between harvest cycles, days or hours

Having a well-mixed culture is important with regard to nutrient removal because it has shown to improve nutrient exchange with the microalgae (5). To ensure adequate mixing within the OMEGA prototype system, the optical density (OD₇₅₀) was measured with a Hach DR2800 spectrophotometer before and after physically shaking the PBR modules. The percent sedimentation within the PBR tubes was then calculated using **Equation 3.8**.

$$\text{SED} = \frac{OD_{750\text{After}} - OD_{750\text{Before}}}{OD_{750\text{After}}} (100) \quad (3.8)$$

Where,

SED	= Culture sedimentation, %
OD _{750After}	= Culture optical density after shaking PBR modules
OD _{750Before}	= Culture optical density before shaking PBR modules

3.6 OMEGA Prototype Performance

Maintaining a well-mixed microalgal suspension is necessary to prevent anaerobic conditions from developing in the PBR and to maximize nutrient removal rates (5, 6). To limit sedimentation of microalgae in the OMEGA PBRs, cultures were circulated at velocities ranging from 14 to 21 cm sec⁻¹, flow rates that reportedly prevent sedimentation in open ponds (7). Microalgal suspension and mixing were enhanced by swirl vanes, which imparted a helical flow pattern. With the combination of flow rates and swirl vanes, microalgae settling in the PBRs never exceeded 14% of the PBR biomass. The swirl vanes also increased turbulence, which is known to improve light exposure in PBR cultures (5). In cultures grown in laminar flow systems photoinhibition and light limitations are observed, both of which suppress productivity (5, 7, 8). While swirl vanes may have improved suspension and light availability and hence productivity, two difficulties noted with the swirl vanes tested were 1) increase biofouling on the walls of the PBR in their vicinity and 2) increased drag, which increased pumping energy.

In both experiments 1 and 2, the comparisons of hourly mean DO vs. PAR and DO vs. Fv/Fm are shown in **Figure 3.3**. The increase in photosynthetically generated DO correlates well with PAR from sunrise (06:00) to late afternoon (16:00), although the DO curve is artificially flattened at peak solar irradiance (~12:00) because the DO values

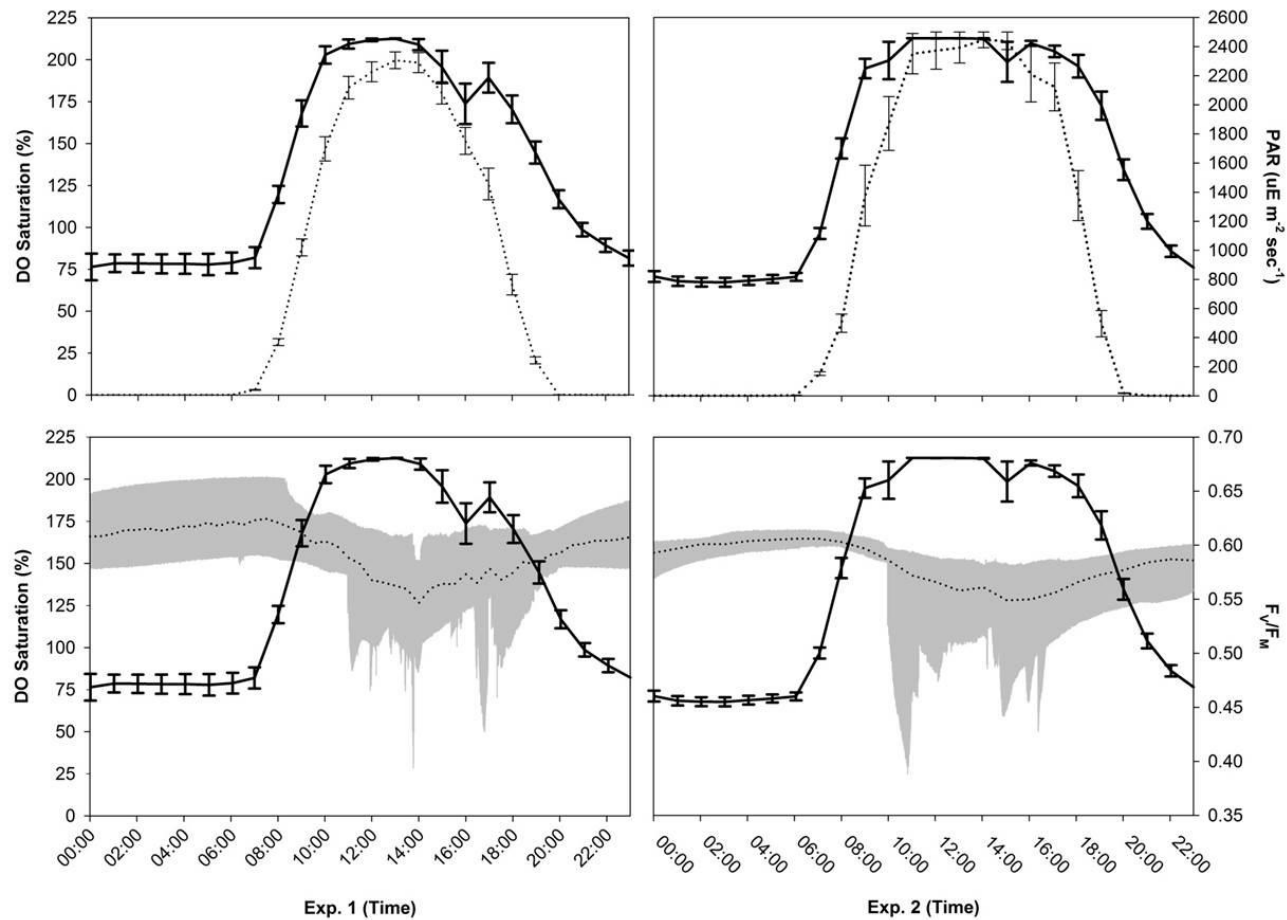


Figure 3.3. DO concentration, PAR and F_v/F_m values for experiment 1 (Left) and experiment 2 (Right). (Top) Mean hourly (\pm SE) concentration photosynthetically generated DO (solid line) increases and decreases as a function of PAR (dotted line). (Bottom) The mean hourly F_v/F_m ratio (dotted line) overlaying the range of data points (shaded area) measured by FRRF indicates that the culture has maintained high photoconversion efficiency. The slight suppression of the F_v/F_m ratio during mid-day is a result of photoinhibition caused by PAR intensity and elevated concentrations of DO (solid line).

exceeded the upper threshold for the oxygen sensors (212% saturation). After 16:00, the decline in DO was due to a combination of decreased photosynthesis, respiration and DO removal by the OSD in the GEHC. The relative contribution of these different factors was not determined.

At peak DO production and peak irradiance, there was a slight photoinhibition indicated by F_V/F_M measurements, which dipped to 0.49 in experiment 1 and 0.54 in experiment 2. Rubio and co-workers (9) noted that in long tubular PBRs DO buildup at high irradiance caused photoinhibition, which they identified as one of the greatest constraints on the scale-up of PBRs. The solution for the OMEGA system is to adjust the ratios of residence time in the PBR to the transfer frequency to the GEHC, which depends on PBR length, the number of GEHCs, and the flow rate. In the OMEGA system the tested residence time of the culture in the PBRs was 20 minutes, based on a PBR length of 3.1 m, a 4.5% transfer to the GEHC, and a PBR flow rate of 86-130 l min^{-1} . In the future, DO as it relates to photoinhibition can be managed for PBRs of a given length using real-time FRRF and DO data in the control logic algorithm to modify GEHC input and flow rates. The size and configuration of the OSD can also be modified to increase the exchange of DO.

3.6.1 GEHC Performance

In addition to DO management, the GEHC was where CO_2 was injected into the culture, both as a source of inorganic carbon for microalgae growth and to control the culture pH. Both carbon availability and pH control are dependent on efficient CO_2 delivery, and both are critical to the productivity and economics of large-scale microalgae cultivation (10-14). Beal *et al.* (15, 16) have shown that commercial CO_2 supply is one of the biggest contributors to overall energy use and cost of microalgal biofuel production.

While the GEHC provided improved CO_2 mass transfer efficiency when compared to traditional sparging methods, diverting only a portion of the culture for CO_2 injection resulted in a pH differential between the PBR and GEHC (**Figure 3.4, top**). This differential was greatest at times of the highest photosynthetic activity, which correlated with the highest PAR and highest gas injection rate during the day when most inorganic carbon was consumed (**Figure 3.4, bottom**). The control system could maintain the pH near the setpoint (7.60), indicating that the mass transfer rate of CO_2 in the GEHC was not exceeded by the rate of carbon removal in the PBR. Thus, the control system could monitor and deliver the amounts of CO_2 demanded by the microalgae. Furthermore, this system reduced CO_2 losses as compared to “on-off” systems that produce hysteresis and potentially large variations from the desired pH setpoint (10, 17). Further improvements in process control may be realized using predictive models to control pumping rates. Rubio *et al.* (9) developed a predictive model capable of estimating carbon depletion in tubular bioreactors based on pH differential, which could be adapted for the OMEGA system by comparing pH in the PBRs versus the GEHC. Further research is needed to determine how such pumping controls could improve energy efficiency and biomass productivity.

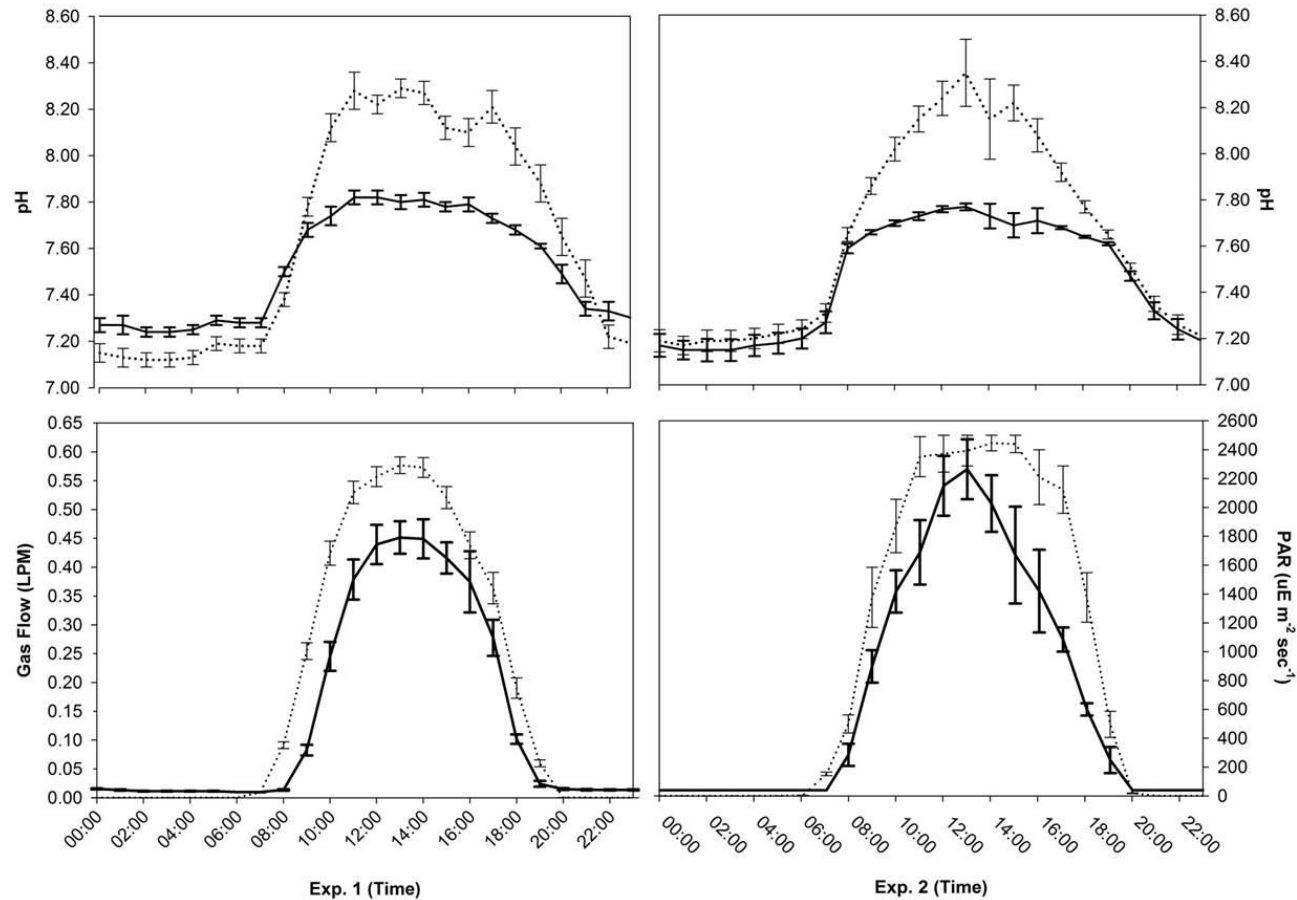


Figure 3.4. The mean hourly (\pm SE) pH, gas flow, and PAR recorded during experiment 1 (**Left**) and experiment 2 (**Right**). (**Top**) pH values measured inside the GEHC (solid line) compared to pH in the PBR (dotted line). The differential between the GEHC and PBRs increases during the day due to carbon assimilation for photosynthesis. The rate of CO₂ injection was controlled to maintain the GEHC pH setpoint during the day. The slow decrease in pH at night is attributed to respiration. (**Bottom**) Gas flow rates (solid lines) indicating CO₂ demand correlated with PAR (dotted lines), and inferred rates of photosynthesis. The pH of the GEHC and PBRs equalize at night due to respiration.

The details of harvesting intervals, biomass production, and carbon utilization for both experiments 1 and 2 are given in **Table 3.1**. Harvesting occurred every 0.83 to 2.79 days, triggered by the depletion of ammonia. It was noted that microalgae accumulated in the settling chamber at the bottom of the GEHC, hence the biomass in the GEHC was higher than in the PBRs, providing an HCF of 2.0 ± 0.1 ($n = 7$) in experiment 1 and 1.4 ± 0.1 ($n = 7$) in experiment 2. These calculated concentration factors were based on the total volume of the GEHC, and therefore do not represent the concentrations at the bottom of the settling chamber.

Harvesting efficiency in the GEHC could be improved by adding coagulants or by integrating an electrocoagulation (EC) system, which produces coagulants *in situ* (18, 19). The EC system is well suited for OMEGA because it has no moving parts and is easily automated (19, 20). Furthermore, by adding a small amount of seawater to the culture isolated in the GEHC, which would increase its ionic strength, would lower the power required for EC and would produce electrolytic chlorine, which could contribute to disinfecting the residual water before release into the environment (20, 21). However, this approach would also lead to the formation of trihalomethanes and other chlorination by-products that are known carcinogens. Chapter 4 discusses the appropriateness of utilizing the EC harvesting process with the OMEGA system in more detail

3.6.2 CO₂ Utilization and Biomass Production

The totalized volume of simulated flue gas (8.5% CO₂, V/V) injected into the GEHC and the biomass produced during experiments 1 and 2 are shown in **Figure 3.5**. The changes in gas utilization, which appear as a “staircase” in the plot, reflect the day/night cycles and the on-demand input of CO₂. The curve slopes upward during light periods due to increased gas flow required to satisfy the carbon demand for photosynthesis by the microalgae. The curve plateaus during dark periods when there is no CO₂ demand. The biomass produced relative to the amount of CO₂ injected was used to calculate the CO₂ utilization efficiency (**Table 3.1**): For experiment 1 the mean efficiency was $53.8\% \pm 4.0\%$ ($n = 9$) and for experiment 2 it was $60.2\% \pm 4.7\%$ ($n = 7$), with values from both experiments ranging from 31.6% to 80.9%. These measured CO₂ conversion efficiencies correspond well to the mass transfer efficiency values obtained in the titration experiment (see **Section 2.4.1: Predicting GEHC Gas Injection Rate and CO₂ Mass Transfer Efficiency**). Gas transfer in the OMEGA GEHC could be improved by using a taller column (greater contact time for rising bubbles), smaller bubbles (greater surface-to-volume ratio), or higher CO₂ concentrations. The site restricted column height, available equipment determined the bubble size, and the CO₂ concentration was chosen to simulate flue gas to determine if it would be adequate to support microalgae cultures in the prototype system.

The observed productivity, normalized to PBR surface area per day, averaged $13.2 \text{ g} \pm 1.9$ ($n = 9$), in experiment 1 and $15.3 \text{ g} \pm 1.6$ ($n = 7$) in experiment 2 (**Table 3.1**). In experiment 1, sampling periods one and three had low biomass yields. The initially low yield, $4.0 \text{ g m}^{-2} \text{ day}^{-1}$, may have been due to a period of culture acclimation. The second low yield on the third harvest cycle ($4.5 \text{ g m}^{-2} \text{ day}^{-1}$) was due to a short incubation

Table 3.1. Harvesting frequency, biomass yields and mass of carbon injected into the GEHC used to calculate carbon conversion efficiency and areal biomass productivity during experiments 1 and 2.

Experiment 1						
Elapsed Time, Days	Days Between Harvest	Biomass Produced, g	Carbon Required, g	Carbon Injected, g	Carbon Conversion Efficiency, %	Biomass Productivity, g m ⁻² day ⁻¹
1.85	1.85	5.2	2.6	5.8	45.0	4.0
2.83	0.98	8.4	4.2	8.2	51.3	12.3
3.66	0.83	2.6	1.3	4.1	31.6	4.5
4.79	1.13	13.4	6.7	13.1	51.1	17.0
6.73	1.94	23.1	11.5	18.0	64.2	17.1
8.75	2.02	15.3	7.7	12.9	59.4	10.9
9.68	0.93	11	5.5	10.1	54.5	17.0
12.5	2.79	29.3	14.7	19.6	74.9	15.1
13.5	1.06	15.2	7.6	14.5	52.5	20.6
Mean (SE)		13.7 (4.6)	6.9 (1.4)	11.8 (1.8)	53.8 (4.0)	13.2 (1.9)
Experiment 2						
0.92	0.92	6.1	3.0	7.1	42.7	9.5
1.87	0.95	8.1	4.1	6.4	63.7	12.3
2.89	1.02	15.4	7.7	11.4	67.7	21.7
4.89	2.00	23.1	11.6	19.3	59.9	16.6
5.88	0.99	12.3	6.2	11.0	56.2	17.8
6.82	0.94	8.3	4.2	8.3	50.2	12.7
8.61	1.79	21.0	10.5	13.0	80.9	16.8
Mean (SE)		13.5 (2.5)	6.8 (1.3)	10.9 (1.7)	60.2 (4.7)	15.3 (1.6)

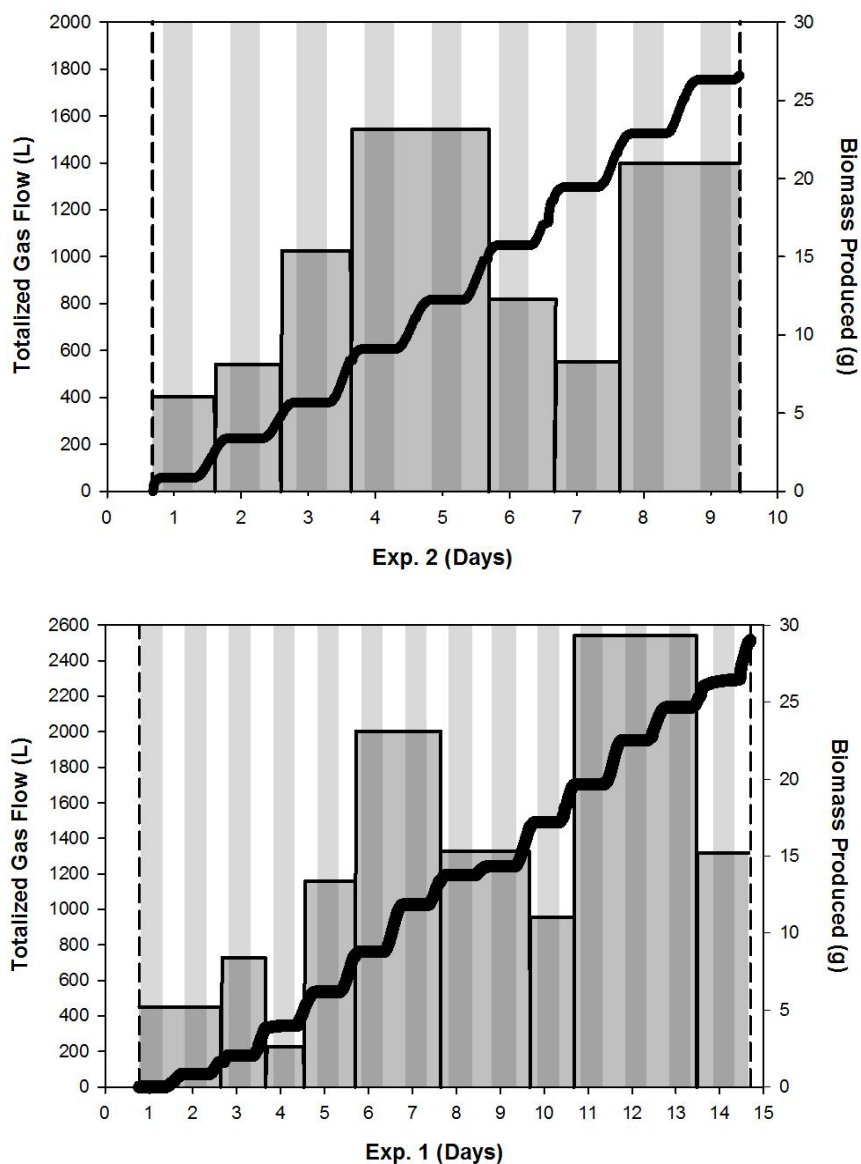


Figure 3.5. Totalized gas flow (8.5% CO₂ V/V) (bold black line) and biomass production (histogram) plotted for experiment 1 (**Bottom**) and experiment 2 (**Top**) with the day/night cycle indicated by vertical stripes. The totalized gas flow has a “staircase” shape because CO₂ was injected on demand; photosynthesis caused injection during the day (slope up), but not at night (plateaus). The histogram shows biomass production in the height of bars (right axis, g) and the time between harvesting in the width of the bars (bottom axis, days).

period with minimal light exposure (**Figure 3.5**). Despite these limitations, the average observed areal productivities were within the range of values reported for open ponds (22-24), although somewhat less than those reported for other PBR systems (25, 26). This disparity with other PBRs may be due to lower nutrient concentrations in the unsupplemented wastewater, the presence of grazers and/or pathogens, or to other limiting culture conditions, such as cool culture temperatures experienced during both experiments. Throughout the course of both trials, the average hourly temperature ranged between 16-23° C due to diurnal shifts in ambient temperature (**Figure 3.6**). This link between microalgal productivity and temperature suggests that site selection must be carefully considered for large-scale OMEGA deployments. However, long-term experiments are required to more fully understand the limiting factors in the OMEGA system and its potential yields.

3.6.3 OMEGA and Wastewater Treatment

The OMEGA system used secondary-treated wastewater FPE as a source of nutrients for microalgae cultures and the concentrations of ammonia, nitrate and phosphate were monitored. The rapid utilization of ammonia required periodic replacement of spent culture medium with fresh FPE. Between 16% and 34% of the total system volume was harvested from the GEHC and replenished to increase the concentration of ammonia (**Figure 3.7**). While ammonia concentration followed a consistent pattern of utilization and replenishment, the corresponding nitrate concentration showed increases, decreases, or no change (**Figure 3.7**). The increases in nitrate were attributed to nitrification by ammonia-oxidizing bacteria, which are known to be present in wastewater (27). The decreases in the nitrate concentration observed in experiment 1 (days 5-8) and experiment 2 (days 1-3 and 4-6) were attributed to the depletion of ammonia and the utilization of nitrate as the microalgae's secondary nitrogen source (**Figure 3.7**). Changes in preferred nitrogen sources have been observed for other microalgae (28).

The calculated rates of ammonia removal varied, but were positive, whereas the rates of nitrate removal were both positive and negative; a “negative removal” rate means nitrate production (**Figure 3.8**). The ammonia removal rate averaged 0.29 ± 0.04 (n = 12) and 0.49 ± 0.03 (n = 11) $\text{mg l}^{-1} \text{hr}^{-1}$ for experiments 1 and 2, respectively. In contrast, nitrate removal rates were predominantly positive during experiment 1 but predominantly negative in experiment 2. In both experiments the actual nitrate concentrations represented the combination of production and utilization at each sampling point. A more effective utilization of total nitrogen can be achieved with longer retention times, and would increase the value of wastewater treatment services provided by OMEGA.

Phosphate concentrations within the microalgal culture ranged between 0.04 and 1.13 mg l^{-1} during experiment 1 and between 0.08 and 7.60 during experiment 2 (**Figure 3.9**). However, several missed sampling events occurred during experiment 1 that prevented calculation of phosphate removal rates. The removal rates were positive in all cases, except for two instances during experiment 2 when slight increases were observed (**Figure 3.10**), and averaged 0.26 ± 0.16 $\text{mg l}^{-1} \text{day}^{-1}$ (n = 5) and 1.18 ± 0.95 $\text{mg l}^{-1} \text{day}^{-1}$ (n = 8) for experiments 1 and 2, respectively. The large standard error calculated for both

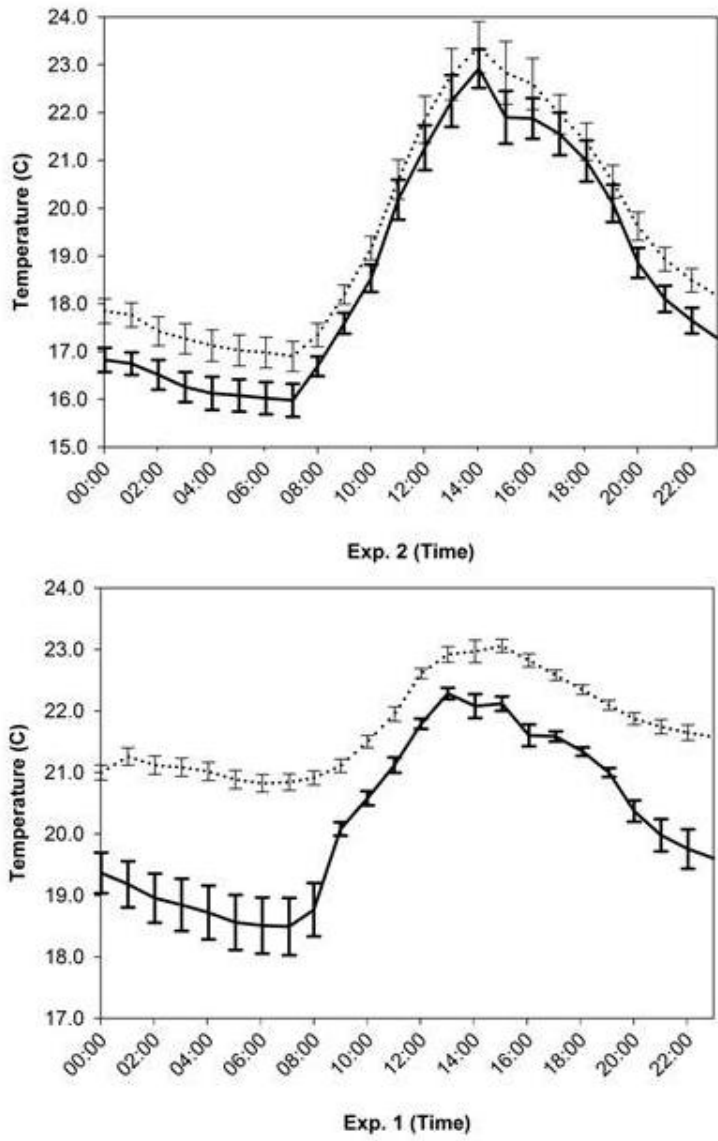


Figure 3.6. The mean hourly temperatures (\pm SE) inside the GEHC (solid lines) and PBR (dotted lines) for experiment 1 and experiment 2. The slightly warmer temperature in the PBR is likely due to the heat capacity of the surrounding seawater and the use of a thermal pool cover during the evening to prevent heat loss.

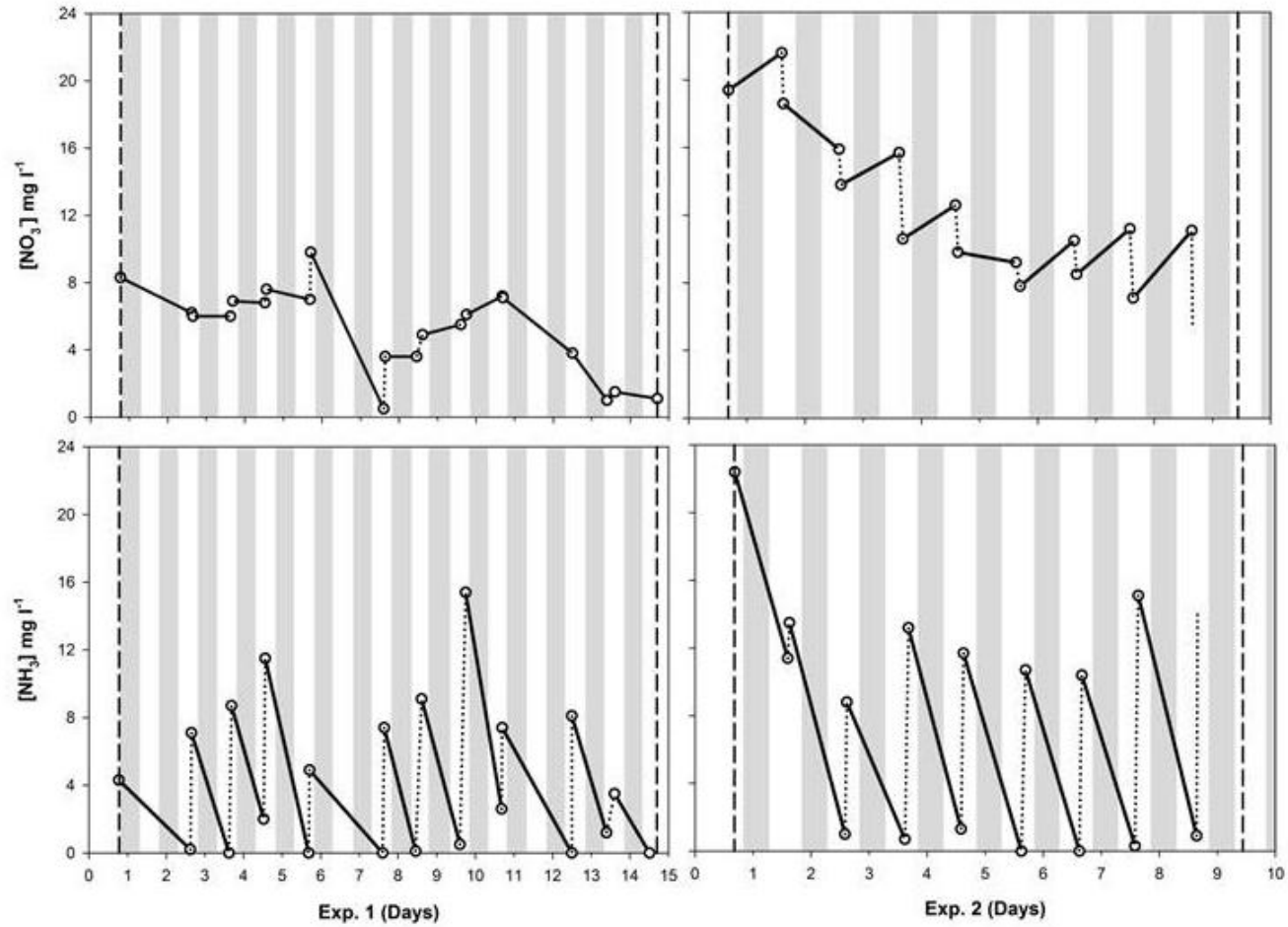


Figure 3.7. Time course for the addition and utilization of ammonia (**Bottom**) and nitrate (**Top**) during experiment 1 and experiment 2. Solid lines represent changes in nutrient concentration between harvest periods, while dotted lines indicate the addition of fresh FPE to replenished nutrients consumed by the microalgae. The day/night cycle is represented by white/gray shading on the vertical bars.

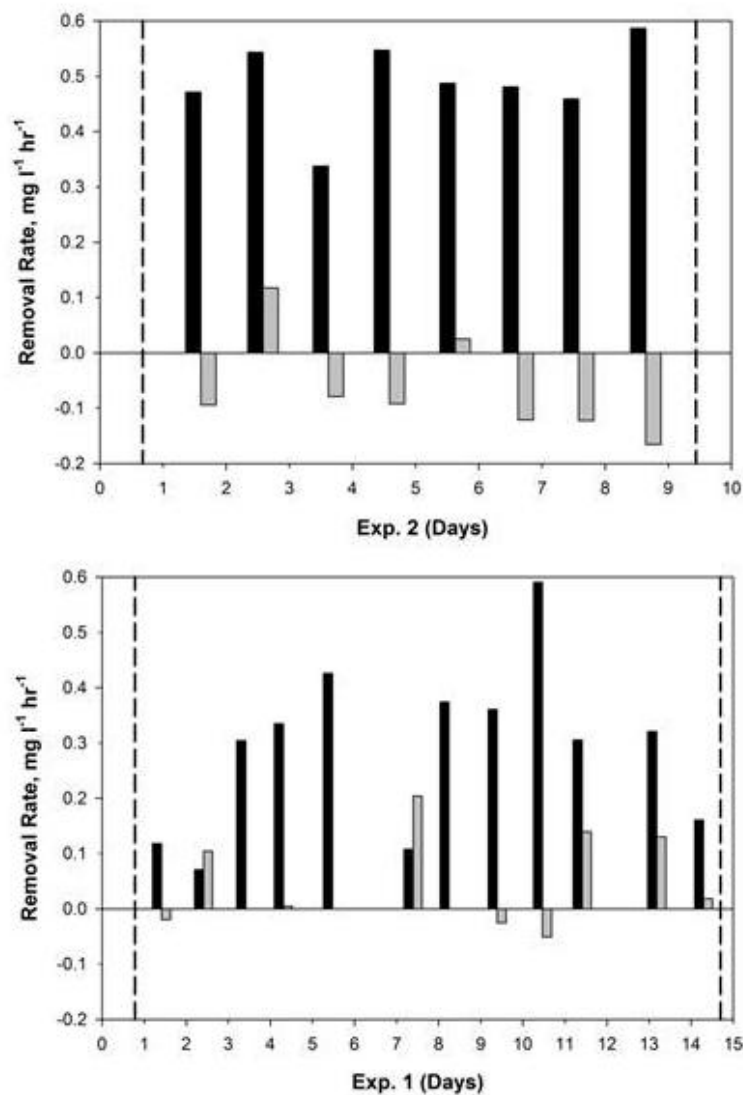


Figure 3.8. Removal rates are shown as positive when nutrients were depleted or negative when nutrient concentrations increased. The ammonia removal rates (black bars) were always positive, but nitrate removal rates (grey bar) were occasionally negative due to nitrification. The microalgae preferred ammonia as their nitrogen source and consume nitrate once the supply of ammonia was exhausted.

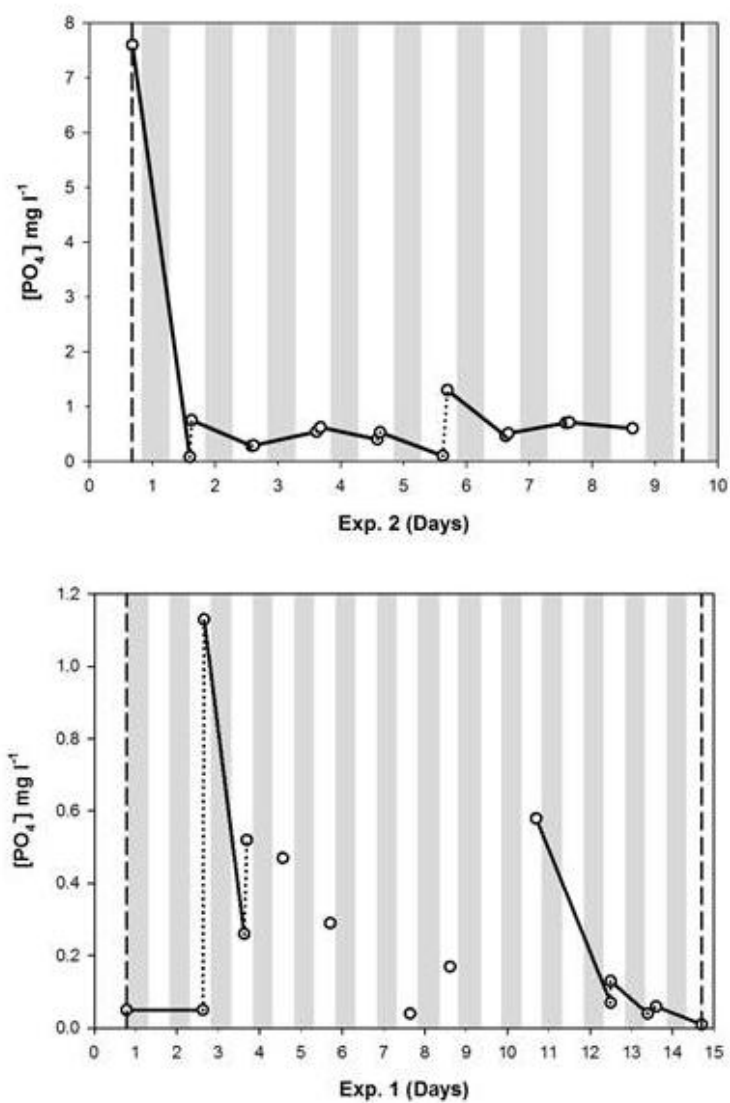


Figure 3.9. Time course for the addition and utilization of phosphate for experiment 1 (**Bottom**) and experiment 2 (**Top**). Solid lines represent changes in nutrient concentration between harvest periods, while dotted lines indicate the addition of fresh FPE to the system. The day/night cycle is represented by white/gray shading on the vertical bars.

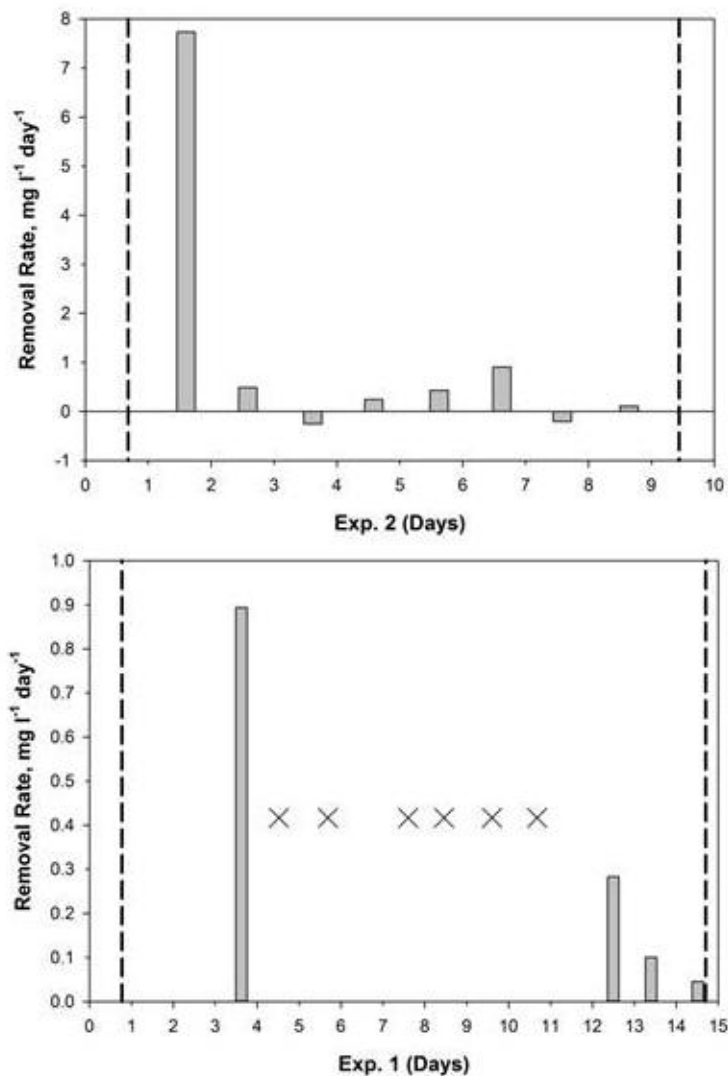


Figure 3.10. Phosphate removal rates for experiment 1 (**Bottom**) and experiment 2 (**Top**). X's signify missing data points between harvest intervals during Experiment 1, which prevented calculation of removal rates. In both experiments, the rate of phosphate recovery increased with increasing concentration.

experiments was caused by more rapid phosphate depletion with increasing concentration available within the culture media. For example, the initial phosphate concentration of 7.6 mg l^{-1} during experiment 2 was reduced to 0.1 mg l^{-1} in less than 24 hours, yielding the highest removal rate of $7.7 \text{ mg l}^{-1} \text{ day}^{-1}$. Similarly, the greatest removal rate observed during experiment 1 ($0.89 \text{ mg l}^{-1} \text{ day}^{-1}$) corresponded with the highest concentration measured during the study period (1.13 mg l^{-1}). This could be attributed to consumption by microalgae, as they are known to exhibit “luxury uptake” of phosphorus, where excess concentrations are stored within the cells (6).

These results indicate that microalgae growing in a prototype OMEGA system can contribute to biological nutrient removal in wastewater treatment. It is well established that microalgae in ponds and other PBR designs can effectively remove nutrients from wastewater (29-32). It has also been demonstrated that microalgae can remove heavy metals (32, 33) and organic contaminants, including surfactants, phenols, and hydrocarbons (32, 34-36). Research reported elsewhere indicates that the OMEGA system can also contribute to the removal of pharmaceuticals and personal care products as well as compounds of emerging concern (37).

3.7 Conclusion

OMEGA has the potential of co-locating microalgal cultivation with two major waste-streams from coastal cities: wastewater and CO₂. By situating OMEGA systems in the vicinity of offshore wastewater outfalls and CO₂ sources, such as near-shore power plants, OMEGA can transform these waste-streams into resources that produce biofuels and treat wastewater without competing with agriculture for water, fertilizer, or land (2). The experiments presented here explored the technical feasibility of OMEGA, using a 110-liter prototype system that was built and tested over a 23-day period. Based on results obtained during prototype testing, the following observations and research needs have been identified:

- 1) The areal productivity of the OMEGA prototype averaged 14.1 g m⁻² day⁻¹ of biomass during two experiments lasting a total of 23 days. These productivity numbers, which are similar to those reported for ponds and PBR systems, demonstrate the viability of the OMEGA concept as a microalgal cultivation process.
- 2) Efficient utilization of supplemental CO₂, a major operational expense, is needed to improve the economics of large scale microalgae cultivation. The OMEGA configuration evaluated during this period satisfied this criterion by converting CO₂ into biomass with greater than 50% efficiency, a significant improvement compared to the 10-20% reported for conventional sparging.
- 3) Photoinhibition is a major obstacle known to reduce biomass yields in PBR systems. However, microalgae cultivated using the OMEGA prototype exhibited only slight photoinhibition, as indicated by F_V/F_M , despite high light levels and supersaturated DO concentrations. This is likely caused by the helical flow pattern generated by swirl vanes. Optimization of swirl vane design and placement in the PBR is needed to reduce pumping energy requirements.
- 4) Microalgae effectively recovered >90% of ammonia from secondary-treated FPE, indicating that OMEGA has ability to perform wastewater treatment services. Further research is needed to fully assess the wastewater treatment capacity of an OMEGA deployment.
- 5) The prototype system was not designed for energy efficiency or cost effectiveness. The materials and design were intended for convenient

construction and experimentation within the limits of the space available on site. Configurations optimizing the efficiency of a large-scale OMEGA deployment are needed.

- 6) Utilization of robust process control algorithms that optimize growth conditions within the PBR is necessary to maximize biomass production and lower operating costs.

3.8 Acknowledgements

Parts of this work are published in the following paper:

P. Wiley *et al.*, Microalgae cultivation using offshore membrane enclosures for growing algae (OMEGA). *Journal of Sustainable Bioenergy Systems* 3, 18 (2013).

3.9 References

1. J. Trent, in *International Workshop on Offshore Algae Cultivation*. (Lolland, Denmark, 2009), pp. 274.
2. J. Trent, P. Wiley, S. Tozzi, B. McKuIn, S. Reinsch, Research Spotlight: The future of biofuels: is it in the bag? *Biofuels* 3, 521 (2012).
3. P. E. Wiley, J. E. Campbell, B. McKuIn, Production of biodiesel and biogas from algae: A review of process train options. *Water Environment Research* 83, 326 (2011).
4. APHA, *Standard methods for the examination of water and wastewater*. W. E. Federation, Ed., Washington, APHA Water Environment Federation, Alexandria, 1998.
5. P. Carlozzi, G. Torzillo, Productivity of Spirulina in a strongly curved outdoor tubular photobioreactor. *Applied Microbiology and Biotechnology* 45, 18 (1996).
6. A. Richmond, *Handbook of Microalgal Culture: Biotechnology and Applied Phycology*. Wiley-Blackwell, 2004.
7. J. Doucha, K. Livansky, Productivity, CO₂/O₂ exchange and hydraulics in outdoor open high density microalgal (*Chlorella* sp.) photobioreactors operated in a Middle and Southern European climate. *Journal of Applied Phycology* 18, 811 (2006).
8. H. Quiang, H. Guterman, A. Richmond, Physiological Characteristics of Spirulina platensis cultured at ultra-high cell densities. *Journal of Phycology* 32, 1066 (1996).
9. F. Rubio, F. Fernández, J. Pérez, F. Camacho, E. Grima, Prediction of dissolved oxygen and carbon dioxide concentration profiles in tubular photobioreactors for microalgal culture. *Biotechnology and Bioengineering* 62, 71 (1999).

10. M. Berenguel, F. Rodríguez, F. Ación, J. García, Model predictive control of pH in tubular photobioreactors. *Journal of Process Control* 14, 377 (2004).
11. J. Doucha, F. Straka, K. Lívanský, Utilization of flue gas for cultivation of microalgae (*Chlorella* sp.) in an outdoor open thin-layer photobioreactor. *Journal of Applied Phycology* 17, 403 (2005).
12. B. S. Ferreira, H. L. Fernandes, A. Reis, M. Mateus, Microporous hollow fibres for carbon dioxide absorption: Mass transfer model fitting and the supplying of carbon dioxide to microalgal cultures. *Journal of Chemical Technology & Biotechnology* 71, 61 (1998).
13. E. Grima, J. Pérez, F. Camacho, R. Medina, Gas-liquid transfer of atmospheric CO₂ in microalgal cultures. *Journal of Chemical Technology and Biotechnology* 56, 329 (1993).
14. P. Talbot, M. Gortares, R. Lencki, J. de la Noüe, Absorption of CO₂ in algal mass culture systems: A different characterization approach. *Biotechnology and Bioengineering* 37, 834 (1991).
15. C. M. Beal, R. E. Hebner, M. E. Webber, R. S. Ruoff, A. F. Seibert, The energy return on investment for algal biocrude: results for a research production facility. *BioEnergy Research* 5, 341 (2012).
16. C. M. Beal *et al.*, Comprehensive Evaluation of Algal Biofuel Production: Experimental and Target Results. *Energies* 5, 1943 (2012).
17. A. Carvalho, L. Meireles, F. Malcata, Microalgal reactors: a review of enclosed system designs and performances. *Biotechnology Progress* 22, 1490 (2006).
18. S. Gao *et al.*, Electro-coagulation-flotation process for algae removal. *Journal of Hazardous Materials* 177, 336 (2009).
19. P. Holt, G. Barton, C. Mitchell, The future for electrocoagulation as a localised water treatment technology. *Chemosphere* 59, 355 (2005).
20. G. Mouedhen, M. Feki, M. Wery, H. Ayedi, Behavior of aluminum electrodes in electrocoagulation process. *Journal of Hazardous Materials* 150, 124 (2008).
21. G. Azarian, A. Mesdaghinia, F. Vaezi, R. Nabizadeh, D. Nematollahi, Algae removal by electro-coagulation process, application for treatment of the effluent from an industrial wastewater treatment plant. *Iranian Journal of Public Health* 36, 57 (2007).
22. P. Chen *et al.*, Review of the biological and engineering aspects of algae to fuels approach. *International Journal of Agricultural & Biological Engineering* 2, 1 (2009).
23. J. Park, R. Craggs, A. Shilton, Wastewater treatment high rate algal ponds for biofuel production. *Bioresource Technology* 102, 35 (2011).
24. O. Pulz, Photobioreactors: production systems for phototrophic microorganisms. *Applied Microbiology and Biotechnology* 57, 287 (2001).

25. Y. Lee, Microalgal mass culture systems and methods: Their limitation and potential. *Journal of Applied Phycology* 13, 307 (2001).
26. Y. Shen, W. Yuan, Z. Pei, Q. Wu, E. Mao, Microalgae Mass Production Methods. *Transactions of the ASABE* 52, 1275 (2009).
27. L. Downing *et al.*, Nitrogen Removal from Wastewater Using a Hybrid Membrane-Biofilm Process: Pilot-Scale Studies. *Water Environment Research* 82, 195 (2010).
28. Y. S. Yun, S. B. Lee, J. M. Park, C. I. Lee, J. W. Yang, Carbon dioxide fixation by algal cultivation using wastewater nutrients. *Journal of Chemical Technology and Biotechnology* 69, 451 (1997).
29. D. Aitken, B. Antizar-Ladislao, Achieving a Green Solution: Limitations and Focus Points for Sustainable Algal Fuels. *Energies* 5, 1613 (2012).
30. L. Christenson, R. Sims, Production and harvesting of microalgae for wastewater treatment, biofuels, and bioproducts. *Biotechnology Advances* 29, 686 (2011).
31. L. B. Christenson, R. C. Sims, Rotating algal biofilm reactor and spool harvester for wastewater treatment with biofuels by-products. *Biotechnology and Bioengineering* 109, 1674 (2012).
32. L. E. de-Bashan, Y. Bashan, Immobilized microalgae for removing pollutants: review of practical aspects. *Bioresource Technology* 101, 1611 (2010).
33. H. V. Perales-Vela, J. M. Pena-Castro, R. O. Canizares-Villanueva, Heavy metal detoxification in eukaryotic microalgae. *Chemosphere* 64, 1 (2006).
34. Q. Gao, Y. Wong, N. Tam, Removal and biodegradation of nonylphenol by different *Chlorella* species. *Marine Pollution Bulletin* 63, 445 (2011).
35. Y. Ghasemi, S. Rasoul-Amini, E. Fotooh-Abadi, The biotransformation, biodegradation and bioremediation of organic compounds by microalgae *Journal of Phycology* 47, 969 (2011).
36. R. Munoz, B. Guieysse, Algal–bacterial processes for the treatment of hazardous contaminants: a review. *Water Research* 40, 2799 (2006).
37. E. P. Kolodziej *et al.*, Municipal wastewater treatment using an OMEGA photobioreactor. *Water Research* Under Review.

Chapter 4: The Future of the OMEGA Concept

4.1 Introduction

The 110-liter OMEGA prototype system operated at the California Department of Fish and Game Wildlife Veterinary Care and Research Center in Santa Cruz, CA proved effective at recovering nutrients from wastewater while sustaining microalgal areal productivities comparable to other cultivation approaches (see **Chapter 3**). To test the feasibility of the proposed configuration at a larger scale, a 1500-liter system was constructed and deployed in an abandoned dissolved air flotation tank located at the San Francisco Southeast Wastewater Treatment Plant (SF SEP). The deployment consisted of four PBR tubes (20.3 cm diameter x 10 m long) constructed of 15-mil linear-low density polyethylene (LLDPE) attached to schedule 40 PVC (10.2 cm) manifolds that connected the PBRs to a centrifugal circulation pump. The system featured swirl vanes (**Figure 2.2**) a gas exchange and harvesting column (GEHC) (**Figure 2.6** and **Figure 4.1**) and utilized the same process control logic utilized by the smaller system operated in Santa Cruz (see **Section 2.5: Process Automation and Data Collection**). The system inoculum consisted of SF SEP secondary final plant effluent (FPE) blended with a mixed culture of green microalgae. Similar to the Santa Cruz deployment, harvesting and refilling the system was performed with the GEHC (see **Section 3.4: Harvesting Procedures, Microalgal Yields and CO₂ Utilization Efficiency**). The operation of the 1500-liter system functioned continuously from February 2012 until decommissioning in June 2012. Unfortunately, estimates regarding areal productivity and nutrient removal rates of this deployment have not yet been determined. However, the success of the SF SEP system lies with the stability of continuous operation, which provides evidence of the soundness of the process control logic and system configuration.

Despite the advances of the OMEGA concept described in this text, there are still operational challenges associated with marine biofouling and techniques needed to improve microalgal harvesting. This chapter addresses these concerns by assessing the impact of marine biofouling on microalgal photosynthesis within OMEGA PBR modules and presents preliminary data on the performance of an electrochemical process developed to improve the microalgal harvesting efficiency of the GEHC. The chapter concludes with a broader discussion of future work and necessary next steps required to advance the development of the OMEGA technology.

4.2 Impact of Biofouling on Microalgal Photosynthesis within OMEGA PBRs

Any full-scale OMEGA deployment must have means to control marine biofouling, which refers to the undesirable accumulation of organisms on submerged surfaces (*1-3*). Development of a biofouling film begins almost immediately with the adsorption of organic material onto newly immersed surfaces, which increases in density and complexity over time (*1, 4*). Biofouling is problematic for OMEGA because it will



Figure 4.1. The 1500-liter OMEGA system deployed at the SF SEP. **(Top)** The system consisted of four PBR tubes 10 m in length connected to a centrifugal circulation pump. **(Bottom)** A scaled version of the GEHC was constructed for supplemental CO₂ injection and as a harvesting location.

add bulk and increase drag on the PBR modules, which may compromise their structural integrity (1, 5). Furthermore, biofouling on OMEGA PBRs will limit transmittance of photosynthetically active radiation (PAR) and suppress rates of microalgal photosynthesis. This presents economic challenges as it will decrease microalgal biomass yields, dampen the performance of OMEGA as a wastewater nutrient recovery process and elevates the operation and maintenance costs of the OMEGA system. To assess the impact of biofouling on the performance of OMEGA, CO₂ consumption, serving as a proxy for photosynthetic activity of microalgae cultivated in a biofouled and clean PBR were compared.

4.2.1 Quantifying the Impacts of Biofouling on Microalgal Photosynthesis

Two identical independent OMEGA systems, each featuring one PBR and one GEHC, were constructed to quantify the impacts of biofouling on microalgal photosynthesis. The PBR modules were deployed in a seawater tank located at the California Department of Fish and Game, Marine Wildlife Veterinary Care and Research Center in Santa Cruz, CA (Lat: 36° 57' 13", Long: -122° 3' 56"), with GEHCs mounted on the exterior of the tank. Heavily biofouled LLDPE PBR tubes, recovered after being deployed for 12-weeks in Moss Landing Harbor, were transported back to the Santa Cruz facility. Once on site, one of the LLDPE PBRs was cleaned to remove the biofouling, while the other remained coated with a biofilm. The two LLDPE PBRs were then cut open and wrapped around two isolated 120-liter polyurethane PBRs deployed in the seawater tank and held in place with zip ties, producing a biofouled system (treatment) and clean system (control) (**Figure 4.2**).

Each system was inoculated with a 120-liters of microalgae mixed with secondary wastewater FPE collected from the Santa Cruz Wastewater Treatment Facility. The flow was circulated through the PBRs at a rate of 75-lpm, with 10% of the total system volume per minute diverted through the GEHC supplemental CO₂ injection. The supervisory control and data acquisition system (SCADA) injected 8.5% CO₂ (V/V) when the pH exceeded 8.25 in response carbon demand exerted by photosynthesizing microalgae. The SCADA system recorded the totalized gas flow for both systems, which was used as a surrogate for rates of photosynthesis (see **Section 2.5.1: Monitoring and Controlling the GEHC with the HMI**).

The experimental data collected over the course of eight days clearly demonstrate that biofouling strongly suppresses photosynthetic activity as represented by CO₂ demand (**Figure 4.3**). Three days into the experiment, the biofouled PBR consumed 77% less CO₂ than the clean PBR. To ensure that this variation was caused by biofouling and not the biological condition of the cultures, the contents of the PBRs were mixed and both systems were re-inoculated to ensure uniform culture density. Then, the sleeves were swapped such that the treatment become the control and vice versa for the remainder of the experiment. This manipulation confirmed that biofouling was the strongest factor influencing rates of photosynthesis, as a similar trend was observed with the biofouled system using 59% less CO₂.

These results suggest that any OMEGA deployment must have means to remove or prevent biofouling from accumulating on the surface of PBRs. If anti-fouling agents are used to prevent marine biofouling, they must be non-toxic to prevent harming the surrounding ecosystem (3, 5). Several authors have described non-toxic anti-fouling compounds designed for ship hulls that could be applicable to the OMEGA system (2-5). However, any such compound must provide good light transmittance, be able to withstand the flexibility of the OMEGA PBRs and be cost effective. Mechanical cleaning methods could also be developed to remove marine biofouling, provided that they are energy efficient, cost effective and non-damaging to the PBRs. Whether these requirements are met will depend on the frequency of cleaning, which will be site-specific and seasonal.

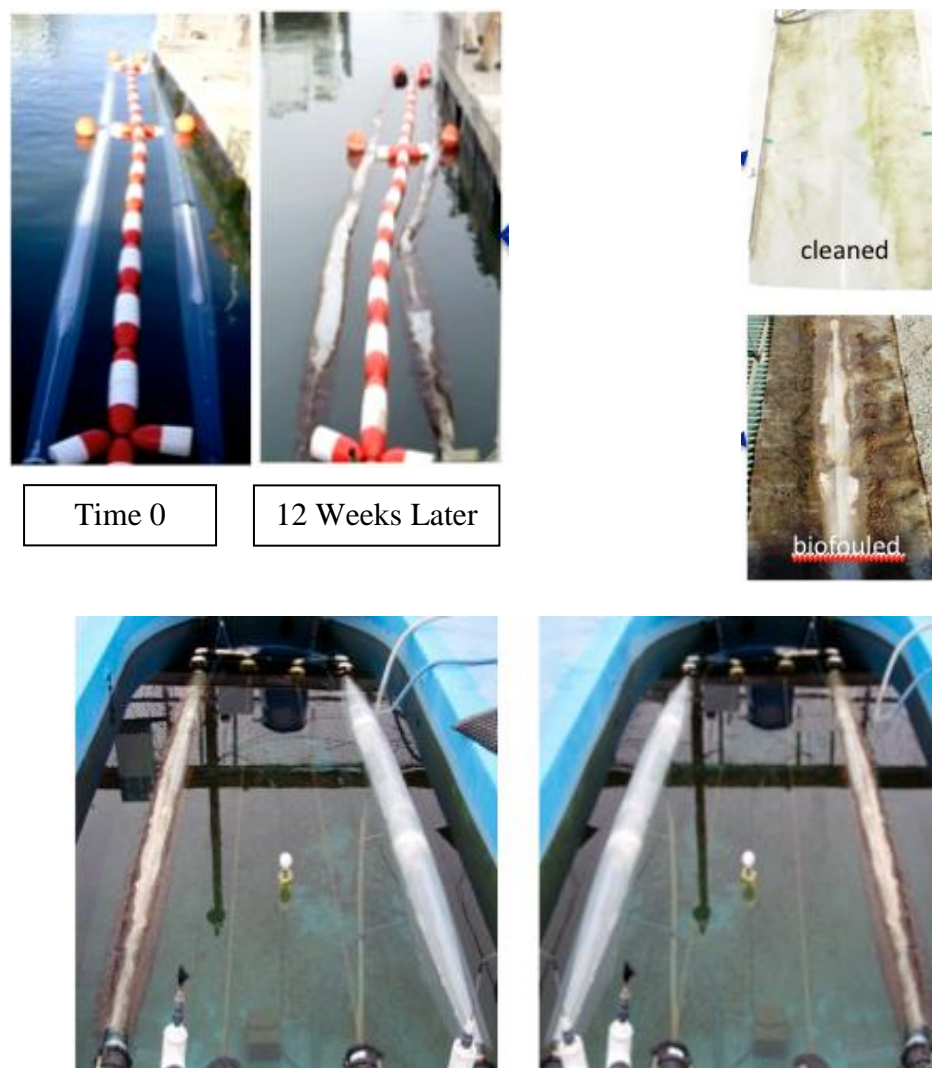


Figure 4.2. (Top Left) The biofouled LLDPE PBR tubes deployed at Moss Landing Harbor at Time 0 and 12 weeks later. (Top Right) The PBR tubes were removed from the harbor and transported to the OMEGA test facility in Santa Cruz, where one on the modules was cleaned while biofouling on the other was left intact. (Above) The biofouled (treatment) and clean (control) LLDPE tubes were cut into sleeves and wrapped around PBR modules deployed in a seawater tanks. The CO_2 consumption, used as a proxy for photosynthetic activity, was used to quantify the light attenuating effects of biofouling. The sleeves were swapped after three days to ensure that biofouling was the driving force inhibiting photosynthesis.

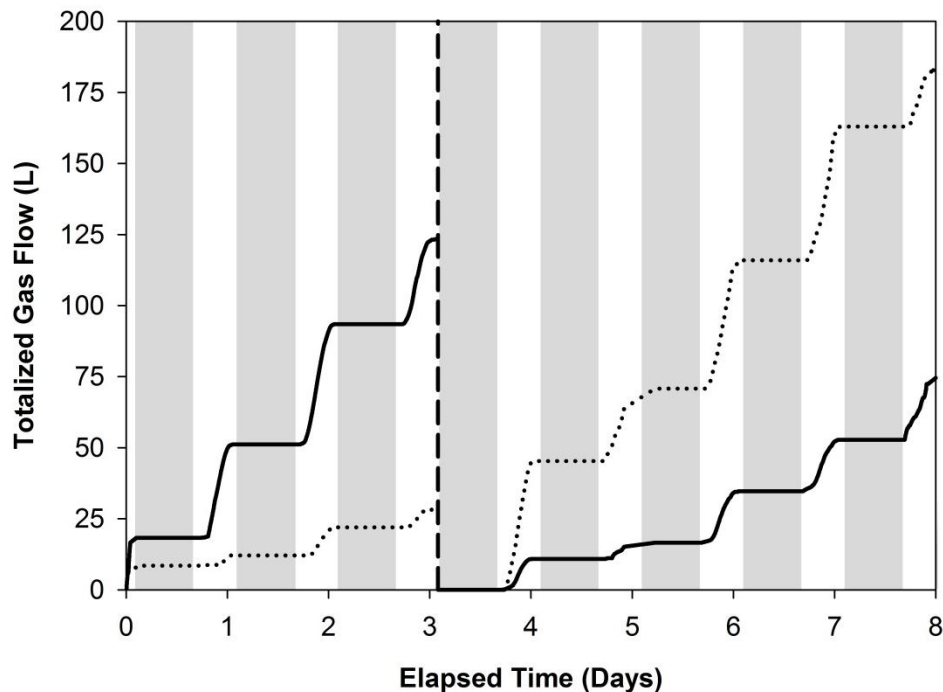


Figure 4.3. The totalized gas flow rate used to express rates of photosynthesis for biofouled and clean OMEGA PBRs. The dotted line during the first three days of the experiment represents CO_2 consumed by the microalgal culture in the biofouled PBR, while the solid line designates the clean PBR. The sleeves were switched at day three (dashed vertical line) and produced a similar trend, indicating that biofouling is the dominant factor suppressing photosynthesis. The grey and white vertical stripes signify the day night cycle, during which time photosynthesis ceases and no CO_2 was demanded by the microalgae.

While surface cleaning of OMEGA modules is essential to ensure efficiency operation, allowing biofouling to accumulate on the underside of the PBRs could prove advantageous as the infrastructure would provide habitat for an extensive community of sessile and associated organisms (6). It is known that introduced surfaces in the marine environment become colonized and can form “artificial reefs” or act as “fish aggregating devices,” which increase local species diversity and expand the food web (7, 8). A large-scale deployment of OMEGA systems may also act as floating “turf scrubbers” and function to absorb anthropogenic pollutants, improving coastal water quality (9).

4.3 Improving Microalgal Harvesting Procedures for the OMEGA System

Harvesting microalgae is a major expense, accounting for an estimated 20-30% of the total biomass production cost (10, 11), making the lack of widely adopted and energy efficient harvesting technologies a major obstacle inhibiting microalgal biofuel

production (12). Challenges associated with microalgal harvesting stem from their small size, low specific gravity and negative surface charges that produce stable suspensions throughout the water column (13-18). These surface charges attract counter ions from the bulk solution, producing a diffuse ionic cloud that surrounds the microalgal cell (19). This diffuse ionic cloud together with the microalgal cell surface charge forms the electrical double layer (EDL) (19). As microalgal cells approach each other in solution, their EDLs overlap such that the concentration of counter ions increases (20), resulting in an electrostatic barrier that prevents the formation of larger aggregates that facilitate liquid-solid separation (**Figure 4.4**). Measurement of this electrical potential, referred to as the zeta potential, indicates the apparent surface charge of suspended particles (21) and directly impacts the efficiency of microalgal harvesting systems (22).

Destabilizing microalgal suspensions is performed using coagulants that either (1) decrease the zeta potential, which reduces electrostatic repulsion between cells and facilitates flocculation, (2) remove suspended particles as they bind to insoluble coagulants that precipitate from solution, or (3) a combination of both mechanisms (23, 24). Henderson et al. (22) observed aggregation and clear separation of microalgal cells from the culture broth when aluminum sulfate was used as a coagulant, but noted poor separation when the zeta potential was stronger (more negative) than -10 mV. To assess the stability of microalgae cultivated using the OMEGA prototype, zeta potential measurements were collected using ZetaPlus zeta potential analyzer (Brookhaven Instruments, Holtsville, NY). Samples collected during prototype operation demonstrated a strongly negative zeta potential that ranged from -9.69 mV and -24.34 mV with a mean of -17.57 ± 0.31 mV ($n = 100$) for pH values between 7.59 and 10.23 (**Figure 4.5**). This strongly negative zeta potential suggests that sedimentation in the GEHC without addition of coagulants will yield a poorly compacted sludge. Indeed, this was observed during operation of the 110-liter prototype, which only concentrated the biomass by a factor of 2.0 ± 0.1 ($n = 7$) for experiment 1 and 1.4 ± 0.1 ($n = 7$) for experiment 2 (see section **3.6.1: GEHC Performance**). Therefore, the design of the GEHC must be expanded to include means for improving microalgal harvesting efficiency.

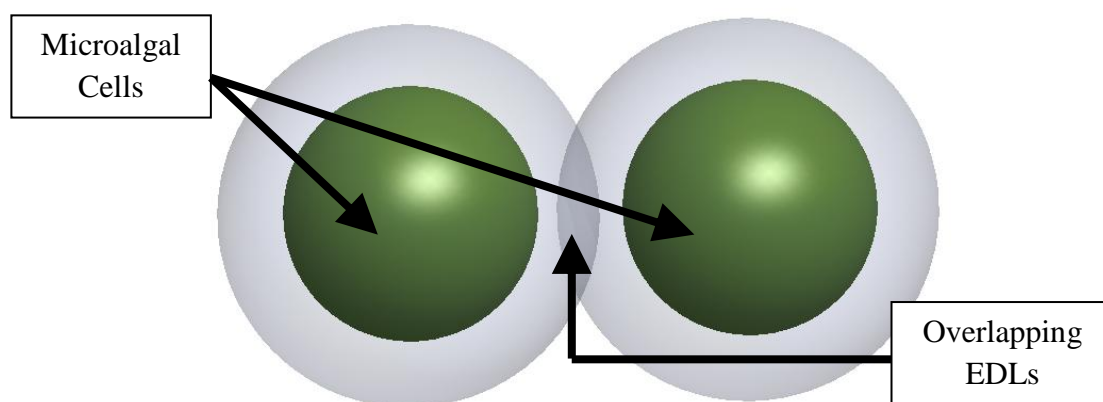


Figure 4.4. Illustration of microalgal cells as they approach each other in the bulk solution. Overlapping EDLs produce an electrostatic force that prevents aggregation and keeps cells suspended in the culture broth.

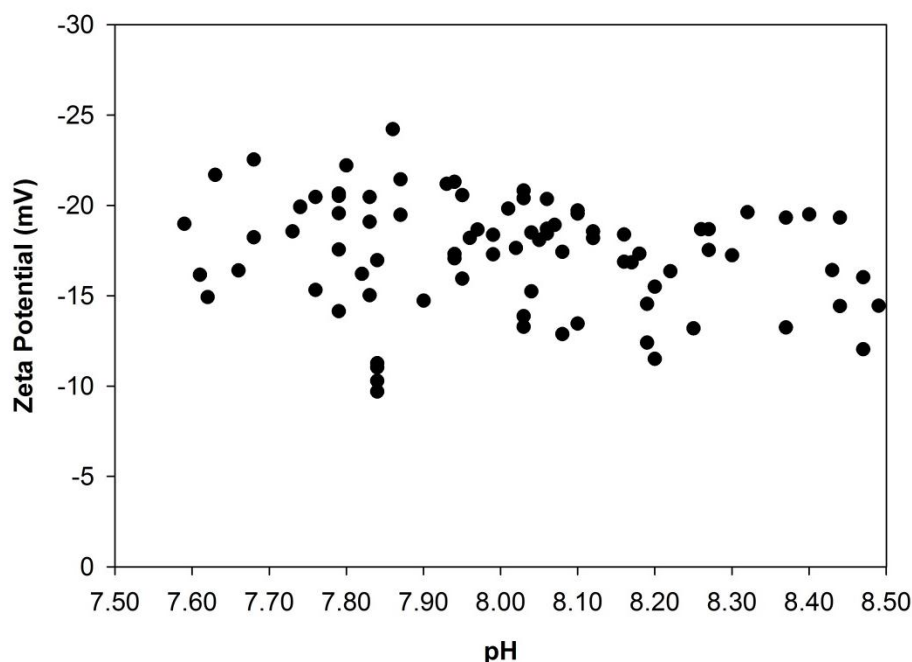


Figure 4.5. Zeta potential of microalgae cultivated using the OMEGA prototype with changing pH. The zeta potential remains strongly negative regardless of pH, indicating that coagulating agents are needed to improve the sedimentation efficiency in the GEHC.

4.3.1 Harvesting Through the GEHC

A full-scale OMEGA deployment constructed using the proposed configuration would consist of multiple GEHCs that would serve as both harvesting locations and effluent discharge points (**Figure 4.6**). Efficient separation of microalgae from the wastewater in the GEHC is necessary to improve the economics of biomass production, and is also required from a wastewater treatment perspective, as it will be necessary to reduce TSS and chemical oxygen demand (COD) of OMEGA final effluent.

During prototype operation at the Santa Cruz location, the GEHC was isolated from the PBR and drained into a barrel. The microalgae was then concentration using suspended air flotation (SAF), which has proven to be an effective, inexpensive, high-rate harvesting system for recovering microalgal biomass from wastewater (17). SAF units generate electrically charged microbubbles using surfactants that adhere to microalgae flocculated with coagulating agents. The microbubbles then force the biomass to the surface of the containment vessel as the bubbles rise through the water column. The biomass is then skimmed from the surface and further dewatered to produce a dry microalgal cake (**Figure 4.7**). While SAF is effective at harvesting microalgae, integrating this technology into the GEHC is challenging because it would require each

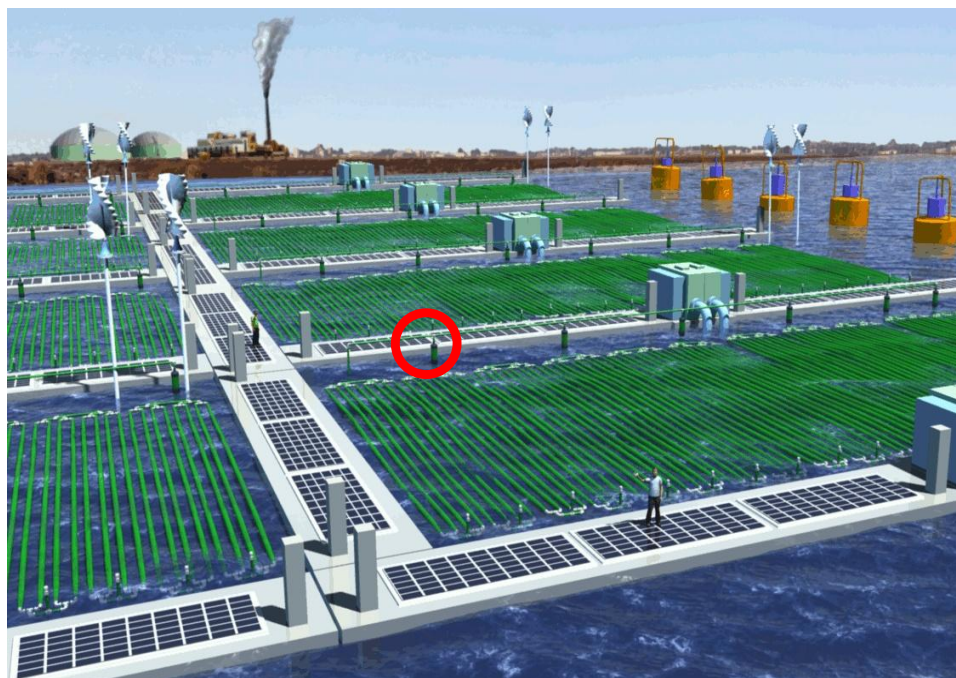


Figure 4.6. Conceptual illustration of a full-scale OMEGA deployment. The red circle identifies one of many GEHCs distributed throughout the system. The GEHC serves as both a harvesting point and an effluent discharge point.

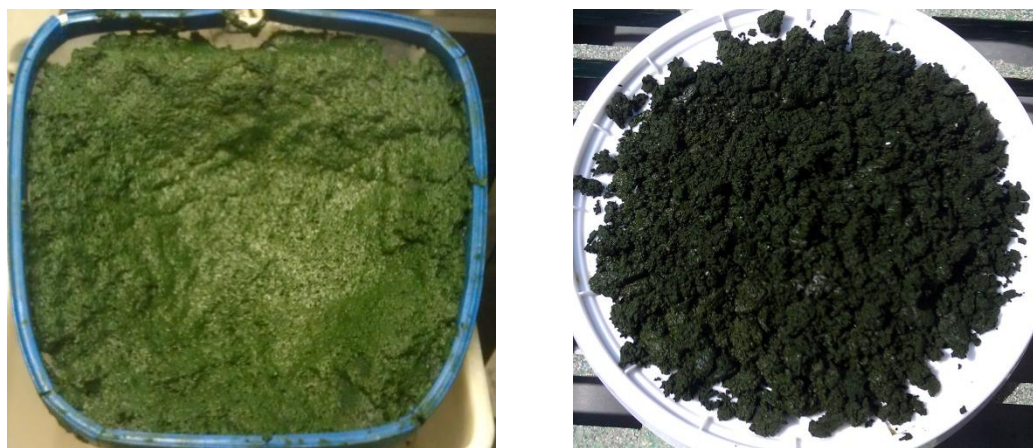


Figure 4.7. (Left) Microalgae removed from the surface of a harvesting barrel using a pool skimmer after being thickened with Suspended Air Flootation. (Right) The biomass was then squeezed by hand to produce a more concentrated microalgal paste.

GEHC to have a skimming mechanism to remove thickened biomass and means of chemical injection. A more appropriate technique to improve microalgal harvesting in the GEHC would be to use coagulants and sedimentation. Using this approach, harvesting would occur in batches, where microalgal biomass would be removed through the GEHC drain valve and pumped to a central location for further dewatering. Once the microalgae are removed, the clear supernatant would be discharged to the receiving water as final effluent.

Electrocoagulation (EC), which generates coagulating agents *in situ*, is a suitable technology for OMEGA because it has no moving parts, needs little maintenance, requires only electricity as an input, is amenable to automation and can be easily integrated into the GEHC (25-27). To evaluate the technical feasibility of this approach, an EC system was constructed and incorporated into the GEHC.

4.3.2 Construction and Operation of an EC Unit for the GEHC

The EC process developed for the OMEGA system was designed to generate coagulants that destabilize microalgal suspensions *in situ*, through the electrochemical oxidation of consumable aluminum electrodes mounted on the exterior of the GEHC (**Figure 4.8**). The electrode assembly, consisting of an anode and cathode (137 x 24 x 4.8 mm each), were held together using non-conductive plastic spacers that provided an electrode gap of 0.25 or 0.50 cm. The electrodes were then inserted into a section of clear schedule 40 PVC (2.54 cm I.D.) with plastic unions on both ends to facilitate rapid installation and removal from the GEHC plumbing (**Figure 4.9**). Wires attached to each electrode were connected to stainless steel machine screws threaded into the clear PVC housing to provide connection to the DC power supply used operate the process. The plumbing was configured such that the GEHC could be isolated from the PBR when EC system was initiated. Once isolated from the PBR, the GEHC pump could recycle the contents of the GEHC past the EC electrodes and through a static mixer until the desired coagulant dose was reached. Once the desired dose was achieved, the GEHC pump could be stopped, providing time for the coagulated microalgae to collect in the GEHC settling chamber (see **Figure 2.6**).

Control and operation of the EC system was performed using the SCADA system, which utilized several field devices, sensors and equipment to measure pH, temperature, conductivity, voltage, amperage, and provided a source of DC power to run the process (**Table 4.1**). Data from the field devices were transmitted to a human-machine interface (HMI) created using LookoutDirect Software (Automation Direct, Cumming, GA) by a DL06 programmable logic controller (PLC) (Automation Direct, Cumming, GA) contained in Control Cabinet B with other electronics used by the EC harvester (**Figure 4.10**). The harvesting HMI enabled operators to enter several process control parameters essential to efficient EC operation, including desired coagulation dosing rate, harvest volume and amperage to be applied to the electrodes (**Figure 4.11**). Operators could also set a timer that would change the polarity of the electrodes to prevent the formation of an insulating passivation layer on the anodes that results from prolonged operation (28). This insulating layer is detrimental to EC operation because the applied voltage must be increased to overcome the additional resistance, resulting in greater power consumption.

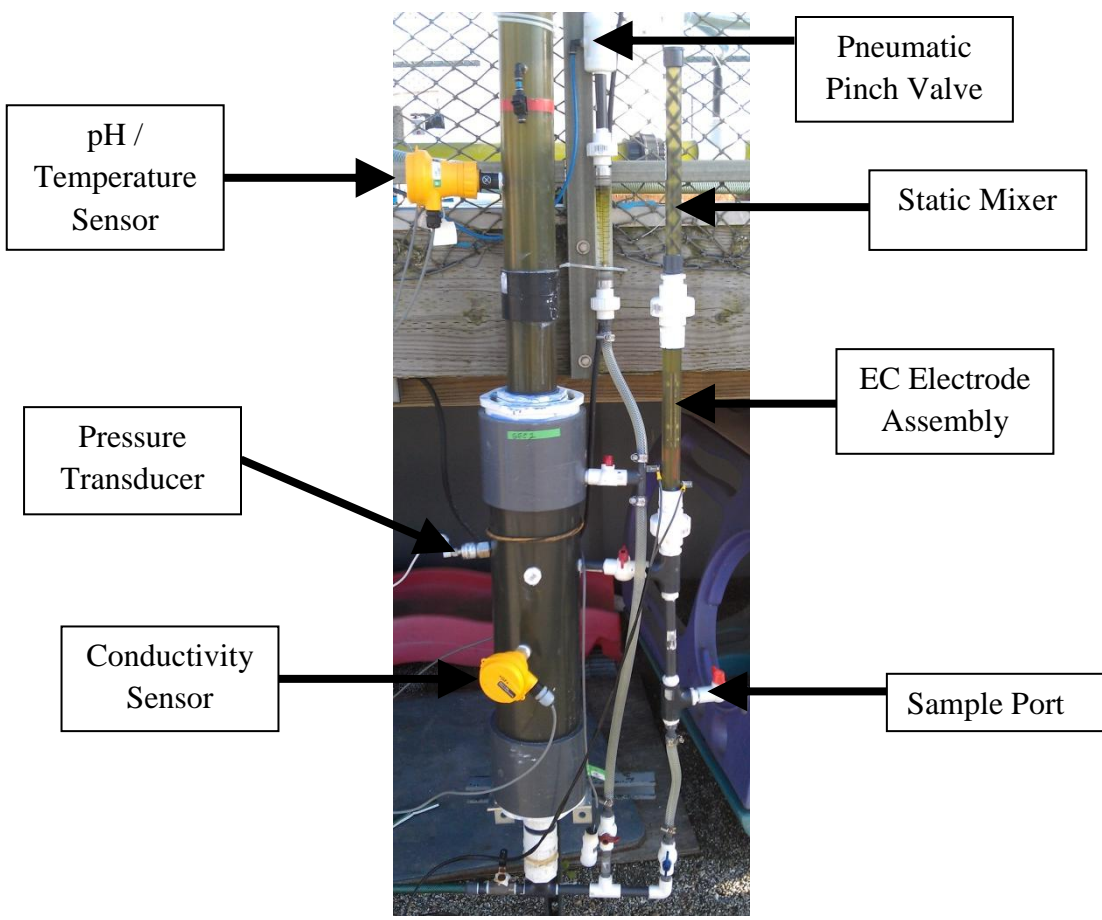


Figure 4.8. Installation of the EC system into the GEHC. Valves in the plumbing isolated the GEHC from the PBR enabling the GEHC pump to recycle flow between the EC electrode plates. Once the desired coagulant dose was delivered, the GEHC was designed to act as a sedimentation pit to collect flocculated microalgal biomass.

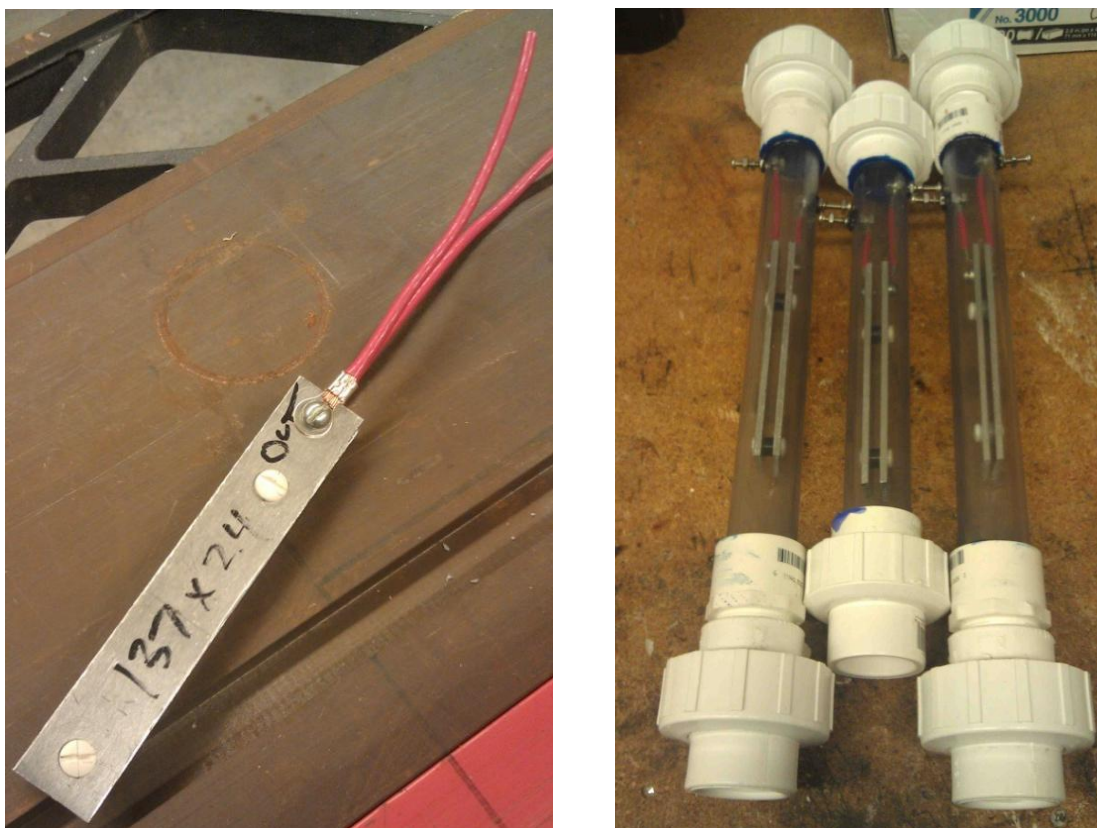


Figure 4.9. (Left) Freshly fabricated aluminum electrodes with wires for the anode and cathode. The electrodes were held together using non-conductive plastic screws and spacers to prevent shorting. (Right) The electrode assembly was inserted inside transparent PVC tubes with union-style end caps to make installation and removal from the GEHC plumbing fast and easy.

Table 4.1. Description and location of the sensors and equipment used by the EC harvesting system.

Sensor / Equipment	Manufacturer and Model Number	Input Signal	Output Signal	Scale	Location	Function
DC Current Transducer	Automation Direct, DCT100-42-24-S	none	4-20 mA	0-50 amps	Control Cabinet B	Measured the current output of the DC power supply. The PLC used this value to control the current output of the DC power supply.
DC Voltage Transducer	CR Magnetics, CR5311-50	none	0-10 VDC	0-50 VDC	Control Cabinet B	Measured the voltage output of the DC power supply. This value was used to calculate the power consumed during EC operation.
DC Power Supply	Acopian, Y030LX2400	0-10 VDC	not used	Maximum Output 0-30 VDC, 0-24 amps	Control Cabinet B	The DC power supply provided the power needed to dissolve aluminum into solution for coagulating microalgae. The power supply was operated in "constant current" mode to deliver consistent dosing.
Relay 1	Automation Direct, 755-2CD-24D	12 VDC	none	Digital On/Off	Control Cabinet B	Pressing "Start" on the HMI closed this relay and started the DC power supply to initiate EC harvesting process.
Relay 2	Automation Direct, 755-2CD-24D	12 VDC	none	Digital On/Off	Control Cabinet B	Activating this relay changed the polarity of the aluminum electrodes to prevent passivation. The frequency is established using the HMI.
pH Sensor	GF Signet, 2750 (combined with temperature sensor)	none	0-10 VDC	0-14	GEHC	Measured pH in the GEHC and was used to calculate the solubility of dissolved aluminum and the molar fractions using ionization constants.

Temperature Sensor	GF Signet, 2750 (combined with pH sensor)	none	0-10 VDC	0-50 C	GEHC	Measured temperature in the GEHC and was used by the PLC to calculate ionization constants using the van't Hoff equation.
Conductivity Sensor	GF Signet, 2850	none	4-20 mA	0-10,000 $\mu\text{S cm}^{-1}$	GEHC	Measured the conductivity in the GEHC to establish a relationship between conductivity and power consumption during EC operation.

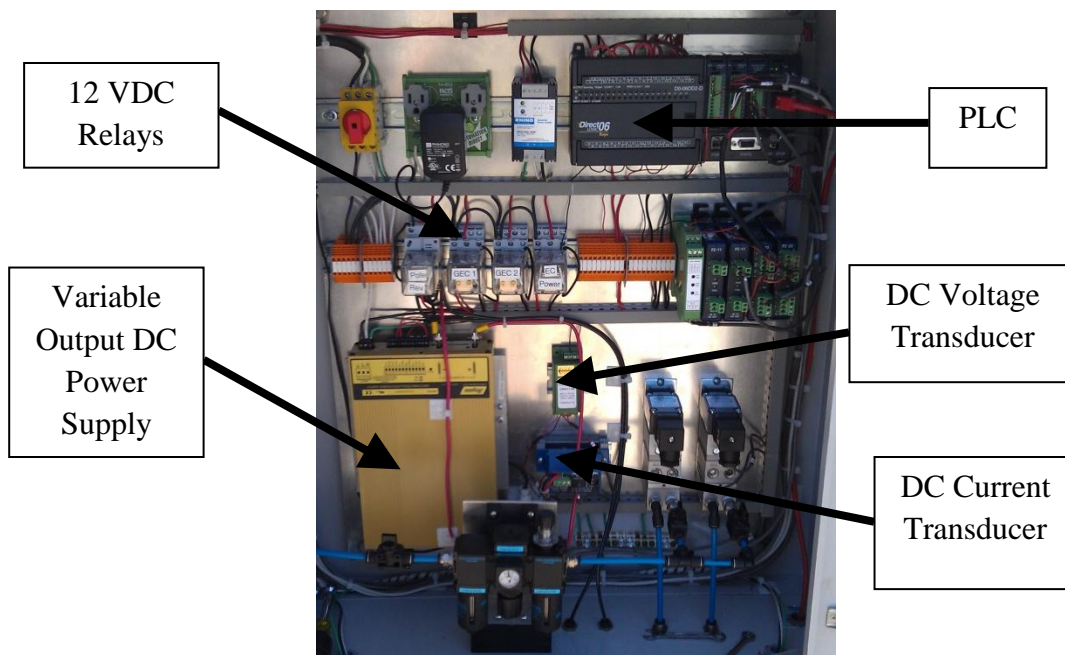


Figure 4.10. Control Cabinet B containing electronics for operating the EC harvest system. The EC process is a low-maintenance, energy efficient process that can be controlled precisely with automation tools.

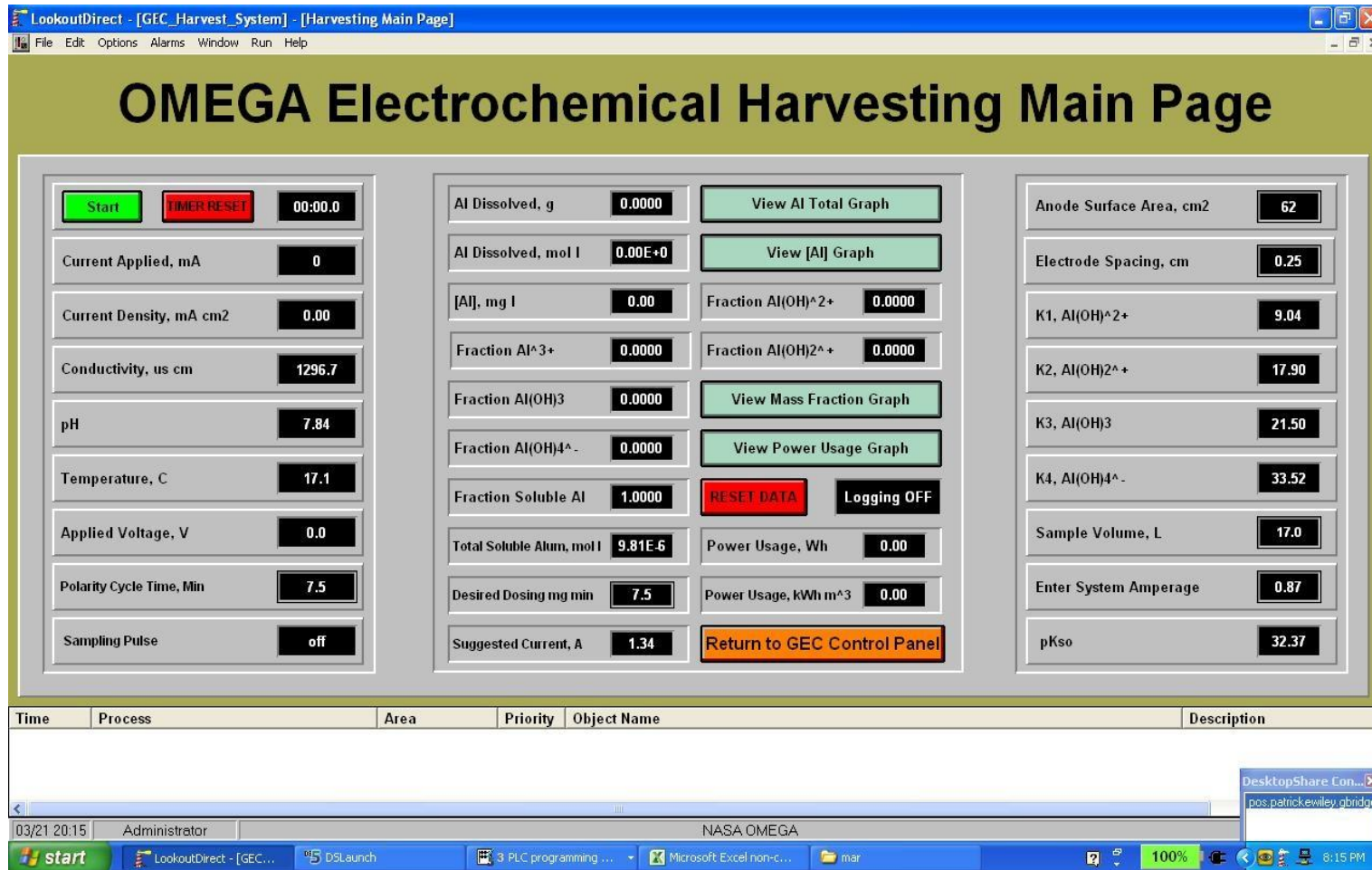


Figure 4.11. The HMI for operating the EC harvesting system. Boxes with the double border accept operator inputs that control coagulant dosing, polarity cycling and calculate power usage. Operators begin the harvest cycle by clicking the green “Start” button, which automatically initiates data logging. The system stops automatically once the desire coagulant dose has been delivered. Molar mass fractions and total soluble aluminum are calculated using ionization constants, pH and temperature.

Upon entry of the desired process control parameters, the EC harvest cycle was initiated by clicking the “Start” button on the HMI. Once engaged, the “Start” button closed a relay that energized the DC power supply, thereby delivering the specified current to the electrodes and dissolving aluminum into solution. The total amount of aluminum ($[Al]_T$) dissolved into solution during EC operation could be quantified using Faraday’s Law (**Equation 4.1**), given that the PLC measured the magnitude and duration of electrical current applied to the electrodes.

$$w = \frac{ItM}{zF} \quad (4.1)$$

Where,

w	= Aluminum dissolved into solution, g Al cm ⁻²
I	= Current density, A cm ⁻²
t	= Time, seconds
M	= Molecular weight of aluminum, g mol ⁻¹
z	= Number of electrons involved in the redox reaction, 3
F	= Faraday’s constant, 96,485 C mol ⁻¹

Several monomeric species, described with **Equations 4.2 – 4.5**, with different coagulation properties are produced when the aluminum generated by EC is released into solution and hydrolyzed.



Using pH values measured during EC operation, the PLC determined $[Al^{3+}]$, mass fraction of each aluminum species (α_i) using ionization constants (K_i) (**Equations 4.6 – 4.11**) and calculated the solubility of aluminum generated using the K_{s0} (**Equation 4.12**) to quantify the formation of precipitates. The van’t Hoff equation was used by the PLC to automatically adjust these constants using temperature measurements in the GEHC (**Equation 4.13**).

$$Al^{3+} = \frac{[Al]_T}{1 + K_1[OH^{-}] + K_2[OH^{-}]^2 + K_3[OH^{-}]^3 + K_4[OH^{-}]^4} \quad (4.6)$$

$$\alpha_1, Al^{3+} = \frac{Al^{3+}}{[Al]_T} \quad (4.7)$$

$$\alpha_2, Al(OH)^{2+} = \frac{[Al^{3+}] \cdot K_1 \cdot [OH^{-}]}{[Al]_T} \quad (4.8)$$

$$\alpha_3, Al(OH)_2^{+} = \frac{[Al^{3+}] \cdot K_2 \cdot [OH^{-}]^2}{[Al]_T} \quad (4.9)$$

$$\alpha_4, Al(OH)_3 = \frac{[Al^{3+}] \cdot K_3 \cdot [OH^{-}]^3}{[Al]_T} \quad (4.10)$$

$$\alpha_5, \text{Al(OH)}_4^- = \frac{[\text{Al}^{3+}] \cdot K_2 \cdot [\text{OH}^-]^4}{[\text{Al}]_T} \quad (4.11)$$

$$\text{Al}_{T,\text{sol}} = \frac{K_{s0}}{[\text{OH}^-]^3} \left(1 + K_1 [\text{OH}^-] + K_2 [\text{OH}^-]^2 + K_3 [\text{OH}^-]^3 + K_4 [\text{OH}^-]^4 \right) \quad (4.12)$$

$$K_i T_2 = K_i T_1 e^{-\frac{\Delta H}{R} \left(\frac{1}{T_2} - \frac{1}{T_1} \right)} \quad (4.13)$$

Where,

K_i	= Ionization constant, unitless
T_2	= Final temperature, K
T_1	= Initial temperature, K
ΔH	= Enthalpy change, kJ mol^{-1}
R	= Ideal gas constant, $8.314 \times 10^{-3} \text{ kJ mol}^{-1}\text{K}^{-1}$

Understanding the molar fraction is important during EC operation because the variable charge density of the hydrolyzed aluminum influences coagulant dosing and provides insight regarding the mechanisms of coagulation. For example, higher proportions of Al^{3+} cations in solution facilitate coagulation through a “charge neutralization” mechanism that reduces electrostatic repulsion and compresses the EDL, enabling particle aggregation due to van der Waals attractive forces (26). In contrast, as aluminum precipitates from solution, microalgae aggregate mostly due to a “sweep-coagulation” mechanism, which does not neutralize particle charges, but rather traps particles within the precipitates, which promotes sedimentation. Given that the pH range observed in the GEHC during prototype operation remained between 7.20 and 7.80 (see **Figure 3.4**), it is likely that a “sweep-coagulation” mechanism will dominate microalgal coagulation due to the limited solubility of aluminum within this pH range (**Figure 4.12**).

When the desired coagulant dose was delivered, as indicated by **Equation 4.1**, the relay activating the DC power supply would automatically disengage, turn off the DC power supply, and terminate the harvest cycle and data logging. At this point, the HMI would display all process data, including power usage expressed as kWh m^{-3} , until the next harvest cycle was initiated.

4.3.3 Preliminary Performance Results of the EC System

Two experimental trials were conducted to measure the power consumption of the EC system and to assess its ability to deliver the desired coagulant dose. During the first experiment, 10 liters of deionized water contained in a plastic bucket was pumped in a closed loop past the aluminum electrodes, which were spaced 0.5 cm apart (**Figure 4.9**). Due to the low conductivity of deionized water, sodium chloride was added to solution to ensure that the power supply could provide adequate voltage to deliver the necessary amperage. The resulting conductivity increased to $937 \mu\text{S cm}^{-1}$, which is similar to values observed for FPE. An aluminum dosing rate of $1 \text{ mg l}^{-1} \text{ min}^{-1}$, requiring 1.7 amps of current, was entered using the HMI and the system was initiated for a ten-minute cycle. Samples were collect at each one-minute interval and analyzed for total aluminum using a Hach DR2800 spectrophotometer (method number 8012). Results from this analysis matched very closely to the total aluminum concentration predicted by the PLC

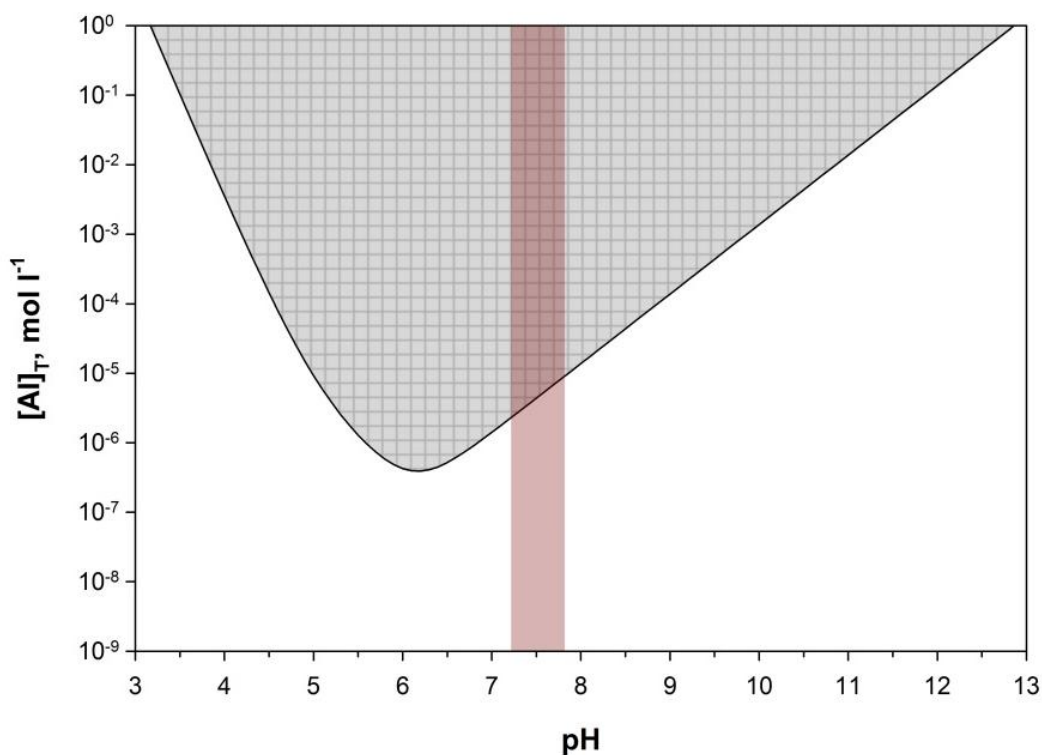


Figure 4.12. Solubility of aluminum as influenced by pH. The gray-shaded region designates the zone of precipitation, while vertical red bar represents the pH range observed in the GEHC during prototype operation. This suggests that a “sweep-coagulation” mechanism will likely dominate this application.

using Faraday’s Law, indicating that the EC system functions as designed (**Figure 4.13**). At the end of the harvest cycle, it was noted that the applied voltage fluctuated between 25.9 and 26.9 VDC to maintain consistent amperage. This corresponds to 0.78 kWh m^{-3} of power consumed when the EC system is operated using the specified parameters. This experimental approach was repeated using microalgae grown in FPE as the solution, rather than distilled water. During this experiment the system was operated for 20 minutes using the same dosing rate of $1 \text{ mg l}^{-1} \text{ min}^{-1}$. As the conductivity of the FPE / microalgal solution was slightly higher than that of the distilled water experiment at $1,006 \text{ }\mu\text{S cm}^{-1}$, the voltage requirements were less, ranging between 21.6 and 24.1. However, because the duration of operation was twice as long, the power consumption for the whole harvest cycle increased to 1.4 kWh m^{-3} . While this is higher than the 0.3 kWh m^{-3} reported by Poelman et al. (29) for the recovery of microalgae from drinking water, it should be noted that the objective of this exercise was to observe overall system functionality and not to optimize coagulant dosing.

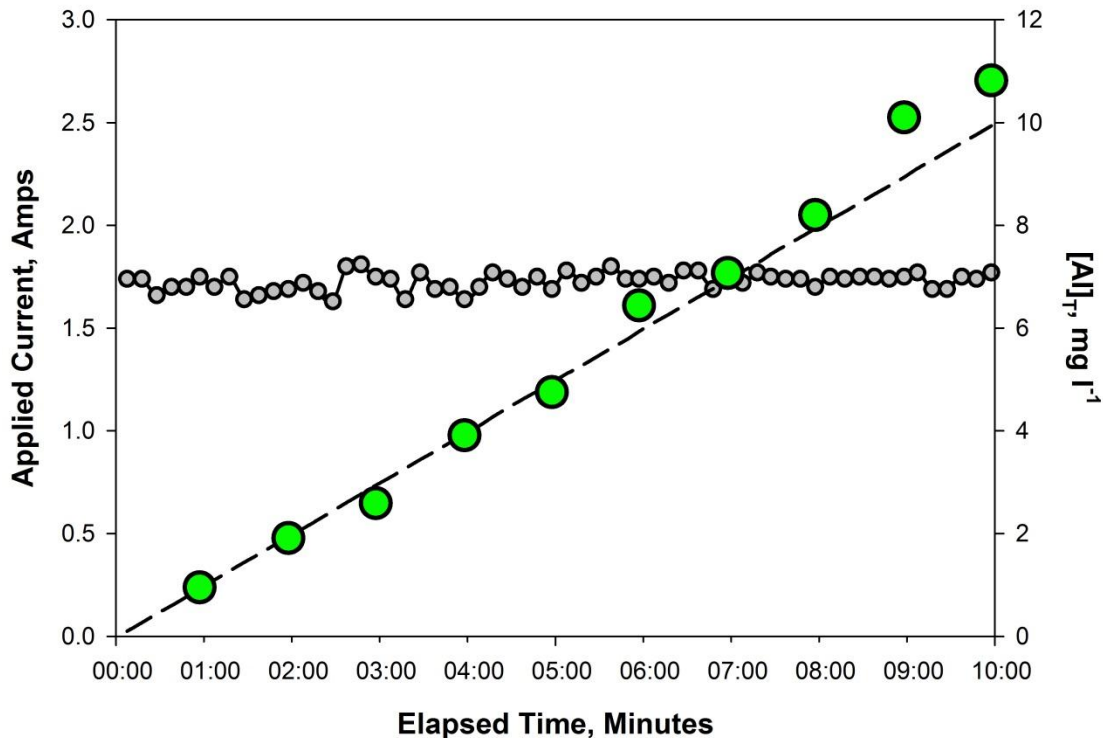


Figure 4.13. Total aluminum concentration predicted by Faraday's Law (dashed line) compared to the actual amount delivered by the EC unit in a sodium chloride solution (green dots). The SCADA system adjusts the voltage of a DC power supply to ensure that the current applied to the electrodes remains constant (gray dots).

When using the EC process to harvest microalgae, the total aluminum concentration measured using the Hach DR 2800 was nearly 40% less than the amount predicted by the PLC for all samples (**Figure 4.14**). Holt et al. (30) observed a similar result when using EC for the destabilization of clay particles, which was attributed to a binding mechanism where coagulants adhere to suspended material and are removed from solution. This type of interaction is likely occurring with the microalgae, as the aluminum concentration measured during the distilled water experiment, which did not contain suspended particles, matched very closely with the theoretical prediction.

The microalgal culture coagulated with the EC system was transferred to a transparent cylinder and allowed to settle overnight. Qualitatively, the separation of the microalgae seemed adequate, as a dense microalgal mat accumulated below clear supernatant (**Figure 4.15**). However, further research is needed to determine the ideal coagulant dose and to improve the energy efficiency of the EC process. Henderson et al. (22) successfully used zeta potential measurements to optimize the dosing of aluminum sulfate for coagulating microalgae. This approach would be applicable to the EC process if a link between microalgal cell density, zeta potential, coagulant dosing, and

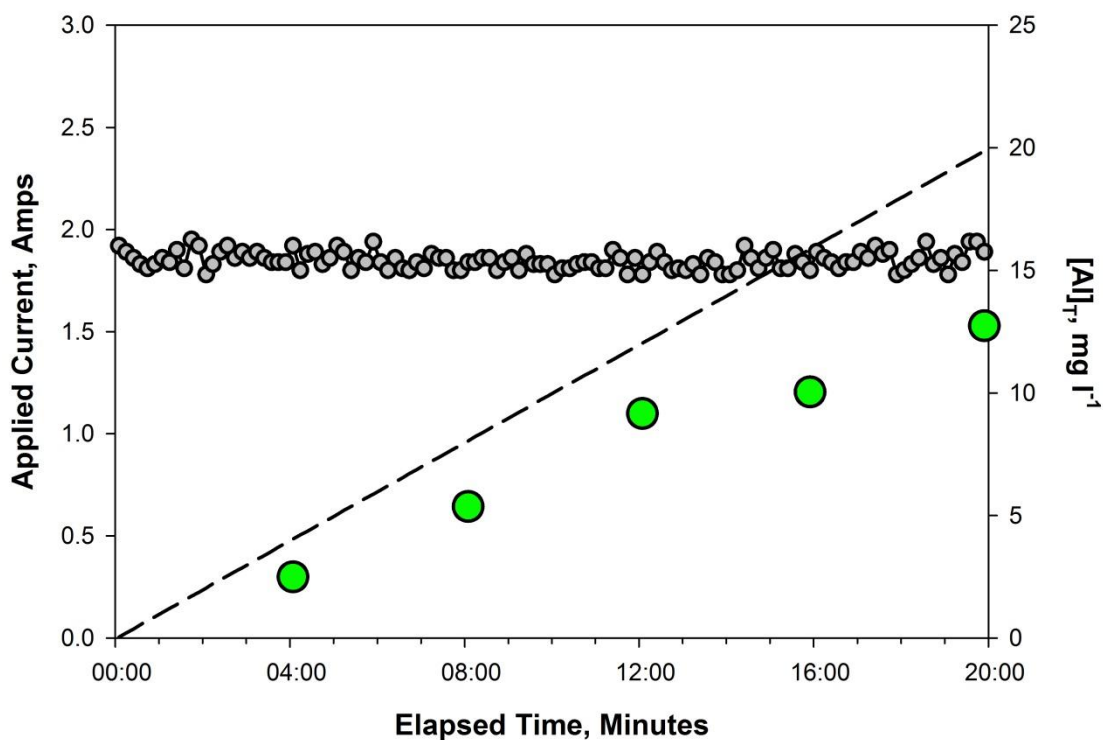


Figure 4.14. Theoretical aluminum concentration predicted with Faraday's Law (dashed line) compared to the actual amount (green dots) measured after an EC cycle was conducted on a microalgal culture. The discrepancy between theoretical and observed dosing is likely due to coagulants binding to the microalgal cells, as current (gray dots), and thus dosing, remained constant throughout the cycle.



Figure 4.15. Sedimentation of microalgal biomass after being subjected to an EC harvest cycle. When used with a GEHC, the dense microalgal mat will be removed, while the clear supernatant is discharged as final effluent.

sedimentation rates can be established. Connecting these parameters would make zeta potential measurements an important process control tool that could efficiently regulate the amount of current applied to the electrodes. However, an inexpensive, flow-through zeta potential field unit capable of interfacing with PLCs does not presently exist.

Energy requirements can be reduced by decreasing the electrode gap and increasing the conductivity of the culture in the GEHC with the addition of surrounding seawater. To quantify the impact of this approach, contents of the GEHC were passed through electrodes with a 0.25 cm gap. The conductivity of the solution, which consisted of microalgae mixed with FPE, was increased to $2,600 \mu\text{S cm}^{-1}$ through the addition of seawater. The system was operated at a current setpoint of 1.1 amps, which required only 4.8 volts. Operating under these conditions would reduce the power consumed during the deionized water experiment from 0.78 to 0.14 kWh m^{-3} . Similarly, the power consumed during the microalgal harvest cycle would have been reduced from 1.4 to 0.29 kWh m^{-3} , performance numbers predicted to make EC more economically viable than use of liquid coagulants (29).

In addition to the previously described knowledge gaps, research identifying the ideal placement and configuration of the electrodes within the GEHC is needed. This configuration must provide adequate coagulant mixing and enable easy replacement and inspection of the electrodes. Furthermore, systems enabling automatic removal of microalgal biomass that has accumulated in the GEHC settling chamber following EC and discharge of the clear supernatant as OMEGA final effluent must be developed.

4.4 Concluding Thoughts

OMEGA has the potential of co-locating microalgae cultivation with wastewater treatment to produce a biofuel feedstock that does not compete with agriculture for water, fertilizer, or land (31). This work provides credibility to the OMEGA approach, as the prototype system had an overall areal productivity of $14.1 \text{ g m}^{-2} \text{ day}^{-1}$, with peaks above $20 \text{ g m}^{-2} \text{ day}^{-1}$, which is consistent with reported U.S. average microalgae productivity of $13.2 \text{ g m}^{-2} \text{ day}^{-1}$ (32). Additionally, the microalgae consistently removed >90% of the ammonia from the secondary-treated FPE, suggesting that a scaled-up system could also provide effective wastewater treatment services.

Many open questions remain with regard to the feasibility of large-scale OMEGA systems. The small-scale prototype OMEGA systems were intended for experimentation and were not designed for energy efficiency or economical scale up. For large-scale OMEGA deployment dense configurations of PBRs, improved hydrodynamics, optimized pumping and mixing, more sophisticated process control algorithms and effective harvesting protocols will be needed to increase yields, improve the energy return on investment, and lower operating costs. Advances forward osmosis (FO) membrane technology and PBR manufacturing are needed to fully ingrate FO into OMEGA modules and ensure reliable operation. In addition, questions about the impact of biofouling, concerns about engineering systems that can cope with marine environments and issues around both environmental impact and environmental regulations will need to be answered. It remains to be seen if the need for sustainable biofuels will drive the innovation necessary to address these questions to develop large-scale OMEGA systems.

4.5 Acknowledgements

Parts of this work are published or are currently being reviewed for publication in the following papers:

- P. Wiley *et al.*, Microalgae cultivation using offshore membrane enclosures for growing algae (OMEGA). *Journal of Sustainable Bioenergy Systems* 3, 18 (2013).
- Harris, L., S. Tozzi, P. Wiley, C. Young, J. Richardson, K. Clark, J. Trent (2013). Potential impact of biofouling on the proposed offshore membrane enclosures for growing algae (OMEGA). *Bioresource Technology*. Under review.
- J. Trent, P. Wiley, S. Tozzi, B. McKuin, S. Reinsch, Research Spotlight: The future of biofuels: is it in the bag? *Biofuels* 3, 521 (2012)

4.6 References

1. J. D. Zardus, B. T. Nedved, Y. Huang, C. Tran, M. G. Hadfield, Microbial biofilms facilitate adhesion in biofouling invertebrates. *The Biological Bulletin* 214, 91 (2008).
2. J.-P. Maréchal, C. Hellio, Challenges for the development of new non-toxic antifouling solutions. *International Journal of Molecular Sciences* 10, 4623 (2009).
3. J. A. Callow, M. E. Callow, Trends in the development of environmentally friendly fouling-resistant marine coatings. *Nature Communications* 2, 244 (2011).
4. C. M. Kirschner, A. B. Brennan, Bio-Inspired antifouling strategies. *Annual Review of Materials Research* 42, 211 (2012).
5. M. Schultz, J. Bendick, E. Holm, W. Hertel, Economic impact of biofouling on a naval surface ship. *Biofouling* 27, 87 (2011).
6. L. Harris *et al.*, Potential impact of biofouling on the proposed offshore membrane enclosures for growing algae (OMEGA). *Bioresource Technology* Under review, (2012).
7. J. H. Bailey-Brock, Fouling community development on an artificial reef in Hawaiian waters. *Bulletin of Marine Science* 44, 580 (1989).
8. F. Kerckhof, B. Rumes, A. Norro, T. Jacques, S. Degraer, Seasonal variation and vertical zonation of the marine biofouling on a concrete offshore windmill foundation on the Thornton Bank (southern North Sea). (2010).
9. W. Mulbry, P. Kangas, S. Kondrad, Toward scrubbing the bay: Nutrient removal using small algal turf scrubbers on Chesapeake Bay tributaries. *Ecological Engineering* 36, 536 (2010).
10. R. Levine, A. Oberlin, P. Adriaens, A Value Chain and Life Cycle Assessment Approach to Identify Technological Innovation Opportunities in Algae Biodiesel. *Nanotech* 3, 1 (2009).
11. E. Molina Grima, E. Belarbi, F. Ación Fernández, A. Robles Medina, Y. Chisti, Recovery of microalgal biomass and metabolites: process options and economics. *Biotechnology Advances* 20, 491 (2003).
12. N. Uduman, Y. Qi, M. Danquah, G. Forde, A. Hoadley, Dewatering of microalgal cultures: A major bottleneck to algae-based fuels. *Journal of Renewable and Sustainable Energy* 2, 012701 (2010).
13. W. Bare, N. Jones, E. Middlebrooks, Algae removal using dissolved air flotation. *Journal of the Water Pollution Control Federation* 47, 153 (1975).
14. R. Craggs, P. McAuley, V. Smith, Wastewater nutrient removal by marine microalgae grown on a corrugated raceway. *Water Research* 31, 1701 (1997).

15. W. Oswald, E. Lee, B. Adan, K. Yao, New wastewater treatment method yields a harvest of saleable algae. *WHO Chronicle* 32, 348 (1978).
16. M. Teixeira, M. Rosa, Comparing dissolved air flotation and conventional sedimentation to remove cyanobacterial cells of *Microcystis aeruginosa* Part I: The key operating conditions. *Separation and Purification Technology* 52, 84 (2006).
17. P. Wiley, K. Brennehan, A. Jacobson, Improved Algal Harvesting Using Suspended Air Flotation. *Water Environment Research* 81, 702 (2009).
18. P. E. Wiley, J. E. Campbell, B. McQuin, Production of biodiesel and biogas from algae: A review of process train options. *Water Environment Research* 83, 326 (2011).
19. H. Ohshima, *Theory of Colloid and Interfacial Electric Phenomena*. Academic Press, 2006.
20. J. Goodwin, *Colloids and Interfaces with Surfactants and Polymers: An Introduction*. Wiley, 2004.
21. T. Cosgrove, *Colloid Science: Principles, Methods and Applications*. Wiley-Blackwell, Oxford, 2005.
22. R. Henderson, S. Parsons, B. Jefferson, Successful removal of algae through the control of Zeta potential. *Separation Science and Technology* 43, 1653 (2008).
23. J. Duan, J. Gregory, Coagulation by hydrolysing metal salts. *Advances in Colloid and Interface Science* 100, 475 (2003).
24. C. Huang, J. Pan, *Coagulation Approach to Water Treatment*. Encyclopedia of Surface and Colloid Science (2006), pp. 1049-1064.
25. A. Bukhari, Investigation of the electro-coagulation treatment process for the removal of total suspended solids and turbidity from municipal wastewater. *Bioresource Technology* 99, 914 (2008).
26. M. Mollah *et al.*, Fundamentals, present and future perspectives of electrocoagulation. *Journal of Hazardous Materials* 114, 199 (2004).
27. E. Ofir, Y. Oren, A. Adin, Comparing pretreatment by iron of electro-flocculation and chemical flocculation. *Desalination* 204, 87 (2007).
28. P. Holt, G. Barton, C. Mitchell, The future for electrocoagulation as a localised water treatment technology. *Chemosphere* 59, 355 (2005).
29. E. Poelman, N. De Pauw, B. Jeurissen, Potential of electrolytic flocculation for recovery of micro-algae. *Resources, Conservation and Recycling* 19, 1 (1997).
30. P. Holt, G. Barton, M. Wark, C. Mitchell, A quantitative comparison between chemical dosing and electrocoagulation. *Colloids and Surfaces A: Physicochemical and Engineering Aspects* 211, 233 (2002).

31. J. Trent, P. Wiley, S. Tozzi, B. McQuin, S. Reinsch, Research Spotlight: The future of biofuels: is it in the bag? *Biofuels* 3, 521 (2012).
32. U. S. DOE, “National Algal Biofuels Technology Roadmap” U.S. Department of Energy, Office of Energy Efficiency and Renewable Energy, Biomass Program, 2010.